

**STABILITY ANALYSIS AND CONTROL OF  
STOCHASTIC POWER SYSTEMS**

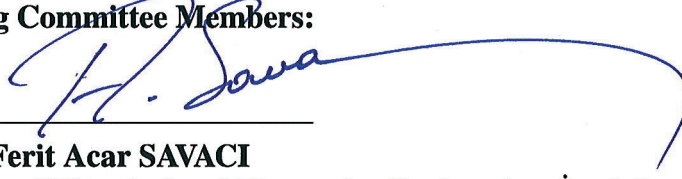
**A Thesis Submitted to  
the Graduate School of Engineering and Sciences of  
İzmir Institute of Technology  
in Partial Fulfillment of the Requirements for the Degree of  
DOCTOR OF PHILOSOPHY  
in Electronics and Communication Engineering**

**by  
Serpil YILMAZ**

**July 2019  
İZMİR**

We approve the thesis of **Serpil YILMAZ**

**Examining Committee Members:**



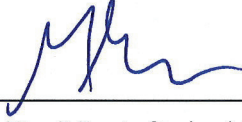
**Prof. Dr. Ferit Acar SAVACI**

Department of Electrical and Electronics Engineering, İzmir Institute of Technology



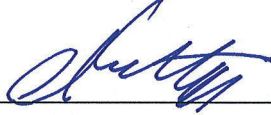
**Prof. Dr. Enver TATLICIOĞLU**

Department of Electrical and Electronics Engineering, İzmir Institute of Technology



**Assoc. Prof. Dr. Mustafa A. ALTINKAYA**

Department of Electrical and Electronics Engineering, İzmir Institute of Technology



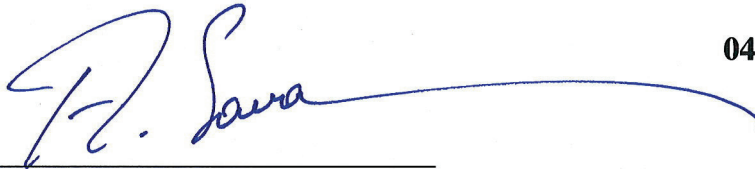
**Assoc. Prof. Dr. Engin KARATEPE**

Department of Electrical and Electronics Engineering, Dokuz Eylül University



**Assist. Prof. Dr. Mehmet Emre ÇEK**

Department of Electrical and Electronics Engineering, Dokuz Eylül University



**04 July 2019**

**Prof. Dr. Ferit Acar SAVACI**

Department of Electrical and Electronics Engineering  
İzmir Institute of Technology



**Prof. Dr. Enver TATLICIOĞLU**

Head of the Department of  
Electrical and Electronics Engineering

**Prof. Dr. Aysun SOFUOĞLU**

Dean of the Graduate School of  
Engineering and Sciences



# ACKNOWLEDGMENTS

I would like to express my sincere gratitude to my advisor, Prof. Dr. Ferit Acar Savacı, for directing me towards a variety of interesting research areas and for his endless support for my development as an independent researcher. It has been honor for me to have Prof. Dr. Ferit Acar Savacı as my Ph.D. advisor. I would like to thank him from the bottom of my heart for his patient guidance, encouragement and advice.

I would also like to express my sincere thanks to the committee members, Prof. Dr. Enver Tatlıcıođlu, Assoc. Prof. Dr. Mustafa A. Altınkaya, Assoc. Prof. Dr. Engin Karatepe and Assist. Prof. Dr. Mehmet Emre ek. I would like to thank each of them individually for providing me with valuable feedback and comments.

I would like to thank the Scientific and Technological Research Council of Turkey, TÜBİTAK BİDEB for supporting me during my education with 2211-E PhD Scholarship.

Finally, I would like to extend my deepest gratitude and love to my beloved family, for their love and constant support. Very special thanks to my sister, Zeynep Yılmaz, who has supported me all my life. I am grateful to have such a wonderful sister.

# ABSTRACT

## STABILITY ANALYSIS AND CONTROL OF STOCHASTIC POWER SYSTEMS

Increase of the electricity generation and the growth of global electricity consumption lead to an increase in the power fluctuations. In this dissertation, we have proposed a novel approach by modeling these fluctuations as alpha-stable Levy processes. We have focused on the stability analysis and control for stochastic single machine infinite bus system with an emphasis on (1) understanding the effect of impulsive and asymmetric power fluctuations on the rotor angle stability, and (2) developing control rule for synchronism in the presence of Wiener and alpha-stable Levy type power fluctuations. We have investigated the basin stability over the parameter space of mechanical power and damping parameters in the presence of alpha-stable Levy type load fluctuations. The probabilities of returning to the stable equilibrium point have been calculated for different characteristic exponent and skewness parameters of alpha-stable Levy motion to see the effect of impulsive and asymmetric load fluctuations. It has been shown that the impulsiveness and/or asymmetry in the distributions of the load fluctuations can cause the instability of the rotor angle. Hence, the synchronism is lost and the rotor angle despite being stable in the sense of probability, might not be stable in the mean square sense. Furthermore, we have studied the control of the rotor angle stability of single machine infinite bus power system in the presence of Wiener type stochastic fluctuations by minimizing the stochastic sensitivity function. We have also derived an analytical expression for the rotor angle dispersion of single machine infinite bus system in the presence of alpha-stable Levy type power fluctuations. The control rule for the minimization of the rotor angle dispersion has been achieved.

# ÖZET

## STOKASTİK GÜÇ SİSTEMLERİNİN KARARLILIK ANALİZİ VE KONTROLÜ

Elektrik üretiminin artması ve küresel elektrik tüketiminin büyümesi güç dalgalanmalarında artışa yol açmaktadır. Bu tezde, bu dalgalanmaları alfa-kararlı Levy rassal süreçler olarak modelleyerek yeni bir yaklaşım önerildi. Stokastik tek makine sonsuz bara güç sistemlerinde (1) dürtüsel ve asimetrik güç dalgalanmalarının rotor açısı kararlılığı üzerindeki etkisinin anlaşılmasına, ve (2) Wiener ve alfa-kararlı Levy tipi güç dalgalanmaları altında senkronizasyon için kontrol kuralı geliştirilmesine önem verilerek kararlılık analizi ve kontrolüne odaklanıldı. Yük dalgalanmalarının dağılımındaki dürtüsellik ve/veya asimetrinin, rotor açısının kararsızlığına neden olabileceği gösterildi. Bu nedenle, senkronizasyonun kaybıyla birlikte, rotor açısı dağılım açısından kararlı olmasına rağmen, ortalama kare anlamında kararlı olmayabilir. Alfa-kararlı Levy tipi yük dalgalanmalarının varlığında mekanik güç ve sönüm parametrelerine bağlı olarak rotor açısının kararlılığının sağlandığı başlangıç koşullarının kümesi bulundu. Dürtüsel ve asimetrik yük dalgalanmalarının etkisini incelemek için farklı karakteristik üstel ve simetri (çarpıklık) parametreleri seçildi ve rotor açısının kararlı denge noktasına geri dönme olasılıkları hesaplandı. Ayrıca, Wiener tipi stokastik dalgalanmaların varlığında rassal hassasiyet fonksiyonunu en aza indirerek, tek makineli sonsuz bara güç sistemlerinde rotor açısı kararlılığının kontrolü incelendi. Alfa-kararlı Levy tipi güç dalgalanmalarının varlığında tek makineli sonsuz bara sisteminin rotor açısı saçılımı için analitik bir ifade çıkarıldı. Rotor açısı saçılımını en aza indirgeyen kontrol kuralı elde edildi.

To the memory of my beloved father, Yaşar YILMAZ

# TABLE OF CONTENTS

|  |      |
|--|------|
| LIST OF FIGURES .....  | ix   |
| LIST OF TABLES .....   | xii  |
| LIST OF SYMBOLS .....  | xiii |
| LIST OF ABBREVIATIONS .....  | xiv  |
| CHAPTER 1. INTRODUCTION .....  | 1    |
| 1.1. Power System Stability .....  | 1    |
| 1.1.1. Rotor Angle Stability .....   | 3    |
| 1.1.2. Frequency Stability .....   | 4    |
| 1.1.3. Voltage Stability .....   | 5    |
| 1.2. Rotor Dynamics and The Swing Equation .....   | 6    |
| 1.3. Single Machine Infinite Bus Power System .....  | 8    |
| CHAPTER 2. STABILITY OF STOCHASTIC NONLINEAR DYNAMICAL SYS-<br>TEMS .....                                    | 12   |
| 2.1. Brownian Motion .....   | 12   |
| 2.1.1. Construction of Brownian Motion as a Random Walk .....  | 13   |
| 2.1.2. Brownian Motion in $\mathbb{R}^m$ .....   | 14   |
| 2.2. Itô Calculus .....  | 15   |
| 2.2.1. Existence and Uniqueness for the Solution of the Itô SDE .....  | 17   |
| 2.2.2. Itô's Lemma .....   | 18   |
| 2.3. Alpha-Stable Lévy Process .....   | 19   |
| 2.4. Stochastic Stability .....  | 24   |
| 2.4.1. Moment Stabilities .....  | 25   |
| 2.4.2. Lyapunov Stability .....  | 26   |
| CHAPTER 3. CONTROL OF STOCHASTIC NONLINEAR DYNAMICAL SYS-<br>TEMS .....                                      | 28   |
| 3.1. Covariance Control .....  | 28   |
| 3.2. Stochastic Sensitivity Analysis for the Nonlinear Dynamical System<br>Perturbed by Wiener Process ..... | 33   |

|   |        |
|---|--------|
| CHAPTER 4. STABILITY ANALYSIS OF STOCHASTIC SINGLE MACHINE INFINITE BUS POWER SYSTEM .....                                | 39     |
| 4.1. Deterministic Single Machine Infinite Bus Power Systems .....  | 40     |
| 4.2. Stochastic Single Machine Infinite Bus Power Systems.....  | 45     |
| 4.3. The Effect of Wiener and $\alpha$ -stable Lévy Power Fluctuations on the Rotor Angle Stability .....                 | 46     |
| 4.3.1. Variation of Basin of Attraction of SEP by Increasing Impulsiveness and/or Skewness.....                           | 46     |
| 4.3.2. Variation of Basin of Attraction of Limit Cycle by Increasing Impulsiveness and/or Skewness.....                   | 48     |
| 4.4. Basin Stability of Stochastic Single Machine Infinite Bus Power System   | 51     |
| <br>CHAPTER 5. CONTROL OF STOCHASTIC SINGLE MACHINE INFINITE BUS POWER SYSTEMS .....                                      | <br>58 |
| 5.1. Controlling the Rotor Angle Stability in SMIB Power Systems by Minimizing Stochastic Sensitivity Function .....      | 58     |
| 5.2. Controlling the Rotor Angle Stability in SMIB Power Systems with $\alpha$ -stable Lévy type power fluctuations ..... | 72     |
| <br>CHAPTER 6. CONCLUSIONS .....  | <br>79 |
| <br>REFERENCES .....  | <br>80 |

# LIST OF FIGURES

| <u>Figure</u>   | <u>Page</u> |
|---|-------------|
| Figure 1.1. Classification of power system stability (Source: (Kundur et al., 2004)) . . . .  | 3           |
| Figure 1.2. Equivalent circuit of Single Machine Infinite Bus (SMIB) power system. . . .  | 9           |
| Figure 1.3. Power-Angle ( $P_e - \delta$ ) Curve. . . . .   | 10          |
| Figure 2.1. Four realizations (trajectories) of one-dimensional sample Brownian motion . . . . .  | 14          |
| Figure 2.2. $\alpha$ -stable density in the case of $\alpha \in \{2.0, 1.4, 0.8, 0.5\}$ , $\beta = 0$ , $\sigma = 1$ , $\mu = 0$ . . . . .                                      | 21          |
| Figure 2.3. $\alpha$ -stable density in the case of $\alpha = 0.8$ , $\beta \in \{-1.0, 0, 0.5, 1.0\}$ , $\sigma = 1$ , $\mu = 0$ . . . . .                                     | 21          |
| Figure 2.4. Trajectories of $\alpha$ -stable Lévy motion in the case of $\alpha = 1.7$ and $\beta = 0$ , $\sigma = 1$ , $\mu = 0$ . . . . .                                     | 22          |
| Figure 2.5. Trajectories of $\alpha$ -stable Lévy motion in the case of $\alpha = 0.7$ and $\beta = 0$ , $\sigma = 1$ , $\mu = 0$ . . . . .                                     | 22          |
| Figure 2.6. Trajectories of $\alpha$ -stable Lévy motion in the case of $\alpha = 1.8$ and $\beta = 1$ , $\sigma = 1$ , $\mu = 0$ . . . . .                                     | 23          |
| Figure 2.7. Trajectories of $\alpha$ -stable Lévy motion in the case of $\alpha = 1.9$ and $\beta = -1$ , $\sigma = 1$ , $\mu = 0$ . . . . .                                    | 23          |
| Figure 4.1. Phase portrait of deterministic SMIB system for $P_m > 1$ . . . . .   | 42          |
| Figure 4.2. Phase portrait of deterministic SMIB system for $D = 0.8 > D_c = 0.414$ and $P_m = 0.5$ . . . . .   | 42          |
| Figure 4.3. Phase portrait of deterministic SMIB system for $D = D_c = 0.414$ and $P_m = 0.5$ . . . . .   | 43          |
| Figure 4.4. Phase portraits of deterministic SMIB system for $D = 0.36 < D_c = 0.414$ and $P_m = 0.5$ . . . . .   | 43          |
| Figure 4.5. Basin of attraction of the stable equilibrium point (SEP) which is colored in blue while the basin of attraction of stable limit cycle is colored in white. . . . . | 44          |
| Figure 4.6. Wiener type fluctuations in the load $\alpha = 2.0$ and $\beta = 0$ . . . . .   | 47          |
| Figure 4.7. Lévy type fluctuations in the load with $\alpha = 1.95$ and $\beta = 0$ . . . . .   | 47          |
| Figure 4.8. Lévy type fluctuations in the load with $\alpha = 1.8$ and $\beta = 0$ . . . . .  | 49          |
| Figure 4.9. Lévy type fluctuations in the load with $\alpha = 1.95$ and $\beta = 1$ . . . . .   | 49          |
| Figure 4.10. Wiener type fluctuations in the load with $\alpha = 2.0$ and $\beta = 0$ . . . . .   | 50          |
| Figure 4.11. Lévy type fluctuations in the load with $\alpha = 1.8$ and $\beta = 0$ . . . . .   | 50          |
| Figure 4.12. Lévy type fluctuations in the load with $\alpha = 1.9$ and $\beta = 1$ . . . . .   | 52          |



|   |    |
|---|----|
| Figure 4.13. Basin stability diagram for deterministic case. ....   | 54 |
| Figure 4.14. Return probability for $P_m = 0.5$ and $D = 0.8$ . ....  | 55 |
| Figure 4.15. Return probability for $P_m = 0.5$ and $D = 0.2$ . ....  | 55 |
| Figure 4.16. Basin stability diagram in the case of $\alpha$ -stable Lévy type power fluctuations<br>with $\alpha = 1.7, \beta = 1$ . ....  | 56 |
| Figure 4.17. Basin stability diagram in the case of $\alpha$ -stable Lévy type power fluctuations<br>with $\alpha = 1.7, \beta = -1$ . ....   | 56 |
| Figure 4.18. Basin stability diagram in the case of $\alpha$ -stable Lévy type power fluctuations<br>with $\alpha = 1.2, \beta = 1$ . ....  | 57 |
| Figure 5.1. Phase portrait of rotor angle $\delta$ vs. rotating speed $w$ of deterministic ( $\epsilon = 0$ )<br>for the initial conditions $\delta(0), \omega(0)$ in the interval of $[-\pi, \pi]$ and $[-10, 10]$ . . | 61 |
| Figure 5.2. Phase portrait of rotor angle $\delta$ vs. rotating speed $w$ of stochastic uncon-<br>trolled SMIB power system ( $\epsilon = 0.001$ ) for $\delta(0) = 1, \omega(0) = 1$ . ....                            | 62 |
| Figure 5.3. Attainability region of the stochastic sensitivity matrix $W$ for $P_m = 1$ ,<br>$D = 0.2$ and the intensity of noisy measurement $c = 0.2$ . ....  | 63 |
| Figure 5.4. Attainability region of the stochastic sensitivity matrix $W$ for $P_m = 1$ ,<br>$D = 0.2$ and the intensity of noisy measurement $c = 0.5$ . ....  | 63 |
| Figure 5.5. Attainability region of the stochastic sensitivity matrix $W$ for $P_m = 1$ ,<br>$D = 0.2$ and the intensity of noisy measurement $c = 0.8$ . ....  | 64 |
| Figure 5.6. Attainability region of the stochastic sensitivity matrix $W$ for $P_m = 1$ ,<br>$D = 0.2$ and the intensity of noisy measurement $c = 1.0$ . ....  | 64 |
| Figure 5.7. The stochastic rotor angle responses over 1000 trajectories (black) with<br>optimal regulators, 95% confidence interval (red), empirical mean (green)<br>for noise intensity with $c = 0.2$ . ....          | 66 |
| Figure 5.8. The stochastic rotor angle responses over 1000 trajectories (black) with<br>optimal regulators, 95% confidence interval (red), empirical mean (green)<br>for noise intensity with $c = 0.5$ . ....          | 66 |
| Figure 5.9. The stochastic rotor angle responses over 1000 trajectories (black) with<br>optimal regulators, 95% confidence interval (red), empirical mean (green)<br>for noise intensity with $c = 0.8$ . ....          | 67 |
| Figure 5.10. The stochastic rotor angle responses over 1000 trajectories (black) with<br>optimal regulators, 95% confidence interval (red), empirical mean (green)<br>for noise intensity with $c = 1.0$ . ....         | 67 |
| Figure 5.11. Phase portrait of rotor angle $\delta$ vs. rotating speed $\omega$ of the deterministic and<br>uncontrolled system for $P_m = 0.5$ . ....  | 68 |
| Figure 5.12. Attainability region of the stochastic sensitivity matrix $W$ for $P_m = 0.5$ ,<br>$D = 0.2$ and the intensity of noisy measurement $c = 0.2$ . ....   | 69 |

|   |    |
|---|----|
| Figure 5.13. Attainability region of the stochastic sensitivity matrix $W$ for $P_m = 0.5$ ,<br>$D = 0.2$ and the intensity of noisy measurement $c = 0.5$ . .....  | 69 |
| Figure 5.14. Attainability region of the stochastic sensitivity matrix $W$ for $P_m = 0.5$ ,<br>$D = 0.2$ and the intensity of noisy measurement $c = 0.8$ . .....  | 70 |
| Figure 5.15. Attainability region of the stochastic sensitivity matrix $W$ for $P_m = 0.5$ ,<br>$D = 0.2$ and the intensity of noisy measurement $c = 1.0$ . .....  | 70 |
| Figure 5.16. The stochastic rotor angle responses over 1000 trajectories with optimal<br>regulators for $P_m = 0.5$ , $D = 0.2$ and the intensity of noise measurements<br>$c = 0.5$ . .....                                    | 71 |
| Figure 5.17. The stochastic rotor angle responses over 1000 trajectories with optimal<br>regulators for noise intensity $c = 1.0$ . .....   | 72 |
| Figure 5.18. The values of the dispersion $\sigma^\alpha$ versus to the minimum settling time with<br>the variation of the characteristic exponent $\alpha$ . .....   | 76 |
| Figure 5.19. The stochastic responses of rotor angle of SMIB subject to $\alpha$ -stable Lévy<br>type power fluctuations with $\alpha = 1.5$ , $\beta = 0$ over 1000 realizations in the<br>presence of optimal regulator. .... | 77 |
| Figure 5.20. The stochastic responses of rotor speed of SMIB subject to $\alpha$ -stable Lévy<br>process with $\alpha = 1.5$ , $\beta = 0$ over 1000 realizations in the presence of<br>optimal regulator. ....                 | 77 |
| Figure 5.21. Phase portrait of the stochastic response of SMIB under $\alpha$ -stable Lévy<br>noise with $\alpha = 1.8$ . .....   | 78 |

# LIST OF TABLES

| <u>Table</u> |  | <u>Page</u> |
|--------------|--|-------------|
| Table 4.1.   | Percentage of Stochastic Trajectories Converging to the SEP. ....                                | 51          |
| Table 5.1.   | Optimal parameters of stochastic sensitivity matrix and the optimal regulator coefficients. .... | 65          |
| Table 5.2.   | Optimal parameters of stochastic sensitivity matrix and the optimal regulator coefficients. .... | 71          |
| Table 5.3.   | The optimal regulator coefficients for $P_m = 1.0$ p.u. ....                                     | 75          |

# LIST OF SYMBOLS

|                                |  |
|--------------------------------|--|
| $J$                            | Total moment of inertia of the rotor masses                                      |
| $\theta_m$                     | Angular displacement of the rotor w.r.t. a stationary axis                       |
| $T_a$                          | Net accelerating torque  |
| $T_m$                          | Mechanical torque supplied by the prime mover                                    |
| $T_e$                          | Electrical torque  |
| $t$                            | Time   |
| $\omega_{sm}$                  | Synchronous speed of the machine   |
| $\delta_m$                     | Angular displacement of the rotor from the synchronously rotating reference axis |
| $P_m$                          | Mechanical power   |
| $P_e$                          | Electrical power   |
| $P_a$                          | Accelerating power   |
| $M$                            | Inertia coefficient  |
| $D$                            | Damping coefficient  |
| $\delta$                       | Rotor angle  |
| $\omega$                       | Rotor speed deviation  |
| $B(t)$                         | Brownian motion  |
| $\xi(t)$                       | Gaussian white noise   |
| $L_\alpha(t)$                  | $\alpha$ -stable Lévy motion   |
| $S_\alpha(\gamma, \beta, \mu)$ | $\alpha$ -stable distribution  |
| $\alpha$                       | Characteristic exponent parameter  |
| $\beta$                        | Skewness parameter   |
| $\gamma$                       | Scale parameter  |
| $\mu$                          | Location parameter   |
| $\mathbf{K}_{CC}$              | Feedback gain matrix   |
| $\mathbf{C}_{r,XX}$            | Reference covariance matrix  |
| $\phi(X)$                      | The asymptotics for the stationary probability density of the state $X$          |
| $D_c$                          | Critical damping level   |

# LIST OF ABBREVIATIONS

|            |  |
|------------|--|
| SMIB ..... | Single Machine Infinite Bus            |
| SDE.....   | Stochastic Differential Equation       |
| pdf.....   | probability density function           |
| SSMIB..... | Stochastic Single Machine Infinite Bus |
| SEP.....   | Stable Equilibrium Point               |

# CHAPTER 1

## INTRODUCTION

Electricity is an essential resource for all aspects of modern life and as a customer what we all expect is that the electricity should always be available when we need at any moment. Although the local outages are usual and accustomed, what is not expected is the massive electric power outages. Power grids are becoming increasingly larger and complex with many connections ever expanding between neighboring systems and proper safeguards should be taken to prevent any potential problem to spread and escalate very quickly. The power system becomes increasingly a target to the attacks, therefore cyber security becomes also an important issue for the energy sector.

According to the North American Electric Reliability Council (NERC) the planning and reliable operation of the power grid should be based on the following key concepts:

1. The power generation and demand should be balanced continuously.
2. The reactive power supply and demand should be balanced to maintain scheduled voltages.
3. The flow on transmission lines should be monitored continuously to avoid overheating.
4. The electric system should be kept in a stable condition- voltage and power (angle) stability limits are set to ensure.
5. The system should be reliably operated even if in the presence of contingency due to the loss of the most important generator or transmission facility.

Since these concepts emphasize the need for understanding stability analysis and control in power systems this chapter reviews some major blackouts occurring over the globe and continues with the summary of the general aspects of power system stability. Further, the rotational dynamic of a machine is discussed and the equivalent electrical representation of the machine is introduced. Finally, since the stability analysis in this dissertation has been based on the rotor angle stability, then the relation between the rotor angle and the electrical output power and the effect of disturbance in the rotor angle on the system stability are explained in a machine connected to a large system through transmission lines which is called as single machine infinite bus system.

## 1.1. Power System Stability

The stability in power systems has been an important problem for long years (Abe et al., 1982; Dobson and Chiang, 1989). The stability problems emerged in the early 1900s have been concerned with the remote main generating stations. The increased use of electric power has led to the increase of the interconnections and the complexity of power systems. Over the years across the globe there have been many major blackouts which mainly began with a single instability event that has led a cascading effect.

In 2003, the branches of a tree have fallen to the transmission line coming from Switzerland to Italy and after this event, the transmission lines coming from France have been also tripped off due to the overload and then the blackout has been occurred in the whole Italy (Corsi and Sabelli, 2004). The another major blackout has occurred on August 14, 2003. The blackout has caused nearly 50 million people in the Midwest and Northeast United States and Ontario, Canada to lack access to electricity and the outage took 4 days in some parts of the United States and more than a week in the parts of Ontario. The blackout has begun with the loss of generation in a power station due to the loss of transmission lines and this has led to the unbalance between the load and generation and as a consequence the power outage has happened in the USA (Liscouski and Elliot, 2004). In 2006, in Continental Europe the blackout has been triggered by the high wind generation in Germany. The imbalance power between supply and demand resulted in splitting the Continental European power system into three separate regions with significant power imbalances in each region (Maas et al., 2007). After these major blackouts the third serious blackout in Continental Europe has occurred in Turkey. The loss of synchronism between the Eastern and the Western subsystems of Turkey has been initiated with the tripping of the Osmanca–Kursunlu line due to the overload. This event has led to the Eastern and Western Turkish subsystems to separate which resulted in the loss of synchronism with the Continental European power system (TEIAS and ENTSO-E, 2015). The most recent massive blackout which is also the largest power outage in the country's history has occurred in March 2019 in Venezuela. As a result of the sharp decrease in turbines rotational speed in the largest hydroelectric power plant, the power system has experienced subsequent collapses which caused the entire country to be lack of electricity for more than a week.

CIGRE Study Committee 38 and IEEE Power System Dynamic Performance Committee have developed a report called IEEE CIGRE Joint Task Force which defines the power system stability as:

**Definition 1.1** *Power system stability is the ability to regain a state of operating equilibrium following a physical disturbance for a given initial operating condition (Kundur et al., 2004).*



The power system stability is classified as rotor angle stability, frequency stability and voltage stability depending on their physical character. The classification can be further divided into subcategories as small-disturbance or large-disturbance stability depending on the size of the disturbance and the short term or long term stability depending on the time frame of the disturbance involved in power system (Kundur et al., 1994) as shown in Figure 1.1. These disturbances can be resulted from such as the faults occurred in the system, the changes in load, generator trip or the loss of transmission facility.

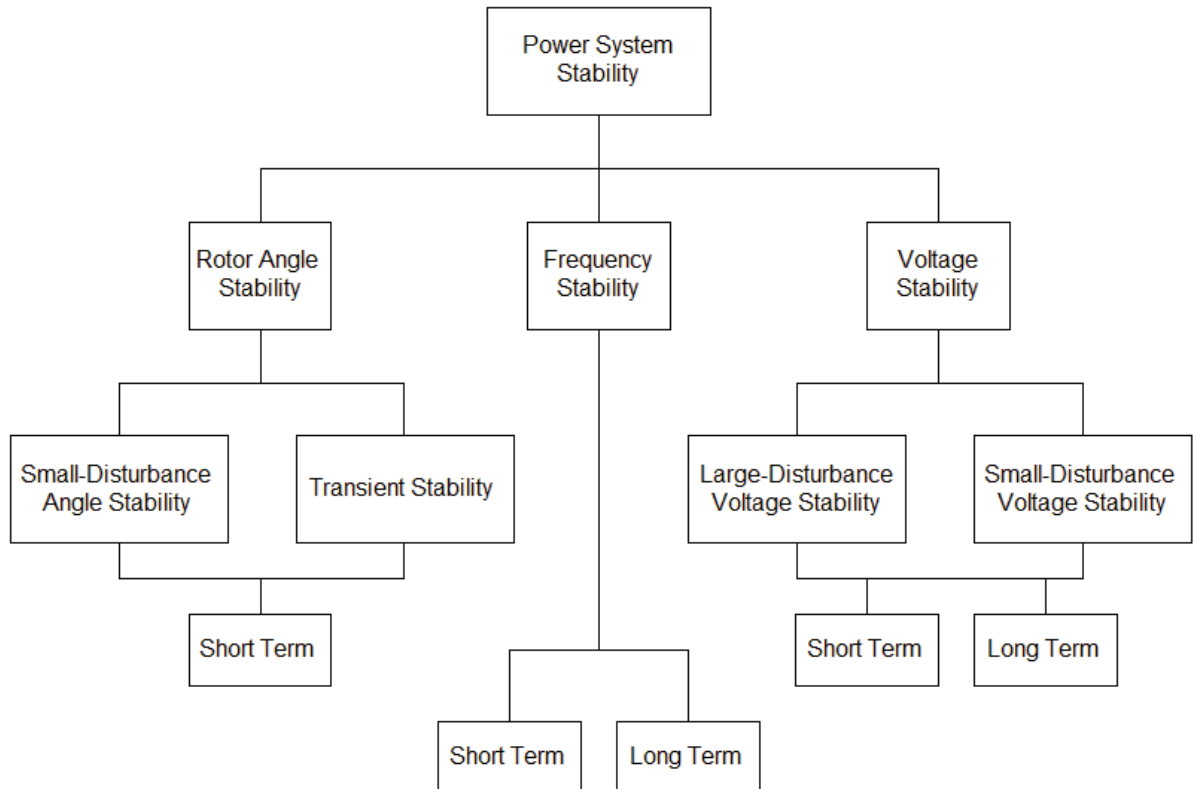


Figure 1.1. Classification of power system stability (Source: (Kundur et al., 2004))

The details of power system stability shown in Figure 1.1 have been expressed as follows:

### 1.1.1. Rotor Angle Stability

**Definition 1.2** Rotor angle stability is the ability of interconnected machines of a power system to remain in synchronism following a disturbance (Kundur et al., 2004).

In the steady-state, the input mechanical torque of each machine is exactly equal to the output electrical torque of each machine in the opposite direction and the speed remains constant. The minor oscillations of rotor angles in the power system constantly occur when machine rotors accelerate or slow down to maintain the balance between the electrical output power and mechanical input power.

However, the presence of disturbance in the system causes an imbalance between the mechanical and electrical torque leading to oscillations in the rotor angle. The run of one machine temporarily faster than another machine leads to the advance of the angular position of its rotor relative to the angular position of the slower machine. By transferring the part of the load from the slow machine to the fast machine provides the reduction in the speed difference and hence angular separation. Beyond a certain limit, the angular separation increases and the power transfer decreases and this leads to the increase of the angular separation further.

In the presence of the loss of synchronism of a machine, the power system is designed to disconnect the unstable machine from the grid to protect the power plant from physical damage since the machines are usually the most expensive units in power system.

The rotor angle stability can be divided into categories: small-disturbance angle stability and transient stability which are described as follows:

- (i) Small-disturbance angle (or steady state) stability represents the stability phenomenon in which synchronism is maintained in power systems under sufficiently small disturbances.
- (ii) Transient stability represents the ability of the power system to maintain synchronism when subjected to a severe transient disturbance due to the changes in load, generator trip or the loss of transmission facility.

As shown in Figure 1.1 the time frame of interest in small signal stability and transient stability are given as short-term which are on the order 10-20 seconds and 3-5 seconds, respectively.

### **1.1.2. Frequency Stability**

**Definition 1.3** *Frequency stability is the ability of a power system to keep the frequency steady after a disturbance caused by significant imbalance between generation and load (Kundur et al., 2004).*

Under the stable operating conditions, interconnected power systems are required to have the same frequency. In the presence of major disturbances the power system breaks into

separate islands and the generation in any island may substantially exceed or go beyond to the required demand, therefore each island in the grid should maintain the balance between generation and demand. Because the imbalance between the generation and demand causes the frequency of system to vary. When the generation exceeds demand, the system frequency increases and when the generation is less than demand the frequency decreases. It is practically accepted that frequency can deviate slightly. However significant deviations in the frequency can cause generator turbine blades to be damaged.

### 1.1.3. Voltage Stability

**Definition 1.4** *Voltage stability is the ability of a power system to maintain the voltages in the system within acceptable limits following a disturbance (Kundur et al., 2004).*

Voltage instability or voltage collapse refers to the progressive fall in voltage until stable operating voltages can no longer be maintained. The major reason of the progressive drop in voltage is the imbalance of reactive power supply and demand which is caused by such as the increase of real or reactive loads, the reach of power transfer a high level, the generation trip or the loss of transmission facilities. If the required reactive power cannot be supplied promptly, voltages decay and this can cause voltage instability.

There can be also a relation with the progressive decline in voltage and the rotor angle stability. Low voltages can occur as a result of the loss of synchronism of machines due to the out of step in rotor angles. Voltage instability is analyzed by  $V - Q$  and  $P - V$  curves which refer to voltage relative to reactive power and power relative to voltage, respectively.

According to the  $V - Q$  analysis, under stable operating conditions the increase in voltage requires the reactive power to increase while the decrease in voltage results in the decrease of the reactive power requirement. However, when the voltage at bus is decreased but the corresponding reactive power requirement begins to increase, the system becomes unstable. The level of voltage at which stable system becomes unstable is called as the critical voltage and the corresponding reactive power level is called as the reactive margin.

Beyond the voltage level, contingency analysis should be conducted for the voltage stability. The real power system capability over a transmission facility is described by  $P - V$  analysis. A high level of power transfer causes the voltage cannot maintain stable. After the occurrence of contingency, the operating conditions determined by  $P - V$  curve are adjusted to keep the system stable.

The voltage stability can be divided into the following subcategories:

- (i) Large-disturbance voltage stability is the ability to maintain steady voltages in the pres-

ence of a large disturbance due to the faults occurring in the system, the generation trip or, the loss of transmission facility.

- (ii) Small-disturbance voltage stability is the ability to keep steady voltages in the presence of small perturbations such as incremental load changes in the system.

Voltage instability can takes gradually about a few seconds or ten minutes. The time frame can be classified as a short-term or a long-term.

## 1.2. Rotor Dynamics and The Swing Equation

Based on the law of rotation, the rotational dynamics of a synchronous machine is governed by the following equation:

$$J \frac{d^2 \theta_m}{dt^2} = T_a = T_m - T_e \quad (1.1)$$

where

$J$  denotes the total moment of inertia of the rotor masses ( $kg.m^2$ )

$\theta_m$  is the angular displacement of the rotor w.r.t. a stationary axis (rad)

$T_a$  is the net accelerating torque ( $N.m$ )

$T_m$  is the mechanical torque supplied by the prime mover ( $N.m$ )

$T_e$  is the electrical torque ( $N.m$ )

$t$  denotes time in seconds ( $s$ ).

The angular displacement of the rotor w.r.t. a stationary axis  $\theta_m$  is defined as

$$\theta_m = \omega_{sm} t + \delta_m \quad (1.2)$$

where  $\omega_{sm}$  is the synchronous speed of the machine and  $\delta_m$  is the angular displacement of the rotor from the synchronously rotating reference axis .

The time derivative of (1.2) is given as:

$$\frac{d\theta_m}{dt} = \omega_{sm} + \frac{d\delta_m}{dt} \quad (1.3)$$

and the second derivative of (1.2) is as follows:

$$\frac{d^2\theta_m}{dt^2} = \frac{d^2\delta_m}{dt^2} \quad (1.4)$$

where the rotor angular velocity  $d\theta_m/dt$  equals to the synchronous speed when  $d\delta_m/dt = 0$ .

The rotor speed from synchronism is denoted by  $d\delta_m/dt$ . By substituting (1.4) in (1.2) the following equation is obtained:

$$J \frac{d^2\delta_m}{dt^2} = T_a = T_m - T_e . \quad (1.5)$$

Let

$$\omega_m \equiv \frac{d\delta_m}{dt} \quad (1.6)$$

and since the torque times angular velocity equals to the power multiplying (1.5) by  $\omega_m$ , then the following equation is obtained:

$$J\omega_m \frac{d^2\delta_m}{dt^2} = P_a = P_m - P_e \quad (1.7)$$

where  $P_m$  is the mechanical power,  $P_e$  is the electrical power and  $P_a$  denotes the accelerating power due to the unbalance between  $P_m$  and  $P_e$ .

The angular momentum of the rotor  $J\omega_m$  is called as the inertia constant of the machine at synchronous speed  $\omega_{sm}$  and it is denoted by  $M_m$ .

$$M_m \frac{d^2\delta_m}{dt^2} = P_a = P_m - P_e . \quad (1.8)$$

By expressing the power angle and angular speed in electrical radians and electrical radians per second rather than mechanical radians and mechanical radians per second, the relations are given respectively as:

$$\delta \equiv \frac{\delta_m}{p/2} \quad \text{and} \quad \omega_s \equiv \frac{\omega_{sm}}{p/2} \quad (1.9)$$

where  $p$  is the number of poles then the swing equation can be written as:

$$M \frac{d^2 \delta}{dt^2} = P_a = P_m - P_e. \quad (1.10)$$

where the inertia coefficient

$$M = \frac{2HS_{mach}}{\omega_s} \quad (1.11)$$

$S_{mach}$  is the three-phase rating of the machine and

$$H = \frac{0.5J\omega_{sm}^2}{S_{mach}}. \quad (1.12)$$

In the presence of damping torque the swing equation takes the following form

$$M \frac{d^2 \delta}{dt^2} = P_a = P_m - P_e - P_D \quad (1.13)$$

where the damping power

$$P_D = D \frac{\partial \delta}{dt} \quad (1.14)$$

and  $D$  is the damping coefficient.

The system in (1.13) can be rewritten as the two first-order equations:

$$\begin{aligned} \frac{d\delta}{dt} &= \omega \\ M \frac{d\omega}{dt} &= P_a = P_m - P_e - P_D \end{aligned} \quad (1.15)$$

where  $\delta$  is the rotor angle and  $\omega$  is the rotor speed deviation.

### 1.3. Single Machine Infinite Bus Power System

For the sake of understanding, stability analysis and control in this dissertation have been discussed in single machine infinite bus system. Single machine infinite bus (SMIB)

power system is a system in which a machine connected to an infinite bus through a transmission line as shown in Figure 1.2. The bus whose voltage and frequency remain constant is called as the infinite bus.

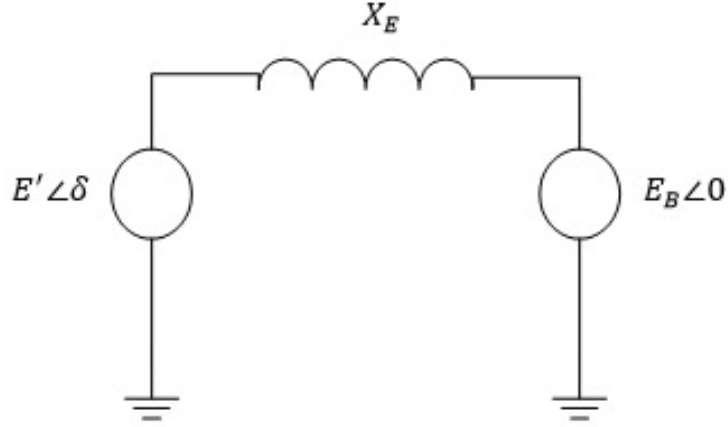


Figure 1.2. Equivalent circuit of Single Machine Infinite Bus (SMIB) power system.

The complex internal voltage of the machine is represented by  $E' \angle \delta$  and the complex infinite bus voltage is represented by  $E_B \angle 0$  and  $X_E$  denotes the total reactance between the machine and infinite bus in Figure 1.2.

The classical model in power systems represents the machine in a simple but very useful way. In the SMIB power system shown Figure. 1.2 the machine has been represented by classical model which has two dynamic variables given in (Rogers, 2012) as:

1. the angle of the machine's internal voltage
2. the machine's speed deviation from synchronous speed.

The dynamics of the SMIB system are described by the following equations:

$$\begin{aligned} \frac{d\delta}{dt} &= \omega \\ M \frac{d\omega}{dt} &= P_m - P_{max} \sin \delta . \end{aligned} \quad (1.16)$$

The electrical power output  $P_e$  transmitted to the infinite bus is given by

$$P_e = \frac{E' E_B}{X_E} \sin \delta \quad (1.17)$$



where the maximum power is transmitted to the infinite bus when the angle  $\delta = 90^\circ$ ; then

$$P_{max} = \frac{E' E_B}{X_E} . \quad (1.18)$$

In the steady state, there is a balance between the mechanical power  $P_m$  and the electrical power  $P_e$  such as

$$P_m = P_e = P_{max} \sin \delta \quad (1.19)$$

and the rotor angle can be found using (1.19) as:

$$\delta_0 = \sin^{-1} \left( \frac{P_m}{P_{max}} \right) \quad \text{or} \quad \delta_{max} = \pi - \sin^{-1} \left( \frac{P_m}{P_{max}} \right) . \quad (1.20)$$

The stability of a SMIB can be analyzed by using the power-angle curve ( $P_e - \delta$ ) shown as in Figure 1.3.

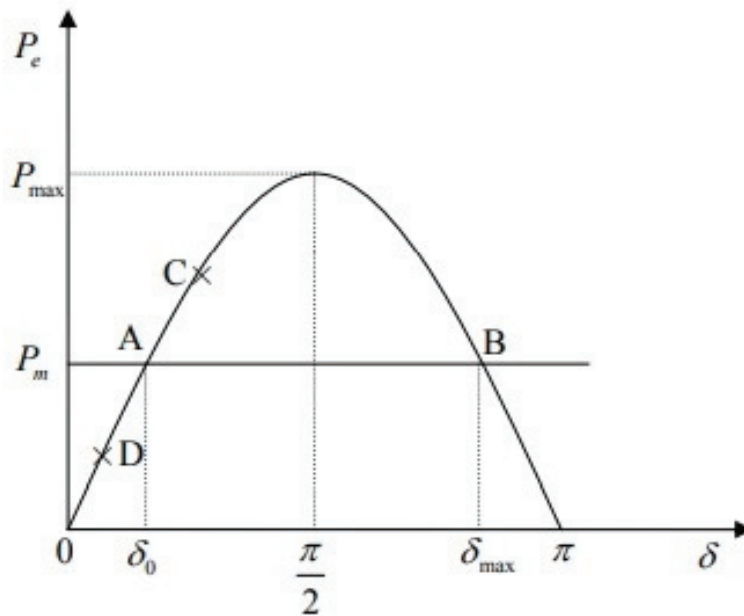


Figure 1.3. Power-Angle ( $P_e - \delta$ ) Curve.

In the steady state, the solutions of (1.19) represented by  $\delta_0$  and  $\delta_{max} = \pi - \delta_0$  have been shown in Figure 1.3 which corresponds to the point *A* and *B*, respectively. Consider a machine which delivers a constant mechanical power  $P_m$  and operates at steady-state synchronous speed with a rotor angle of  $\delta_0$ . In this case  $P_m$  is equal to the electrical output power  $P_e$  represented by the point *A* shown in Figure 1.3.

When the load is suddenly increased to a value corresponding to the point *C* on the power-angle curve, the electrical power exceeds the mechanical power and hence the accelerating power becomes negative. This causes the rotor to slow down and the angle  $\delta$  will decrease to the point *A* but due to the inertia of rotor, the rotor angle decrease from  $\delta_0$  to the further angle corresponding to the point *D*. At this point mechanical power exceeds the electrical power and the accelerating power is positive then the rotor cannot remain at synchronous speed, it starts to accelerate and the rotor angle advances to the value corresponding to the point *C*. In the absence of damping, the rotor oscillates in this sequence indefinitely.

However, when the operating rotor angle is  $\delta_{max}$  which corresponds to the point *B* and when the rotor angle is perturbed, the mechanical power exceeds the electric power which causes the rotor to accelerate. The rotor angle increases and the electrical power decreases further. Hence, the presence of disturbance in the rotor angle results in the continuous increase in the rotor speed which lead to the system become unstable.

## CHAPTER 2

# STABILITY OF STOCHASTIC NONLINEAR DYNAMICAL SYSTEMS

The stability theory of stochastic differential equations has become a very popular research in applications from various fields such as engineering, physics, biological systems, economics and finance. This chapter begins with the review of Brownian motion (Wiener process) since the noise is generally assumed to be Gaussian in dynamical systems described by stochastic differential equations. Then the construction of Wiener process is introduced. Further, Itô stochastic differential equations, existence and uniqueness for the solution of Itô stochastic differential equation, and general remarks on the solution process are discussed. It is also possible to consider the extreme events in the dynamical systems which can be described by alpha-stable Lévy process ( $\alpha$ -stable Lévy process). The properties of such processes are given and the effects of distribution parameters on the  $\alpha$ -stable Lévy motion are analyzed. Finally, the stability analysis in stochastic systems based on the mean square stability are discussed.

### 2.1. Brownian Motion

The study of random differential equations has begun with the investigation of Brownian motion which lead to the development in the theory of stochastic processes.

In 1826-27, Robert Brown observed the irregular motion of pollen particles suspended in water and he noticed that the motions of two distinct particles appear to be independent. This motion is referred to as Brownian motion. In the 1920's, American mathematician Norbert Wiener, studied on a mathematical theory of Brownian motion called the theory of Wiener process.

The Brownian motion (Wiener process) can be defined in the following way (Soong, 1973):

**Definition 2.1** : *A real-valued stochastic process  $B(t)$  which indicates the position of a particle at time  $t$  is called a Brownian motion (Wiener process) if*

1.  $B(t)$ ,  $t \geq 0$  are continuous functions of  $t$ ;

2.  $B(t) - B(s)$  is normally distributed having zero mean and  $(t - s)$  variance for all  $t \geq s \geq 0$ ;
3.  $B(t)$  has independent increments, i.e., for any finite sequence of times  $0 < t_1 < t_2 < \dots < t_n$ , the random variables

$$B(t_1), B(t_2) - B(t_1), \dots, B(t_n) - B(t_{n-1})$$

are independent.

### 2.1.1. Construction of Brownian Motion as a Random Walk

The generation of the samples of Brownian motion  $B(t)$  is given as: For a given interval  $[0, T]$  consider a mesh  $\{t_i = i\tau : i = 0, 1, \dots, N\}$  on  $[0, T]$  with fixed natural number  $N$  and  $\tau = T/N$ .

For a given finite sequence  $\xi_i, i = 1, 2, \dots, N$  of independent Gaussian variables with mean 0 and variance  $\tau$  (i.e.  $\xi_i = N(0, \tau)$ ), let

$$B^\tau(0) = 0 \text{ a.e.} \tag{2.1}$$

and for  $i = 1, 2, \dots, N$  compute

$$B^\tau(t) = B^\tau(t_{i-1}) + (t - t_{i-1})\xi_i \tag{2.2}$$

for  $t \in (t_{i-1}, t_i]$  The process  $\{B^\tau(t) : t \in [0, T]\}$  converges to the Brownian motion process  $B(t)$  on  $[0, T]$  when  $\tau \rightarrow 0$ .

Figure 2.1 presents four realizations of one-dimensional Brownian motion  $B(t)$  obtained by computer simulation with  $T = 1$  and  $\tau = 0.001$ .

Almost all sample paths of the Wiener process are continuous in time, but they are in fact non-differentiable for time  $t \geq 0$ . The non-differentiability implies that there is no velocity of the particle under observation at every instant of time.

To express the non-differentiability for fixed  $t$ , the distribution of the difference quotient is given as:

$$\frac{1}{\tau}(B(t + \tau) - B(t)) \tag{2.3}$$

which is a Gaussian distribution with zero mean and  $(1/\tau)$  variance.

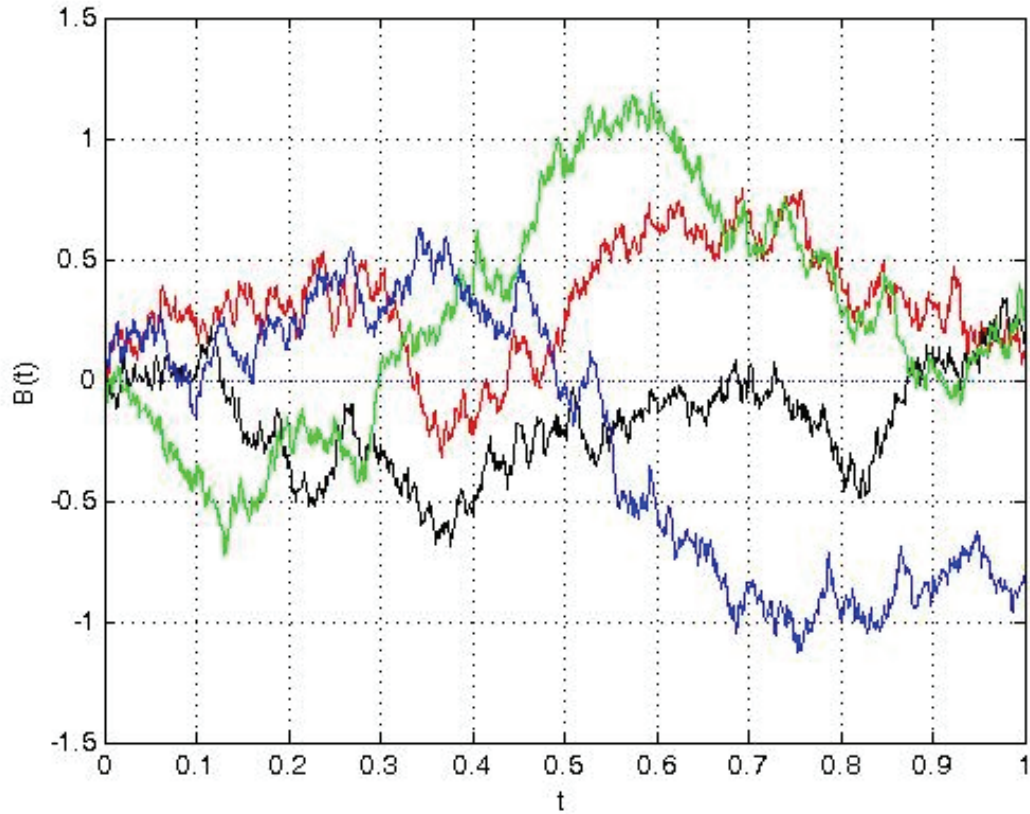


Figure 2.1. Four realizations (trajectories) of one-dimensional sample Brownian motion

As  $\tau \rightarrow 0$ , this normal distribution diverges and therefore the difference quotient cannot converge with positive probability to a finite random variable in a probabilistic sense (Rogers, 2012).

Gaussian white noise  $\xi(t)$  can be symbolically expressed with the time derivative of the Brownian motion (Wiener process)

$$\dot{B}(t) = \frac{dB(t)}{dt} \equiv \xi(t) \quad (2.4)$$

and conversely the Brownian motion (Wiener process) can also be symbolically expressed as the time integral of the white noise:

$$B(t) = \int_0^t \xi(s) ds \quad (2.5)$$

### 2.1.2. Brownian Motion in $\mathbb{R}^m$

A stochastic vector process  $\mathbf{B}(t) = [B_1(t), B_2(t), \dots, B_m(t)]$  is an  $m$ -dimensional Brownian motion (Wiener process) if

1. each component  $B_i(t)$  is a 1-dimensional Wiener process,
2. the processes  $B_i(t)$  are mutually independent .

for each  $i = 1, 2, \dots, m$ .

### 2.2. Itô Calculus

The presence of uncertainties and randomness in the systems described by ordinary differential equations lead to the modeling of the systems by random differential equations to include the disturbances. Random differential equations play an important role to model and analyze the uncertainties in the physical or natural systems.

Consider the random differential equations given as:

$$\dot{\mathbf{X}}(t) = \mathbf{F}(\mathbf{X}(t), \mathbf{Y}(t), t), \quad t \in T; \quad \mathbf{X}(t_0) = \mathbf{X}_0 \quad (2.6)$$

where  $\mathbf{X}(t) \in R^n$  with components  $X_i(t)$ ,  $i = 1, 2, \dots, n$ . The vectors  $\mathbf{F}$  and  $\mathbf{X}_0$  are  $n$ -dimensional vectors and the stochastic process  $\mathbf{Y}(t) \in R^m$ .

Itô calculus analyzes a special class of random differential equations in which the dynamical systems are driven by Brownian motion, i.e., the components of stochastic process  $\mathbf{Y}(t)$  in (2.6) are white Gaussian noise:

$$\dot{\mathbf{X}}(t) = \mathbf{F}(\mathbf{X}(t), t) + \mathbf{G}(\mathbf{X}(t), t)\xi(t) \quad t \in T; \quad \mathbf{X}(t_0) = \mathbf{X}_0 \quad (2.7)$$

where the components of stochastic process  $\xi(t) \in R^m$  are Gaussian white noise, the matrix function  $\mathbf{G}(\mathbf{X}(t), t) \in R^{n \times m}$ , and  $\mathbf{X}_0$  is independent of  $\xi(t)$ ,  $t \in T$ .

Equation (2.7) can be rewritten using the formal representation given in (2.4) for the Gaussian white noise as:

$$d\mathbf{X}(t) = \mathbf{F}(\mathbf{X}(t), t) + \mathbf{G}(\mathbf{X}(t), t) d\mathbf{B}(t) \quad t \in T; \quad \mathbf{X}(t_0) = \mathbf{X}_0 \quad (2.8)$$

and the stochastic integral representation is as:

$$\mathbf{X}(t) - \mathbf{X}(t_0) = \int_{t_0}^t \mathbf{F}(\mathbf{X}(s), s) ds + \int_{t_0}^t \mathbf{G}(\mathbf{X}(s), s) d\mathbf{B}(s) \quad t \in T; \quad \mathbf{X}(t_0) = \mathbf{X}_0 \quad (2.9)$$

where  $\mathbf{X}_0$  is independent of the increment  $d\mathbf{B}(t)$ ,  $t \in T$ .

The first integral in the right-hand side of the (2.9) is the ordinary Riemann integral in the mean square sense. However, the second integral in the right-hand side of the (2.9) cannot be interpreted as a Riemann-Stieltjes integral in the mean square sense because when the random variables  $Y_n$  are defined by

$$Y_n = \sum_{k=1}^n X(t'_k) [B(t_k) - B(t_{k-1})], \quad t'_k \in [t_{k-1}, t_k], \quad (2.10)$$

the sum  $Y_n$  does not converge in the mean square sense to a unique limit since the limit of  $\{Y_n\}$  sum depends on the choice of  $t'_k$ .

Therefore, the integral

$$\int_{t_0}^t X(s) dB(s) \quad (2.11)$$

does not exist as a Riemann-Stieltjes integral in the mean square sense.

Consider the second integral in the right-hand side of the (2.9) defined as

$$\int_{t_0}^t \mathbf{G}(\mathbf{X}(s), s) d\mathbf{B}(s) \quad (2.12)$$

where the vector  $\mathbf{X}(t)$  is stochastic process and  $\mathbf{B}(t)$  is  $m$ -dimensional Brownian motion.

This integral can be interpreted as the limit of a random sequence consisting of the summation in the mean square sense.

When the sequence is defined as:

$$\sum_{k=1}^n G[X(t_{k-1}), t_{k-1}] [B(t_k) - B(t_{k-1})] \quad (2.13)$$

where  $0 \leq t_0 < t_1 < \dots < t_k < t_{k+1} \leq T$  and  $G[X(t_{k-1}), t_{k-1}]$  is evaluated at the left-hand endpoint of the time interval on each subinterval  $[t_{k-1}, t_k)$ .



With this interpretation (2.8) or (2.9) is called as the Itô stochastic differential equation (SDE) .

However when the sequence is defined as

$$\sum_{k=1}^n G [X(t_{k-1/2}, t_{k-1/2})] [B(t_k) - B(t_{k-1})] \quad (2.14)$$

where  $t_{k-1/2} = (t_k + t_{k-1})/2$  then (2.8) or (2.9) is called as the Stratonovich stochastic differential equation.

It can be concluded that depending on the interpretation of the second integral of the right-hand side of the (2.7) as Itô sense or Stratonovich sense, (2.8) or (2.9) is called Itô or Stratonovich differential equation, respectively.

On the other hand, the increment after the time instance  $t_{k-1}$  given as  $B(t_k) - B(t_{k-1})$  is independent of  $X(t_{k-1})$  in Itô sense but there may be dependence between the process  $X(t_{k-1/2})$  and the increment  $B(t_k) - B(t_{k-1})$  in Stratonovich sense.

The difference between the two integrals are given in (Sun, 2006) as:

$$(S) \int_{t_0}^t G(X(s), s) dB(s) - (I) \int_{t_0}^t G(X(s), s) dB(s) = \frac{1}{2} \int_0^t \frac{\partial G(X(s), s)}{\partial X} G(X(s), s) ds \quad (2.15)$$

where (S) represents the integral in the Stratonovich sense and (I) represents the integral in the Itô sense,  $X(t)$  and  $B(t)$  are one-dimensional stochastic processes and the right-hand side of the (2.15) is a Riemann integral in the mean square sense.

In general, the term 'stochastic differential equation' is accepted to mean the Itô stochastic differential equation and in this dissertation we consider the Itô stochastic differential equation.

### 2.2.1. Existence and Uniqueness for the Solution of the Itô SDE

Consider the scalar Itô equation

$$X(t) = X_0 + \int_{t_0}^t f(X(s), s)ds + \int_{t_0}^t g(X(s), s)dB(s) \quad (2.16)$$

where  $X(t_0) = X_0$  and the initial condition  $X_0$  is independent of  $dB(t)$ ,  $t \in T = [t_0, \alpha]$ .

The solution process  $X(t)$  of the Itó SDE generated by (2.16) is Markovian. This is an important property which has considerable techniques to obtain the solution process of Itó equation.

**Theorem 2.1** *Let  $f(x, t)$  and  $g(x, t)$ ,  $t \in T$ , be two real functions. Equation (2.16) has a unique mean square solution if the following properties are satisfied (Soong, 1973):*

1. *Both functions are continuous on  $T \times (-\infty, \infty)$  and uniformly continuous in  $t$  with respect to  $x \in (-\infty, \infty)$ .*
2. *For a suitable  $K > 0$ , the growth conditions*

$$f^2(x, t) \leq K^2(1 + x^2), \quad g^2(x, t) \leq K^2(1 + x^2) \quad (2.17)$$

3. *For a suitable  $K > 0$ , the Lipschitz conditions*

$$\begin{aligned} |f(x_2, t) - f(x_1, t)| &\leq K |x_2 - x_1| \\ |g(x_2, t) - g(x_1, t)| &\leq K |x_2 - x_1| \end{aligned} \quad (2.18)$$

The existence and uniqueness theorem can be generalized to the vector case by using the same properties given above.

### 2.2.2. Itó's Lemma

Consider the following Itó SDE which is satisfied by the  $n$ -dimensional vector stochastic process  $X_j(t)$

$$dX_j(t) = F_j(\mathbf{X}, t) dt + \sum_{k=1}^m G_{jk}(\mathbf{X}, t) dB_k(t) \quad \text{for } i = 1, 2, \dots, n. \quad (2.19)$$

Let  $U(\mathbf{X}, t)$  be an arbitrary function of  $\mathbf{X}$  and  $t$ , with continuous partial derivatives  $\frac{\partial U}{\partial t}$ ,  $\frac{\partial U}{\partial X_j}$ ,  $\frac{\partial^2 U}{\partial X_j \partial X_k}$ , ( $j, k = 1, \dots, n$ ).

Then the differentiation of the function is as:

$$dU(\mathbf{X}, t) = \left( \frac{\partial U}{\partial t} + \sum_{j=1}^n F_j \frac{\partial U}{\partial X_j} + \frac{1}{2} \sum_{j=1}^n \sum_{k=1}^n b_{jk} \frac{\partial^2 U}{\partial X_j \partial X_k} \right) dt + \sum_{j=1}^n \sum_{k=1}^m G_{jk} \frac{\partial U}{\partial X_j} dB_k(t) \quad (2.20)$$

where

$$b_{jk} = \sum_{l=1}^m G_{jl}G_{kl} . \quad (2.21)$$

The Itó's lemma has an important application which provides to derive the moment equations for the response of the Itó's SDE.

When a linear Itó differential equation is considered such that

$$d\mathbf{X}(t) = \mathbf{A}\mathbf{X}(t)dt + \mathbf{G}d\mathbf{B}(t) \quad (2.22)$$

and by using Itó's lemma and  $E [d\mathbf{B}(t)]$  then the mean vector satisfies the equation

$$\frac{dE[\mathbf{X}]}{dt} = \mathbf{A}E[\mathbf{X}] \quad (2.23)$$

and the correlation matrix is governed by the following equation

$$\frac{d\mathbf{R}_{XX}}{dt} = \mathbf{A}\mathbf{R}_{XX} + \mathbf{R}_{XX}\mathbf{A}^T + \frac{1}{2}\mathbf{b} \quad (2.24)$$

where  $\mathbf{b} = \mathbf{G}\mathbf{G}^T$ .

### 2.3. Alpha-Stable Lévy Process

Wiener processes have long been provided useful tools for stochastic modeling. However, in the presence of extreme events or fluctuations that cannot be described by Gaussian distributions, alpha-stable processes which are based on the class of impulsive and asymmetric distributions have been introduced to model such fluctuations. Some applications for  $\alpha$ -stable Lévy process can be given as: seismic ground accelerations in (Grigoriu, 1986); income distributions in economical models in (Mandelbrot, 1960); fatigue life of machineries in mechanics in (Frendal and Rychlick, 1992); anomalous diffusion occurring in complex dynamical systems in (Weiss et al., 2004); the power fluctuations in single machine infinite bus power systems in (Yılmaz and Savacı, 2017a,b), power grid frequency fluctuations in (Schäfer et al., 2018) .

A stochastic process  $\{L_\alpha(t) : t \geq 0\}$  is called an  $\alpha$ -stable Lévy motion if

1.  $L_\alpha(0) = 0$ , almost surely (a.s.);
2.  $L_\alpha(t)$  has independent and stationary increments " $dL_\alpha(t)$ ";

$$3. dL_\alpha(t) \doteq L_\alpha(t) - L_\alpha(s) \sim S_\alpha((t-s)^{1/\alpha}, \beta, 0) \quad \text{for any } 0 \leq s < t < \infty.$$

where the increments of the  $\alpha$ -stable Lévy process  $dL_\alpha(t)$  are  $\alpha$ -stable random variables and their distribution which has no analytical expression is denoted by  $\alpha$ -stable distribution  $S_\alpha(\gamma, \beta, \mu)$ .

$S_\alpha(\gamma, \beta, \mu)$  is characterized by the four parameters: the shift parameter  $\mu$  denotes the location,  $\gamma$  is scale parameter, the characteristic exponent (or the index of stability)  $\alpha$  measures the impulsiveness ( $0 < \alpha \leq 2$ ), and the skewness parameter  $\beta$  measures the symmetry of the distribution, where  $\beta = 0$  refers to symmetric distribution,  $\beta < 0$  to left-skewed distribution and  $\beta > 0$  to right-skewed distribution (Samorodnitsky and Taqqu, 1994; Janicki and Weron, 1993; Nikias and Shao, 1995; Applebaum, 2009).

The characteristic function of an  $\alpha$ -stable random variable is given by (Nikias and Shao, 1995; Samorodnitsky and Taqqu, 1994) :

$$\varphi(w) = \begin{cases} \exp\left\{-\sigma^\alpha |w|^\alpha \left[1 - j\beta \text{sign}(w) \tan\left(\frac{\pi\alpha}{2}\right)\right] + j\mu w\right\} & \text{for } \alpha \neq 1 \\ \exp\left\{-\sigma^\alpha |w| \left[1 + j\beta \text{sign}(w) \frac{2}{\pi} \log(|w|)\right] + j\mu w\right\} & \text{for } \alpha = 1 \end{cases} \quad (2.25)$$

where  $\text{sign}(w)$  is signum function. The numerical approximation of  $\alpha$ -stable density functions have been evaluated by the inverse Fourier transform of the characteristic functions of  $\alpha$ -stable distributions (Nolan, 1997) given in (2.25) as:

$$f(x) = \frac{1}{2\pi} \int_{-\infty}^{\infty} e^{-jwx} \varphi(w) dw \quad (2.26)$$

Figure 2.2- 2.3 present the plots of stable densities for the various parameters of characteristic exponent  $\alpha$  and skewness  $\beta$ .

It can be seen from Figure 2.2 that as the value of characteristic exponent “ $\alpha$ ” decreases then the impulsiveness increases and hence the tails of the corresponding distributions become heavier. The skewness of the distribution has been shown in Figure 2.3 in which the increase in the absolute value of the  $\beta$  results in the more asymmetric (skewed) distribution.

Figure 2.4-2.7 show  $\alpha$ -stable Lévy motion for a few different values of the parameter  $\alpha$  and  $\beta$ . It is seen from Figure 2.4-2.5 that the decrease in the parameter of  $\alpha$  causes the bigger jumps of trajectories.

Figure 2.6-2.7 present the effect of the parameter  $\beta$  on the  $\alpha$ -stable Lévy motion. While the skewness parameter is nonzero  $\beta \neq 0$ , a small deviation in the parameter of characteristic exponent  $\alpha$  causes the jumps of trajectories to become bigger.

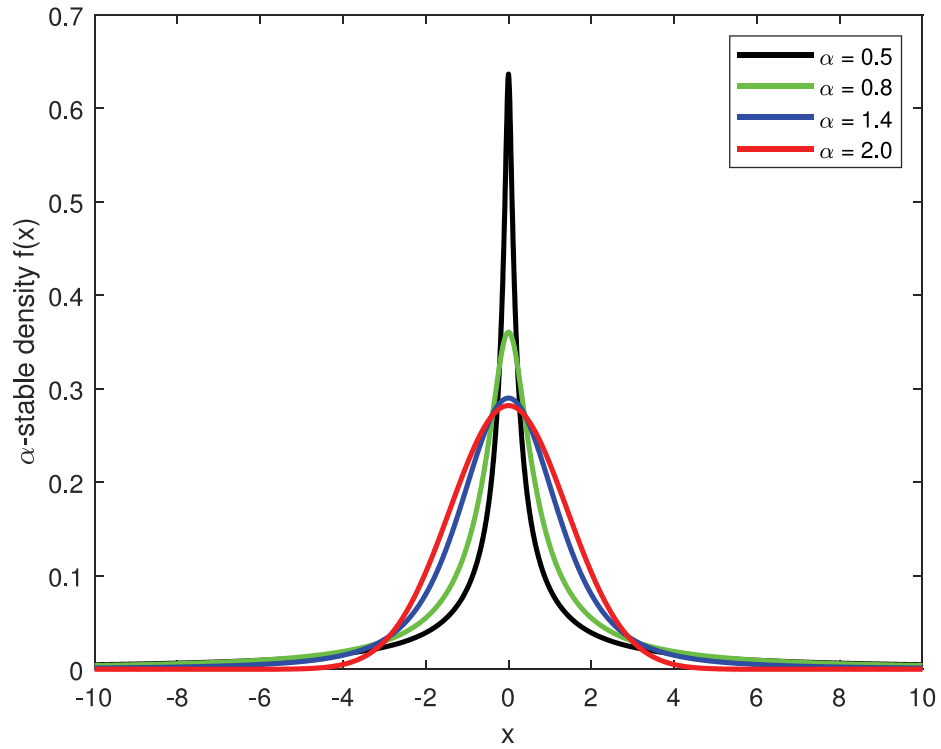


Figure 2.2.  $\alpha$ -stable density in the case of  $\alpha \in \{2.0, 1.4, 0.8, 0.5\}$ ,  $\beta = 0$ ,  $\sigma = 1$ ,  $\mu = 0$ .

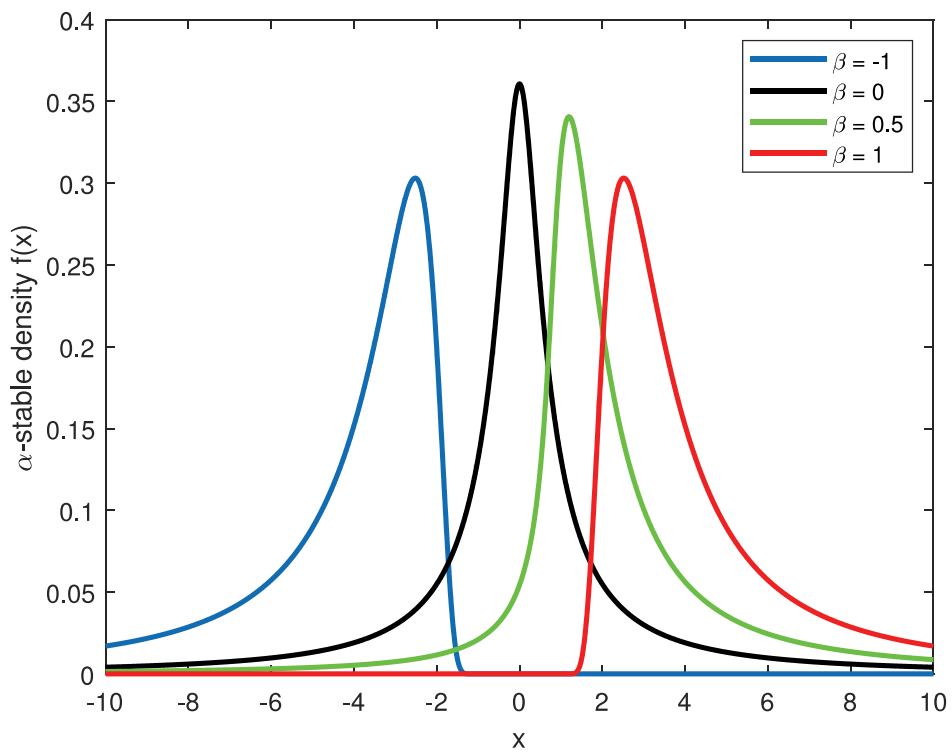


Figure 2.3.  $\alpha$ -stable density in the case of  $\alpha = 0.8$ ,  $\beta \in \{-1.0, 0, 0.5, 1.0\}$ ,  $\sigma = 1$ ,  $\mu = 0$ .

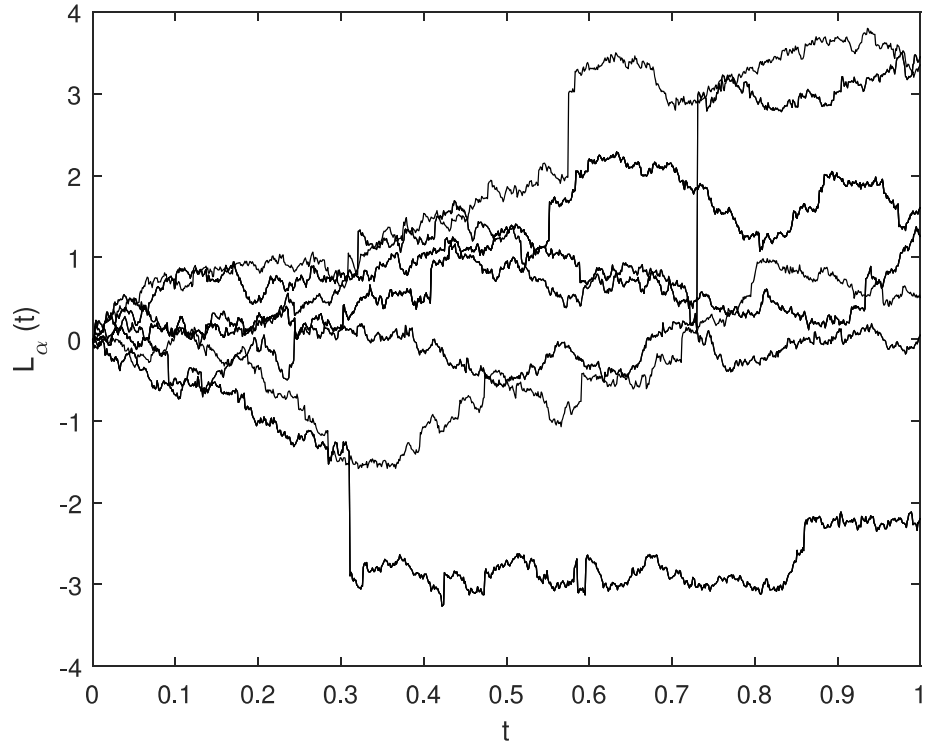


Figure 2.4. Trajectories of  $\alpha$ -stable Lévy motion in the case of  $\alpha = 1.7$  and  $\beta = 0$ ,  $\sigma = 1$ ,  $\mu = 0$ .

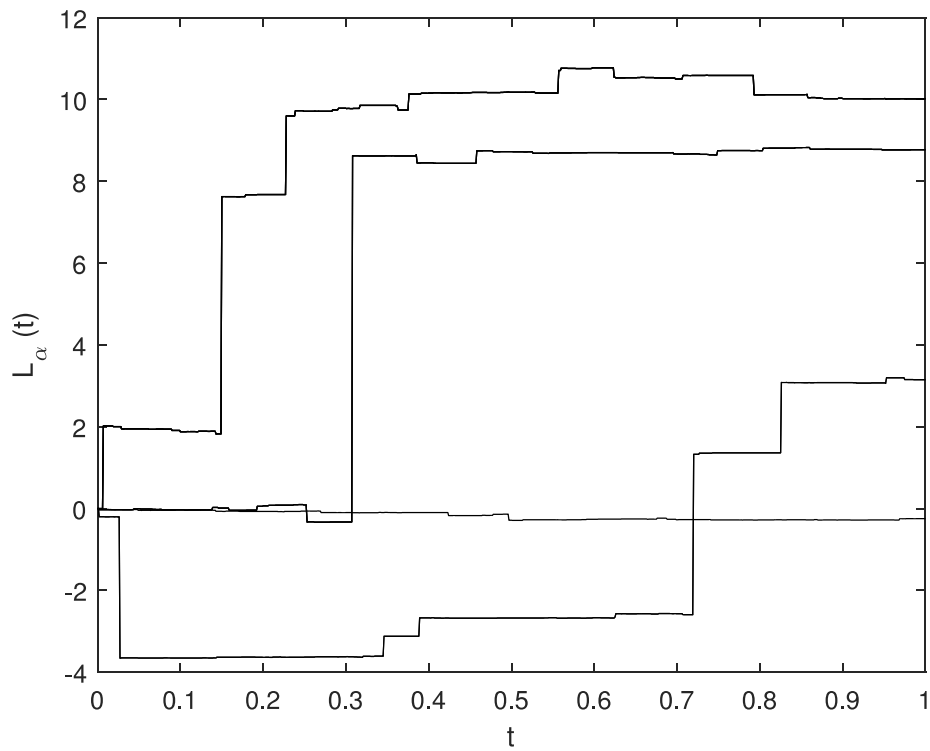


Figure 2.5. Trajectories of  $\alpha$ -stable Lévy motion in the case of  $\alpha = 0.7$  and  $\beta = 0$ ,  $\sigma = 1$ ,  $\mu = 0$ .

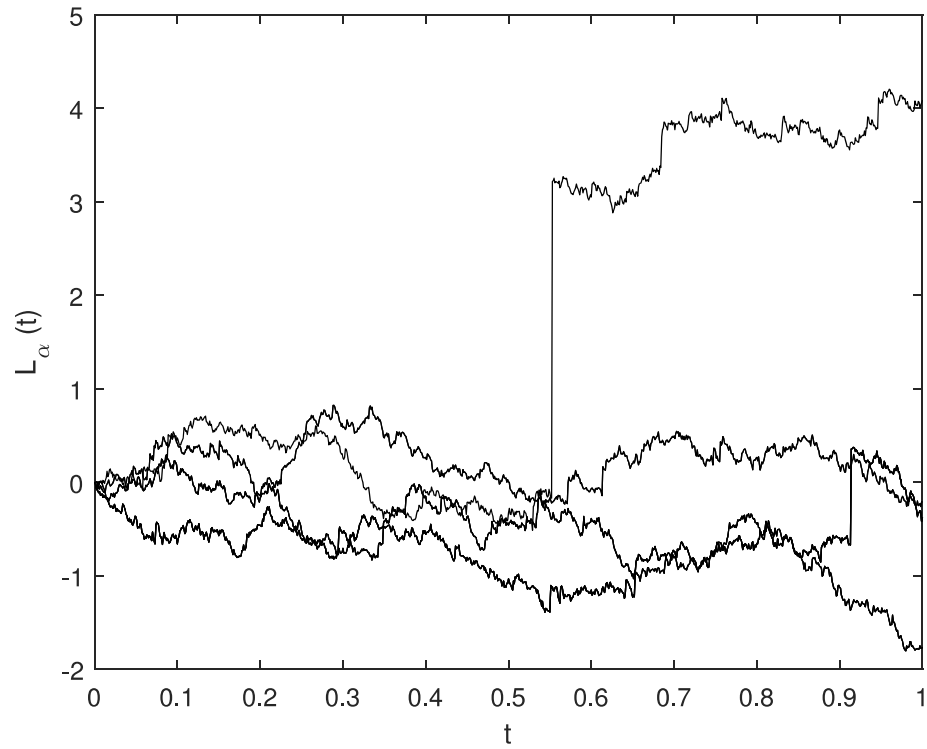


Figure 2.6. Trajectories of  $\alpha$ -stable Lévy motion in the case of  $\alpha = 1.8$  and  $\beta = 1$ ,  $\sigma = 1$ ,  $\mu = 0$ .

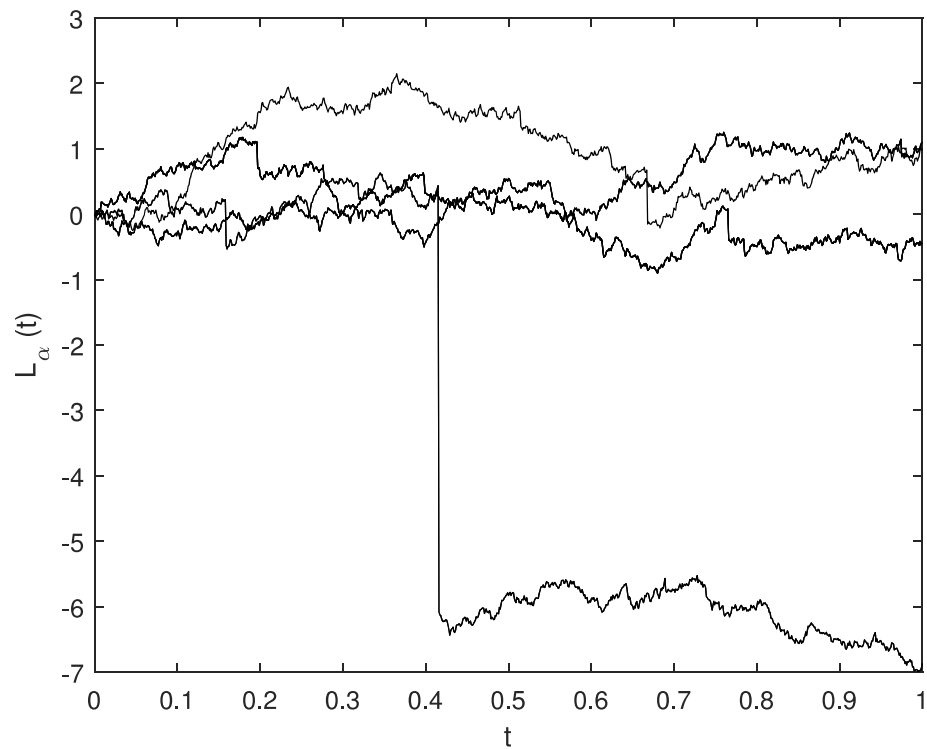


Figure 2.7. Trajectories of  $\alpha$ -stable Lévy motion in the case of  $\alpha = 1.9$  and  $\beta = -1$ ,  $\sigma = 1$ ,  $\mu = 0$ .

**Remark :**

The Lévy processes include random motions whose sample paths are right-continuous with left limits (*cádlág* function) and have countable random jump discontinuities occurring at random times on a finite time interval. Therefore, the Lévy processes include Brownian processes and the Poisson processes (to represent the large and small jumps) (Applebaum, 2009). The Gaussian noise  $W(t) = \frac{dB}{dt}$  is the formal derivative of Wiener process (Brownian motion)  $B(t)$  (Applebaum, 2009) and the increments of the Wiener process " $dB(t)$ " is the special case of  $\alpha$ -stable Lévy motion with  $\alpha = 2$ ,  $\beta = 0$  " i.e.,  $S_2(\gamma, 0, \mu) = N(\mu, 2\gamma^2)$  " Normal (Gaussian) distribution with mean  $\mu$  and variance  $2\gamma^2$  (Samorodnitsky and Taqqu, 1994).

## 2.4. Stochastic Stability

Stochastic modeling plays an important role in the presence of significant uncertainty in the systems. The stability theory of stochastic differential equations has become a very popular research in applications from various fields such as engineering, economic systems and biological systems. The stability phenomenon is essentially a problem of convergence and in this subsection four modes of convergence have been defined and then based on the mean square convergence which deal with second-order stochastic variables and stochastic processes have been explained.

A stochastic process  $X(t)$ ,  $t \in T$  is called a second-order stochastic process, if, the random variables  $X(t_1), X(t_2), \dots, X(t_n)$  are elements of  $L_2$ -space for every set  $t_1, t_2, \dots, t_n$ .

$L_2$ -space represents the linear vector space of the random variables whose second moments are finite with the inner product, the norm and the distance defined in (Soong, 1973) as follows: Let  $X_1$  and  $X_2$  are second-order random variables.

1. The inner product is defined by

$$E \{X_1, X_2\} = \langle X_1, X_2 \rangle . \quad (2.27)$$

2. The norm is defined by

$$\|X\| = \langle X, X \rangle^{1/2} . \quad (2.28)$$

3. The distance between  $X_1$  and  $X_2$  is defined by

$$d(X_1, X_2) = \|X_1 - X_2\| . \quad (2.29)$$



A second-order stochastic process  $X(t)$  is characterized by

$$\|X(t)\|^2 = E \{X^2(t)\} < \infty, \quad t \in T. \quad (2.30)$$

Four modes of convergence of stochastic processes defined in (Soong, 1973) have been given as follows:

**Definition 2.2** A sequence of random variable's  $X_n$  converges in mean square to a random variable  $X$  as  $n \rightarrow \infty$  if

$$\lim_{n \rightarrow \infty} \|X_n - X\| = 0 \quad (2.31)$$

**Definition 2.3** A sequence of random variable  $X_n$  converges in probability to a random variable  $X$  as  $n \rightarrow \infty$  if

$$\lim_{n \rightarrow \infty} P \{|X_n - X| > \epsilon\} = 0 \quad (2.32)$$

for every  $\epsilon > 0$ .

**Definition 2.4** A sequence of random variable  $X_n$  is said to converge almost surely to a random variable  $X$  as  $n \rightarrow \infty$  if

$$P \left\{ \lim_{n \rightarrow \infty} X_n = X \right\} = 1. \quad (2.33)$$

**Definition 2.5** A sequence of random variable  $X_n$  converges in distribution to a random variable  $X$  as  $n \rightarrow \infty$  if their associated distribution

$$\lim_{n \rightarrow \infty} F_{X_n}(x) = F_X(x) \quad (2.34)$$

at every continuity point of  $F_{X_n}(x)$ .

The relationships of four mode convergence can be listed as below:

1. Convergence in mean square implies convergence in probability.
2. Convergence almost surely implies convergence in probability.
3. Convergence in probability implies convergence in distribution.

There have been various methods to study the stability of the solutions of differential equations. The stochastic stability concepts which are based upon convergence in mean square criterion have been considered in the sequel.

### 2.4.1. Moment Stabilities

Let us consider a system of random differential equations whose explicit solution process is represented by  $\mathbf{X}(t)$ . The stability in the mean and stability in the mean square sense have been defined in (Soong, 1973) as follows:

**Definition 2.6** *The system is said to be stable in the mean if*

$$\lim_{t \rightarrow \infty} E|\mathbf{X}(t)| < \mathbf{c} \quad (2.35)$$

where  $\mathbf{c}$  is a finite constant vector.

**Definition 2.7** *The system is asymptotically stable in the mean if*

$$\lim_{t \rightarrow \infty} E|\mathbf{X}(t)| \rightarrow \mathbf{0} \quad (2.36)$$

**Definition 2.8** *The system is said to be mean square stable if*

$$\lim_{t \rightarrow \infty} E|\mathbf{X}(t)\mathbf{X}^T(t)| < \mathbf{C} \quad (2.37)$$

where  $\mathbf{C}$  is a constant square matrix with finite elements.

**Definition 2.9** *The system is asymptotically mean square stable if*

$$\lim_{t \rightarrow \infty} E|\mathbf{X}(t)\mathbf{X}^T(t)| \rightarrow \mathbf{0} \quad (2.38)$$

where  $\mathbf{0}$  is the null matrix.

### 2.4.2. Lyapunov Stability

The stability of stochastic systems in the Lyapunov sense have been developed by (Bertram and Sarachik, 1959) and (Kushner, 1965) with the motivation of the Lyapunov's direct method for the deterministic systems.

The stochastic stability in the Lyapunov sense can be obtained as follows:

**Theorem 2.2** *If there exists a Lyapunov function  $V(\mathbf{X},t)$  defined over the state space which satisfies*

- $V(\mathbf{X},t)$  is continuous in both  $\mathbf{X}$  and  $t$  and its first partial derivatives in these variables exist;

- $V(\mathbf{0}, t) = 0$  and  $V(\mathbf{X}, t) \geq \alpha \|\mathbf{X}\|$  for some  $\alpha > 0$ ;
- $E \{V(\dot{\mathbf{X}}, t)\} \leq 0$

*then the solution of random differential equations  $\mathbf{X}(t)$  is stable in the norm.*

# CHAPTER 3

## CONTROL OF STOCHASTIC NONLINEAR DYNAMICAL SYSTEMS

This chapter focuses on the fundamentals of stochastic control systems for both linear and nonlinear dynamical systems subject to random perturbations. The control of stochastic linear systems have been developed by (Kushner, 1967; Astrom, 1971) using the minimal variance control. In (Kushner, 1967; Astrom, 1971) the optimal control has been also generalized as a variational problem and a control law which minimizes the defined criterion for a given system has been found. In (Skelton et al., 1997) for linear systems a theory has been introduced to design the feedback controller which achieves a specified response covariance. In (Chung and Chang, 1994) by the techniques of stochastic linearization, the nonlinear stochastic system have been linearized and the moment control methods have been applied for the approximated linear system. Stochastic nonlinear systems driven by noise with unknown variance have been stabilized in (Deng and Krstic, 1999) in which the states and tracking error converge to a neighborhood of the origin. In (Sun, 2006) the moments of the nonlinear stochastic system have been controlled by obtaining the probability density function (pdf) of the response. A feedback regulator to minimize the dispersions of the states near the equilibrium has been developed in (Bashkirtseva et al., 2017) based on a quadratic approximation of the quasi-potential proposed in (Mil'Shtein and Ryashko, 1995).

In this chapter, the control of stochastic nonlinear systems in the presence of Wiener-type fluctuations have been explained using the covariance control and the work given in (Ryashko and Bashkirtseva, 2008; Bashkirtseva et al., 2017) based on the stochastic sensitivity analysis subject to Wiener process.

### 3.1. Covariance Control

Controlling the covariance for linear systems subject to Gaussian white noise perturbations which has been presented in (Sun, 2006) is summarized as:

A linear time invariant system is given by

$$\dot{\mathbf{X}} = \mathbf{F}\mathbf{X}(t) + \mathbf{A}\mathbf{U}(t) + \mathbf{G}\mathbf{B}(t) \quad (3.1)$$

where  $\mathbf{X}(t) \in R^n$ ,  $\mathbf{U}(t) \in R^m$  and  $\mathbf{B}(t) \in R^p$ ,  $\mathbf{A}$ ,  $\mathbf{F}$  and  $\mathbf{G}$  are matrices with proper dimensions and the vector of Gaussian white noise process  $\mathbf{B}(t)$  satisfies

$$\begin{aligned} E[\mathbf{B}(t)] &= 0 \\ E[\mathbf{B}(t)\mathbf{B}^T(t+\tau)] &= \sigma_{\mathbf{B}}^2 \delta(\tau) \end{aligned} \quad (3.2)$$

where the positive definite matrix  $\sigma_{\mathbf{B}}^2 \in R^{p \times p}$ .

A full state feedback have been considered as:

$$\mathbf{U}(t) = -\mathbf{K}_{CC}\mathbf{X}(t) \quad (3.3)$$

where  $\mathbf{K}_{CC}$  is the feedback gain matrix. Then (3.1) can be written as

$$\dot{\mathbf{X}} = (\mathbf{F} - \mathbf{A}\mathbf{K}_{CC})\mathbf{X}(t) + \mathbf{G}\mathbf{B}(t). \quad (3.4)$$

Applying Itó's lemma presented in Section (2.2.2), the covariance equation of the response  $\mathbf{X}(t)$  have been obtained as:

$$\frac{d}{dt}\mathbf{C}_{XX}(t) = (\mathbf{F} - \mathbf{K}_{CC}\mathbf{A})\mathbf{C}_{XX}(t) + \mathbf{C}_{XX}(t)(\mathbf{F} - \mathbf{K}_{CC}\mathbf{A})^T + \mathbf{G}\sigma_{\mathbf{B}}^2\mathbf{G}^T, \quad t > 0 \quad (3.5)$$

in which  $\mathbf{C}_{XX}$  is the covariance matrix and in the steady state as  $t \rightarrow \infty$ ,  $\dot{\mathbf{C}}_{XX}(\infty) = 0$ .

For this steady state response of  $\mathbf{X}(t)$  a reference covariance matrix  $\mathbf{C}_{r,XX}$  has been pre-specified such that  $\mathbf{C}_{XX}(\infty) = \mathbf{C}_{r,XX}$  then the following equation have been obtained to determine the gain matrix

$$(\mathbf{F} - \mathbf{K}_{CC}\mathbf{A})\mathbf{C}_{r,XX} + \mathbf{C}_{r,XX}(\mathbf{F} - \mathbf{K}_{CC}\mathbf{A})^T + \mathbf{G}\sigma_{\mathbf{B}}^2\mathbf{G}^T = 0. \quad (3.6)$$

**Theorem 3.1** *To guarantee the existence of the covariance control gain matrix  $\mathbf{K}_{CC}$  which satisfies (3.5),  $\mathbf{C}_{r,XX}$  must satisfy the following condition given in (Hotz and Skelton (1987); Skelton et al. (1997)):*

$$(\mathbf{I} - \mathbf{A}\mathbf{A}^\dagger)(\mathbf{F}\mathbf{C}_{r,XX} + \mathbf{C}_{r,XX}\mathbf{F}^T + \mathbf{G}\sigma_{\mathbf{B}}^2\mathbf{G}^T)(\mathbf{I} - \mathbf{A}\mathbf{A}^\dagger) = 0 \quad (3.7)$$

where  $\mathbf{A}^\dagger$  is the Moore-Penrose inverse of  $\mathbf{A}$ .

The set of all possible feedback gain matrices  $\mathbf{K}_{CC}$  is given by

$$\mathbf{K}_{CC} = \frac{1}{2} \mathbf{A}^\dagger \left( \mathbf{F} \mathbf{C}_{r,XX} + \mathbf{C}_{r,XX} \mathbf{F}^T + \mathbf{G} \sigma_B^2 \mathbf{G}^T \right) \left( 2\mathbf{I} - \mathbf{A} \mathbf{A}^\dagger \right) \mathbf{C}_{r,XX}^{-1} + \mathbf{A}^\dagger \mathbf{L} \mathbf{A} \mathbf{A}^\dagger \mathbf{C}_{r,XX}^{-1} + \left( \mathbf{I} - \mathbf{A} \mathbf{A}^\dagger \right) \mathbf{Z} \quad (3.8)$$

where arbitrary and real  $\mathbf{L} = -\mathbf{L}^T$  and  $\mathbf{Z}$  is an arbitrary real matrix.

The Moore-Penrose inverse, denoted by  $\mathbf{A}^\dagger$  is used to find the inverse of a rank deficient matrix. If the matrix  $\mathbf{A} \in \mathbb{C}^{m \times n}$  is not full rank, i.e.,  $\text{rank}(\mathbf{A}) = r < \min(m, n)$  then the Moore-Penrose inverse  $\mathbf{A}^\dagger = \mathbf{A}^T (\mathbf{A} \mathbf{A}^T)^{-1}$  for  $m < n$ .

Since the reference covariance matrix cannot be specified arbitrarily for a given system the pair of the reference covariance matrix  $\mathbf{C}_{r,XX}$  and the feedback gain matrix  $\mathbf{K}_{CC}$  can be found with the iterative procedure given in (Skelton et al., 1997).

When the system is nonlinear, the moments associated with the solution processes of nonlinear differential equations of the Itó type can be established with the help of the Fokker Planck equation (Soong, 1973).

The stochastic nonlinear dynamic system has been given in the form of Itó equation as in (Sun, 2006):

$$d\mathbf{X}(t) = \mathbf{F}(\mathbf{X}(t), t) dt + \mathbf{G}(\mathbf{X}(t), t) d\mathbf{B}(t), \quad t \geq t_0 \quad (3.9)$$

where the solution process  $\mathbf{X}(t) \in R^n$ , the matrix function  $\mathbf{G}(\mathbf{X}(t), t) \in R^{n \times m}$ , and the Wiener process  $\mathbf{B}(t) \in R^m$  with

$$\begin{aligned} E [d\mathbf{B}(t)] &= 0 \\ E [d\mathbf{B}(t) d\mathbf{B}^T(t + \tau)] &= 2D_{ij} \delta(\tau) \quad i, j = 1, 2, \dots, m. \end{aligned} \quad (3.10)$$

The corresponding Fokker-Planck equation for (3.9) is given as:

$$\frac{\partial F(\mathbf{X}, t | \mathbf{X}_0, t_0)}{\partial t} = - \sum_{j=1}^n \frac{\partial}{\partial X_j} \left[ F_j(\mathbf{X}, t) F + \sum_{i,j=1}^n \frac{\partial^2}{\partial x_i \partial x_j} [(\mathbf{G} \mathbf{D} \mathbf{G}^T)_{ij} F] \right] \quad (3.11)$$

where  $\mathbf{D} \in R^{m \times m}$  denotes the matrix  $\{D_{ij}\}$ .

By using the Fokker-Planck equation (3.11) and letting  $h(\mathbf{X}, t) = X_1^{k_1}(t)X_2^{k_2}(t) \cdots X_n^{k_n}(t)$  the moments equations for  $h(\mathbf{X}, t)$  have been obtained as:

$$\frac{d}{dt}E\{h(\mathbf{X}, t)\} = \sum_{j=1}^n E\left\{F_j \frac{\partial h}{\partial X_j}\right\} + \sum_{i,j=1}^n E\left\{\left(GDG^T\right)_{ij} \frac{\partial^2 h}{\partial X_i \partial X_j}\right\} + E\left\{\frac{\partial h}{\partial t}\right\} \quad (3.12)$$

**Example 3.1** The moment equations  $h(X, t) = X^k$  associated with a simple first-order nonlinear Itó equation having  $F = -X + aX^3$  and  $G = 1$  is given as

$$\dot{m}_k(t) = -k(m_k + a m_{k+2}) + Dk(k-1)m_{k-2} \quad (3.13)$$

where

$$m_k(t) = E\{X^k(t)\}, \quad k = 1, 2, \dots \quad (3.14)$$

It is seen from (3.13) that since the moment equations are coupled and contain of orders higher than  $k$ , to specify the solutions of the infinite hierarchy of moment differential equations becomes a difficult task.

However when the exact stationary pdf of the solution is obtainable then the generalized covariance control for nonlinear systems has been designed using the pdf proposed in (Sun, 2006).

A nonlinear stochastic system is given as:

$$\ddot{X} + h(X, \dot{X}) = U(t) + g(X, \dot{X})B(t) \quad (3.15)$$

where  $h$  and  $g$  are nonlinear functions and  $U = f(X_1, X_2; K_j)$  is a nonlinear feedback control with the control gains  $K_j$ , and the Gaussian white noise  $B(t)$  has zero mean.

A quadratic cost function as a performance measure have been defined as:

$$J = \hat{J} + \beta E[U^2] \quad (3.16)$$

where the moment tracking performance  $\hat{J}$  is as:

$$\hat{J} = \sum_{j,k=0} b_{jk}(m_{jk}^r - m_{jk})^2 \quad (3.17)$$

and the target values for the  $j$ th order moments  $m_{jk}$  are represented by  $m_{jk}^r$ .

The moments of the state variables are given as:

$$m_{jk} = E [X_1^j X_2^k] = \int_{-\infty}^{\infty} \int_{-\infty}^{\infty} x_1^j x_2^k p_{\mathbf{X}}(x_1, x_2) dx_1 dx_2 \quad (3.18)$$

where  $j, k = 0, 1, 2, \dots$ .

To determine the optimal control gains the cost function  $J$  has been minimized with respect to  $K_j$  such that

$$\frac{\partial J}{\partial K_j} = 0, \quad \forall j. \quad (3.19)$$

It is important to remark that for the control design in nonlinear systems using (3.19), the exact stationary pdf  $p_{\mathbf{X}}(x_1, x_2)$  of the response is required. However for nonlinear systems the exact pdf is generally unknown and an alternative procedure was developed in (Wojtkiewicz and Bergman, 2001) to approximate the pdf of the system response by using the maximum entropy principle.

Consider the Itô differential equation

$$dX_j(t) = F_j(\mathbf{X}, t)dt + \sum_{k=1}^m \sigma_{jk}(\mathbf{X}, t)dB_k(t) \quad (3.20)$$

where  $X_j(t)$  is the  $n$ -th dimensional vector stochastic process.

A  $q$ -th order polynomial of the state variables have been defined as

$$H(\mathbf{X}) = \prod_{k=1}^n X_k^{q_k} \quad (3.21)$$

where  $q = \sum_{k=1}^n q_k$  and by applying Itô's lemma given in Section 2.2.2, the  $q$ -th order moment equations of the system can be generated as:

$$\frac{dE [F(\mathbf{X})]}{dt} = E \left[ \sum_{j=1}^n m_j \frac{\partial F(\mathbf{X})}{\partial X_j} + \frac{1}{2} \sum_{j=1}^n \sum_{k=1}^n b_{jk} \frac{\partial^2 F(\mathbf{X})}{\partial X_j \partial X_k} \right] \quad (3.22)$$

where  $b_{jk} = \sum_{l=1}^m \sigma_{jl} \sigma_{kl}$ .



The response of moments up to the qth order probability density function have been constructed as

$$p_{\mathbf{X}}(\mathbf{x}) = \left[ \lambda_0 - \sum_{k=1}^n \lambda_k x_k - \sum_{j,k=1}^n \lambda_{jk} x_j x_k - \cdots - \sum_{q_1, q_2, \dots, q_n=1}^n \lambda_{q_1 q_2 \dots q_n} x_1^{q_1} x_2^{q_2} \cdots x_n^{q_n} \right] \quad (3.23)$$

The coefficients of  $\lambda$  should be chosen such that the entropy in (Sun, 2006):

$$H = E[-\ln p_{\mathbf{X}}(\mathbf{x})] = - \int_{R^n} p_{\mathbf{X}}(\mathbf{x}) \ln p_{\mathbf{X}}(\mathbf{x}) d\mathbf{x} \quad (3.24)$$

is maximized subject to the constraint

$$\int_{R^n} p_{\mathbf{X}}(\mathbf{x}) d\mathbf{x} = 1 . \quad (3.25)$$

Since maximum entropy principle requires the polynomial nonlinear terms and a set of implicit closed nonlinear functions of moments to determine the approximate probability density function then an alternative asymptotics approach can be applied to construct approximate probability density function.

### **3.2. Stochastic Sensitivity Analysis for the Nonlinear Dynamical System Perturbed by Wiener Process**

The analysis and control by using Fokker-Planck-Kolmogorov equation is difficult even for two-dimensional stochastic systems, therefore the alternative asymptotics approaches such as quasi-potential have been developed in (Fredlin and Wentzell, 1984) and by solving the corresponding Hamilton-Jacobi equation, the quasi-potential which provides the minimum action related to the steady-state probability distribution can be obtained. Since this is still a difficult task, a quadratic approximation of the quasi-potential have been proposed in (Mil'Shtein and Ryashko, 1995) for the stability analysis.

The approximation of the quasi-potential in stability problems have been summarized as follows:

Consider the Itô SDE

$$dX = F(X)dt + \epsilon G(X)dB(t) \quad (3.26)$$

where  $X \in R^n$ ,  $B(t) \in R^m$  is Wiener process,  $\epsilon$  is the intensity of noise and  $F(X) \in R^n$  and  $G(X) \in R^{n \times m}$  are sufficiently smooth functions .

In the absence of noise ( $\epsilon = 0$ ), (3.26) is assumed to have the stationary point  $X^*$  (i.e.,  $F(X^*) = 0$ ) and the matrix  $S(X) = G(X)G(X)^T$  is positive definite.

The stationary pdf  $p_X(\mathbf{x})$  of (3.26) satisfies the following Fokker-Planck-Kolmogorov equation

$$\sum_{i=1}^n \frac{\partial}{\partial x_i} [F_i p_X] + \frac{\epsilon^2}{2} \sum_{i=1}^n \sum_{j=1}^n b_{ij} \frac{\partial^2 p_X}{\partial x_j \partial x_k} = 0 \quad (3.27)$$

where  $b_{ij} = [GG^T]_{ij}$ .

Since it is a difficult task to obtain the solution of (3.27) even for 2-dimensional case, the asymptotics for the stationary probability density of the state  $X$ ,  $\phi(X)$  called as quasi-potential are used.

The quasi-potential  $\phi(X)$  can be considered as a variational problem of the minimization of the action functional and  $\phi(X)$  is obtained by solving the Hamilton-Jacobi equation given as follows:

$$\left\langle F(X), \frac{\partial \phi}{\partial X} \right\rangle + \frac{1}{2} \left\langle \frac{\partial \phi}{\partial X}, S(X) \frac{\partial \phi}{\partial X} \right\rangle = 0 \quad (3.28)$$

where the notation  $\langle , \rangle$  represents the inner product and

$$\phi(X^*) = 0, \quad \phi(X) \geq 0. \quad (3.29)$$

The first approximation of the quasi-potential in a neighborhood of the stationary point in (Mil'Shtein and Ryashko (1995)) is written as:

$$\phi(X) = \phi(X^*) + \left\langle (X - X^*), \frac{\partial \phi}{\partial X}(X^*) \right\rangle + \frac{1}{2} \left\langle (X - X^*), \frac{\partial^2 \phi}{\partial X^2}(X^*)(X - X^*) \right\rangle + \mathcal{O}(|X - X^*|^3). \quad (3.30)$$

Since  $\frac{\partial \phi}{\partial X}(X^*) = 0$  in (3.29) and by letting  $V = \frac{1}{2} \frac{\partial^2 \phi}{\partial X^2}(X^*)$  in (3.30) then the quasi-potential becomes in the form as follows:

$$\phi(X) = \phi_1(X) + O(|X - X^*|^3) \quad (3.31)$$

where the quadratic form  $\phi_1(X) = (X - X^*)^T V (X - X^*)$ .

Replacing the  $\phi(X)$  with the quadratic form of the quasi-potential  $\phi_1(X)$  in (3.28), the Hamilton-Jacobi equation can be rewritten as:

$$F^T V + V F + 2V S V = 0 \quad (3.32)$$

where

$$F = \left( \frac{\partial f_i}{\partial x_j}(X^*) \right)_{i,j=1}^n, \quad S = S(X^*) = G(X^*) G^T(X^*) \quad (3.33)$$

and

$$V = \frac{1}{2} \frac{\partial^2 \phi}{\partial x^2}(X^*). \quad (3.34)$$

The matrix  $W = V^{-1}$  corresponds to the stochastic sensitivity matrix which is a unique solution of the Lyapunov's equation

$$F W + W F^T + 2S = 0 \quad (3.35)$$

Based on this quadratic approximation, a feedback regulator to minimize the dispersions of the states near the equilibrium has been developed in (Bashkirtseva et al., 2017).

The control of nonlinear systems by using the stochastic sensitivity analysis has been summarized below :

A nonlinear controlled stochastic system is given as:

$$\dot{X} = f(X) + h(X)U + \epsilon g(X)\xi(t) \quad (3.36)$$

where  $X, f(X) \in R^n$ ,  $h(X) \in R^{n \times l}$ ,  $g(X) \in R^{n \times m}$ -matrix function denotes the dependence of disturbances on the states,  $\xi(t) \in R^m$  is white Gaussian noise,  $\epsilon$  is the noise intensity and the control input  $U \in R^l$  is designed by the feedback regulator with noisy observations  $Y \in R^n$

:

$$\begin{aligned} U &= K(Y - \bar{X}) \\ Y(t) &= X(t) + \epsilon\varphi(X(t))\eta(t) \end{aligned} \quad (3.37)$$

where the equilibrium  $\bar{X}$  satisfies  $F(\bar{X}) = 0$  and the feedback matrix  $K$  is  $(l \times n)$ -constant matrix,  $\varphi(X)$  is the  $n \times m$ -matrix function corresponding to the dependence of disturbances on the states and  $\eta(t) \in R^m$  is white Gaussian noise which is uncorrelated  $\xi(t)$  and satisfies  $E(\eta(t)) = 0$ ,  $E(\eta(t)\eta^T(\tau)) = \delta(t - \tau)I$  with the identity matrix  $I$ .

Let  $X^\epsilon(t)$  be a solution of the system (3.36) and the variable

$$Z(t) = \lim_{\epsilon \rightarrow 0} \frac{X^\epsilon(t) - \bar{X}}{\epsilon} \quad (3.38)$$

characterizes the sensitivity of the equilibrium  $\bar{X}$  to random disturbances of the controlled closed-loop system (3.36) then the first-approximation system can be described by the following SDE as:

$$\dot{Z} = (F + BK)Z + BKR\eta + G\xi \quad (3.39)$$

where

$$F = \frac{\partial f}{\partial x}(\bar{X}), \quad B = h(\bar{X}), \quad R = \varphi(\bar{X}), \quad G = g(\bar{X}). \quad (3.40)$$

Equation (3.39) can be rewritten in the Itô form as:

$$dZ = (F + BK)Zdt + BKRdW_1 + GdW_2 \quad (3.41)$$

where uncorrelated  $W_1(t)$  and  $W_2(t)$  are  $m$ -dimensional Wiener processes with  $dW_1 = \eta(t)dt$  and  $dW_2 = \xi(t)dt$ .

By applying the Itô's rule the dynamics of the second moment  $V(t) = cov(Z(t), Z(t))$  has been obtained as

$$\dot{V} = (F + BK)V + V(F + BK)^T + BK\Phi^T K^T B^T + S \quad (3.42)$$

in which it has a unique stationary solution  $W$  satisfying the following matrix equation

$$(F + BK)W + W(F + BK)^T + BK\Phi^T K^T B^T + S = 0 \quad (3.43)$$

where  $\Phi = RR^T$ ,  $S = GG^T$  and  $W$  quantifies the deviation of the stochastic response of the nonlinear system from the equilibrium which is called as stochastic sensitivity matrix of the equilibrium of system in (Bashkirtseva et al., 2017).

**Theorem 3.2** : For an assigned positive definite stochastic sensitivity matrix  $W$  if there exist  $K$  such that the eigenvalues of the matrix  $(F + BK)$  lie in the left half of the complex plane then an assigned  $W$  is called attainable matrix and satisfies the following conditions in (Bashkirtseva et al., 2017):

$$P_2(FW + WF^T + S)P_2 = 0 \quad (3.44)$$

$$W\Phi^{-1}W - FW - WF^T - S \geq 0 \quad (3.45)$$

where the projective matrix  $P_2 = I - BB^+$ , the superscript “+” denotes the pseudoinversion and  $\geq$  refers to the positive semi-definiteness.

Under these conditions  $W$  is a unique solution of (3.43) and the explicit expression of the feedback coefficient matrix  $K$  can be found in terms of  $W, F, B, \Phi, S$  as:

- (i) If  $\text{rank}(B) = \text{rank}(R) = \text{rank}(G)$ , then for any attainable matrix  $W$  then (3.43) has a solution

$$K = B^{-1} \left( Q^{\frac{1}{2}} H \Phi^{-\frac{1}{2}} - W \Phi^{-1} \right) \quad (3.46)$$

where  $H \in R^{m \times n}$  is an arbitrary orthogonal matrix.

- (i) If  $\text{rank}(B) < \text{rank}(R) = \text{rank}(G)$  then the matrix  $W$  satisfies the following equation

$$P_2 \left( Q^{\frac{1}{2}} H \Phi^{-\frac{1}{2}} - W \Phi^{-1} \right) = 0 \quad (3.47)$$

and then (3.43) has a solution

$$K = B^+ \left( Q^{\frac{1}{2}} H \Phi^{-\frac{1}{2}} - W \Phi^{-1} \right). \quad (3.48)$$

The minimization of the dispersions of the states can be considered as the minimization of the quantitative cost measure  $J(W) = \langle W, Q \rangle$  where  $Q \in R^{n \times n}$  is a positive-definite symmetric matrix and with the constraint of matrix equation given in (3.43), then the Lagrange function  $L(W, K, \Lambda)$  with Lagrange multiplier  $\Lambda \in R^{n \times m}$  is given as:

$$L(W, K, \Lambda) = \langle W, Q \rangle + \langle \Lambda, \mathfrak{J}(W, K) \rangle \quad (3.49)$$

where

$$\mathfrak{J}(W, K) = (F + BK)W + W(F + BK)^T + BK\Phi^T K^T B^T + S. \quad (3.50)$$

The approach of stochastic sensitivity analysis explained in Section (3.2) has provided us to develop the control rule for the rotor angle stability in stochastic SMIB system in the Chapter 5.

## CHAPTER 4

# STABILITY ANALYSIS OF STOCHASTIC SINGLE MACHINE INFINITE BUS POWER SYSTEM

Due to the considerable amounts of power production from high-variable sources such as wind turbines and solar cells and the variable electricity consumptions have made synchronism more important (Dobson, 2013). Some major blackouts occurring such as in the Turkish power system (TEIAS and ENTSO-E, 2015) and in the Italian power system (Corsi and Sabelli, 2004) have been triggered by the tripping of a line which results in the loss of angular stability and hence a loss of synchronism. By the integration of renewable energy sources into the power systems, the rotor angle stability to maintain the synchronism of the interconnected generators would be more severe problem to accomplish. The single machine infinite bus (SMIB) power system is convenient and practical for the understanding of stability analysis.

In (Canizares, 1995) the load level has been considered as a bifurcation parameter and it has been observed that a small perturbation in the load beyond the bifurcation value cause a loss of synchronism of the generator with respect to the infinite bus. The dynamic characteristics for the SMIB system under periodic load disturbance have been studied in (Wang et al., 2015). The SMIB power system with a synchronous generator has been modeled by a third-order differential equation in (Ma et al., 2016) and the responses of rotor angle and rotor speed have been investigated with the change of mechanical power and damping factor which have been considered as the bifurcation parameters.

Besides the deterministic models given in (Canizares, 1995; Wang et al., 2015; Ma et al., 2016), the stochastic models for the disturbances exist in the literature as: In (De Marco and Bergen, 1987) the variations in reactive load power fluctuations have been modeled by Wiener process and a security measure has been proposed to indicate the voltage collapse in power systems. The power fluctuations have been modeled by Gaussian white noise in (Wei and Luo, 2009) and the stability for such a stochastic SMIB (SSMIB) power system have been investigated. In (Lu et al., 2015) the effects of stochastic excitations in SMIB system have been studied by the p-moment stability of rotor angle. In (Shi et al., 2018) the wind power and the load uncertainty in SMIB power system have been modeled by Wiener processes and an analytical method has been proposed to estimate the probability of transient stability under stochastic disturbances.

In these former studies the stochastic fluctuations in electrical power systems either at the loads or at the excitations have been considered as Brownian motion (Wiener process). In (Yılmaz and Savacı, 2017a,b) it has been proposed that the stochastic disturbances occurring in power systems could be more realistically modeled by alpha-stable ( $\alpha$ -stable) Lévy process compared to the modeling by Wiener process. The main motivation for our assumption is that in (Weron, 2007) the stochastic model of the electricity price has been proposed as  $\alpha$ -stable Lévy process and in (Kruczek et al., 2017) the electricity market data have been modeled by using the  $\alpha$ -stable periodic autoregressive model. Since the load has been considered as one of the main factors in determining electricity prices because the sudden demand or supply changes cause sharp spikes in electricity prices then these  $\alpha$ -stable Lévy type fluctuations have been characterized by non-Gaussian, heavy-tailed behavior defined by stable law (Samorodnitsky and Taqqu, 1994).

In the first stage of this chapter, the stochastic fluctuations in SMIB power systems have been modeled as Wiener and  $\alpha$ -stable Lévy processes, respectively and the effect of such fluctuations on the rotor angle stability have been investigated for various parameters of characteristic exponent  $\alpha$  and skewness  $\beta$ . In the second stage of this chapter, the basin stability of SMIB power systems with  $\alpha$ -stable Lévy type fluctuations have been investigated over the parameter space of mechanical power and damping parameter. The probabilities of returning to the stable equilibrium point have been calculated for different characteristic exponent and skewness parameters of  $\alpha$ -stable Lévy type fluctuations to see the effect of impulsive and asymmetric load fluctuations.

#### 4.1. Deterministic Single Machine Infinite Bus Power Systems

The deterministic swing equations in (Kundur et al., 1994) which govern the rotational dynamics of the synchronous machine are given as

$$\begin{aligned}\dot{\delta} &= \omega \\ M\dot{\omega} &= -D\omega + P_m - P_e\end{aligned}\tag{4.1}$$

where  $\delta$  is the relative rotor angle of machine,  $\omega$  is the rotor speed with respect to the synchronous reference,  $P_m$  is the mechanical power,  $P_e$  is the electrical power,  $M$  and  $D$  are the inertia and the damping coefficients, respectively.

The electrical power output  $P_e = P_{max}\sin(\delta)$  in which the maximum output of the machine is  $P_{max} = E' E_B / X_T$  as given in (1.17) and (1.18), respectively.



As stated before  $E' \angle \delta$  is the internal voltage of machine and  $E_B \angle 0$  is the infinite bus voltage;  $X_E$  is the total reactance between the machine and infinite bus. The maximum real power that can be transferred to the infinite bus is fixed as  $P_{max} = 1$  per unit (p.u.) and by defining the state variable  $\begin{bmatrix} x_1 & x_2 \end{bmatrix}^T = \begin{bmatrix} \delta & \omega \end{bmatrix}^T$  then with unit inertia constant (4.1) becomes

$$\begin{aligned} \dot{x}_1 &= x_2, \\ \dot{x}_2 &= -Dx_2 + P_m - \sin(x_1). \end{aligned} \quad (4.2)$$

The equilibrium points of (4.2) satisfy  $x_2^* = 0$  and  $\sin(x_1^*) = P_m$ . By linearizing the state equations around the equilibrium points it can be easily seen that

$$\begin{bmatrix} x_1^* & x_2^* \end{bmatrix}^T = \begin{bmatrix} \delta^* & \omega^* \end{bmatrix}^T = \begin{bmatrix} \arcsin(P_m) & 0 \end{bmatrix}^T \quad (4.3)$$

corresponds to the stable equilibrium point (SEP) while

$$\begin{bmatrix} x_1^* & x_2^* \end{bmatrix}^T = \begin{bmatrix} \delta^* & \omega^* \end{bmatrix}^T = \begin{bmatrix} \pi - \arcsin(P_m) & 0 \end{bmatrix}^T \quad (4.4)$$

corresponds to the saddle point. The SEP is indicated by green circle and the saddle point is indicated by red circle in Figures 4.2- 4.4.

There are multiple equilibria in the state space, " $\delta - \omega$  plane" due to the  $2\pi$  periodicity of the relative rotor angle  $\delta$  while there is only one SEP and one saddle in the corresponding cylindrical state space " $[-\pi, \pi] \times R$ ".

The phase portraits of deterministic SMIB system shown in Figures 4.1 -4.4 have been obtained for the initial values of " $[-\pi, \pi] \times [-10, 10]$ " with different values of the mechanical power  $P_m$  and the damping parameter  $D$ .

It has been clearly seen from (4.4) that there are no fixed points if  $P_m > 1$  and all trajectories converge to the unique rotating orbit as shown Figure 4.1.

The mechanical power have been kept fixed and the phase portraits of deterministic SMIB have been obtained by varying the the value of damping parameter  $D$  relative to the critical damping level  $D_c$ . The critical damping level  $D_c$  which can be obtained by using Melnikov method given in (Guckenheimer and Holmes, 2013) has been defined as the value satisfying the equation of homoclinic bifurcation curve  $P_m = 4D_c/\pi$ . For  $P_m = 0.5$  the critical damping level  $D_c$  has been evaluated theoretically as 0.3927 and numerically as 0.414.

By selecting the value of the damping parameter  $D$  greater than the critical damping level  $D_c$ , it has been observed that the trajectories converge to the SEP as in Figure 4.2.

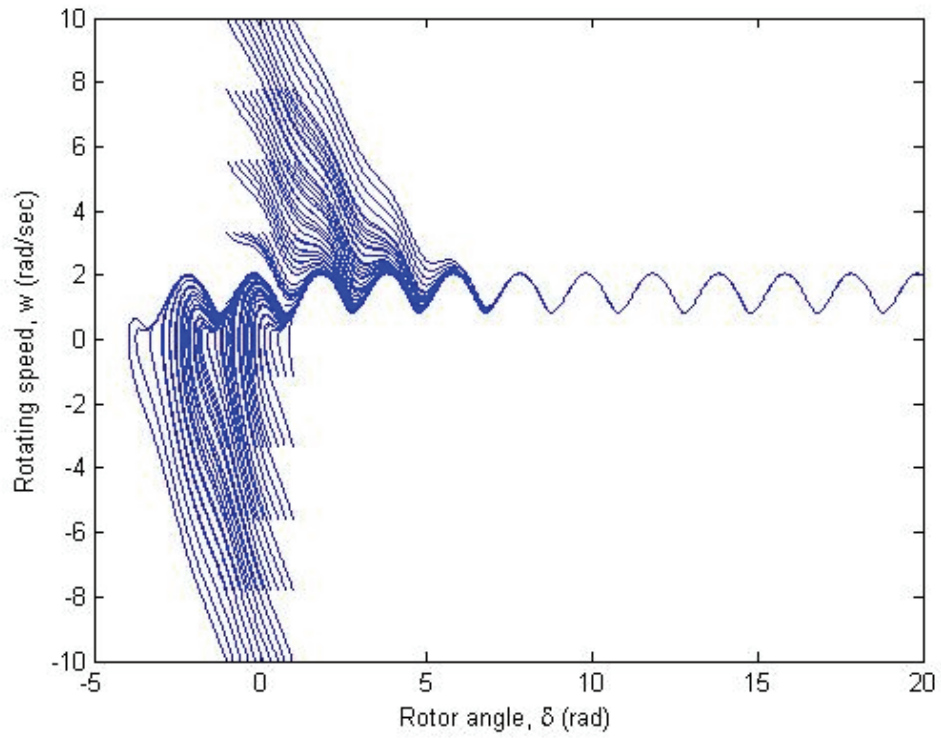


Figure 4.1. Phase portrait of deterministic SMIB system for  $P_m > 1$ .

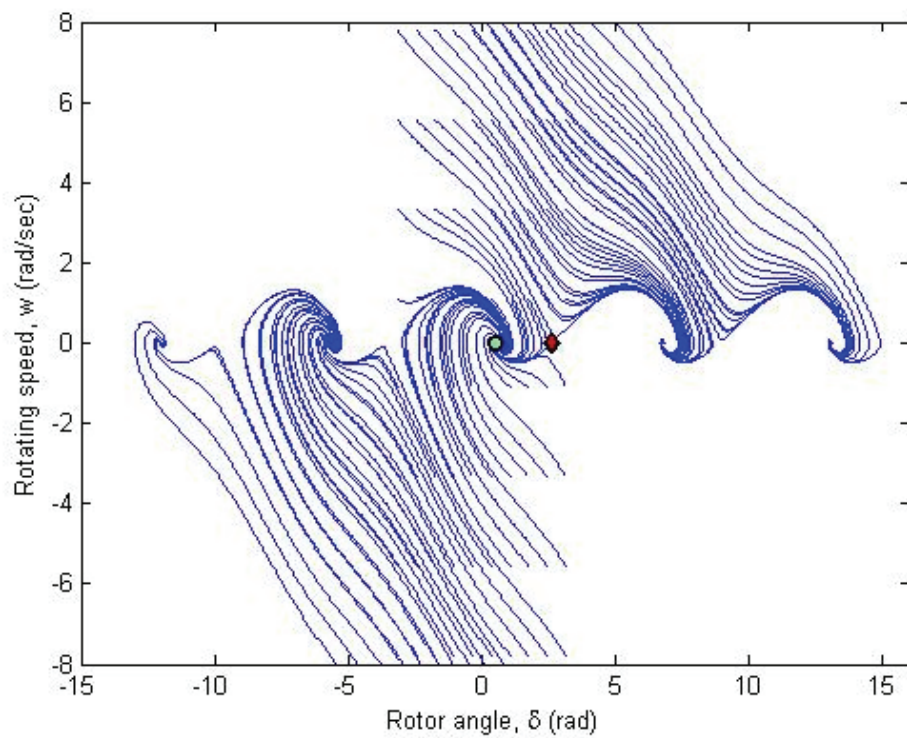


Figure 4.2. Phase portrait of deterministic SMIB system for  $D = 0.8 > D_c = 0.414$  and  $P_m = 0.5$ .

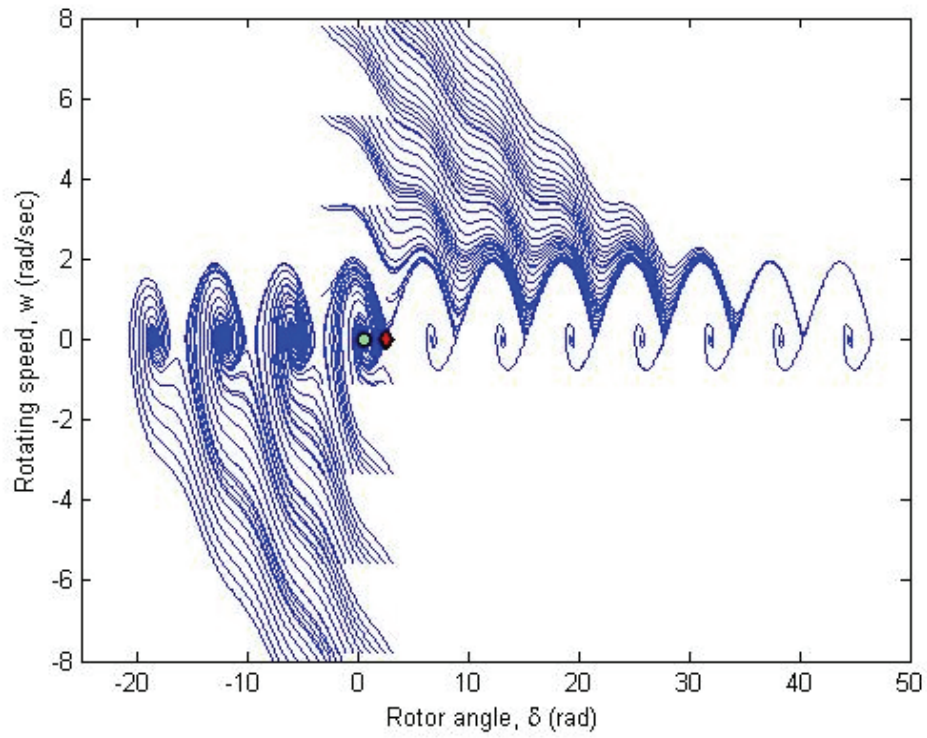


Figure 4.3. Phase portrait of deterministic SMIB system for  $D = D_c = 0.414$  and  $P_m = 0.5$ .

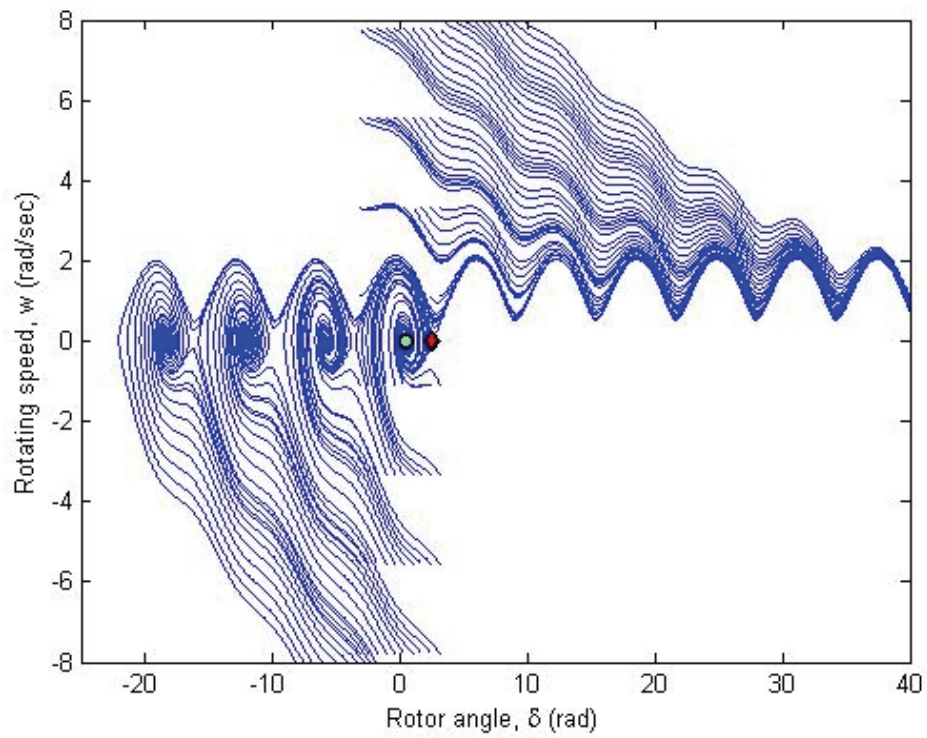


Figure 4.4. Phase portraits of deterministic SMIB system for  $D = 0.36 < D_c = 0.414$  and  $P_m = 0.5$ .

When the value of the damping parameter  $D$  has been chosen as equal to the critical damping level  $D_c$ , it has been observed that all the trajectories converge to the SEP sooner or later as in Figure 4.3.

By choosing the value of the damping parameter  $D$  less than the critical damping level  $D_c$  it has been observed that the system has a SEP and a stable limit cycle as shown in Figure 4.4 and in this bistable case depending on the initial conditions the trajectories converge either to the SEP or to the rotating orbit (limit cycle). The case of rotating orbit is undesired for the rotor angle stability of SMIB.

The basin of attraction can provide an understanding for the stability analysis in deterministic systems. The basin of attraction of each attractor corresponds to the region of all possible initial conditions which lead to trajectories converge on that attractor. The basins of attraction for the bistable case have been computed by using Monte Carlo method and have been presented in Figure 4.5 in which the basin of attraction of SEP is colored in blue while the basin of attraction of stable limit cycle is colored white.

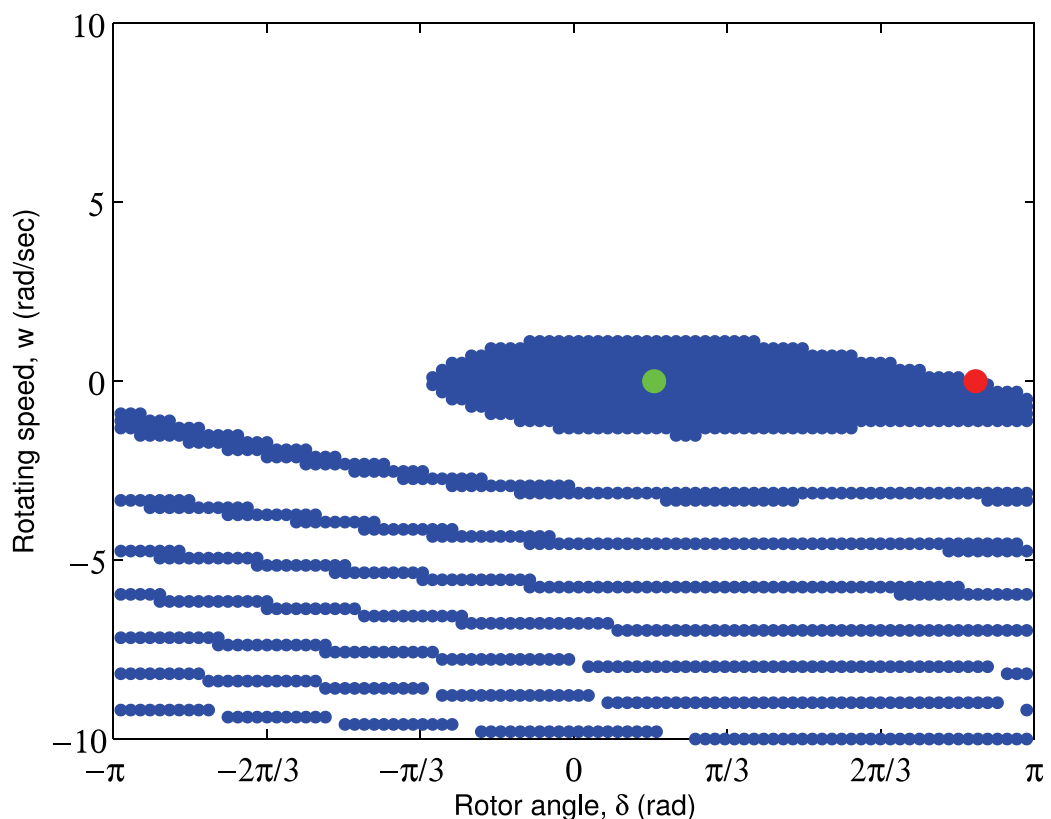


Figure 4.5. Basin of attraction of the stable equilibrium point (SEP) which is colored in blue while the basin of attraction of stable limit cycle is colored in white.

The deterministic model of SMIB given in (4.1) is analogous to the Josephson junction and the classical driven pendulum given in (Strogatz, 2018).

## 4.2. Stochastic Single Machine Infinite Bus Power Systems

In the steady state, there is a balance between the mechanical power and the electrical power and the machine runs at a constant speed which leads to the constant relative rotor angle (i.e., at the equilibrium point  $\dot{\delta} = 0$ ). Due to the random load change, line tripping or loss of machine the imbalance between the mechanical power and the electrical power may result in deviation from the rotational speed which leads to the loss of synchronism.

Under the load fluctuations of Gaussian type, (4.1) have been analyzed in (Wei and Luo, 2009) and in (Lu et al., 2015) where the imbalance between the mechanical power and the electrical power in the SSMIB power system given in (4.1) has been modeled by  $P_L = \epsilon B(t)$  where  $\epsilon$  is the noise intensity and  $B(t)$  is the Brownian motion (Wiener process) and the increments of the Brownian motion  $dB(t)$  is Gaussian random variable (Soong, 1973; Samorodnitsky and Taqqu, 1994).

As it has been proposed in (Yilmaz and Savacı, 2017a,b) the imbalance between the mechanical power and the electrical power in the SSMIB power system given in (4.5) has been modeled by  $P_L(t) = \epsilon L_\alpha(t)$  where  $\epsilon$  is the noise intensity and  $L_\alpha(t)$  is the alpha-stable Lévy process and the increments of the Lévy process  $dL_\alpha(t)$  is  $\alpha$ -stable random variable (Samorodnitsky and Taqqu, 1994).

Our motivation of choosing Lévy type fluctuations is that it admits impulsive and asymmetric fluctuations which can be modeled by  $\alpha$ -stable random variable (Samorodnitsky and Taqqu, 1994). Modeling the imbalance between the mechanical power and electrical power as  $P_L(t) = \epsilon L_\alpha(t)$  and considering the unit inertia constant then the dynamics of the SSMIB can be written as

$$\begin{bmatrix} \dot{\delta} \\ \dot{\omega} \end{bmatrix} = \begin{bmatrix} \omega \\ -D\omega + P_m - P_e \end{bmatrix} + \begin{bmatrix} 0 \\ 1 \end{bmatrix} P_L \quad (4.5)$$

by defining the state variable  $\begin{bmatrix} x_1 & x_2 \end{bmatrix}^T = \begin{bmatrix} \delta & \omega \end{bmatrix}^T$  then (4.5) can be rewritten as:

$$d\mathbf{X}(t) = \mathbf{f}(t, \mathbf{X}(t))dt + \mathbf{g}dL_\alpha(t) \quad (4.6)$$

$$\mathbf{f}(t, \mathbf{X}(t)) = \begin{bmatrix} x_2 \\ -Dx_2 + P_m - \sin x_1 \end{bmatrix}; \quad \mathbf{g} = \begin{bmatrix} 0 \\ \epsilon \end{bmatrix} \quad (4.7)$$

and the increments of the Lévy process  $dL_\alpha(t)$  is  $\alpha$ -stable random variable (Samorodnitsky and Taqqu, 1994).

The Euler-Maruyama method given in (Janicki and Weron, 1993; Kloeden and Platen, 1999) is applied to approximate the numerical solution of (4.7) as:

$$\mathbf{X}_{t_i} = \mathbf{X}_{t_{i-1}} + \mathbf{f}(t_{i-1}, \mathbf{X}(t_{i-1}))\tau + \mathbf{g} \Delta L_{\alpha,i}^\tau \quad (4.8)$$

where the increment of the Lévy process is  $\alpha$ -stable random variable  $\Delta L_{\alpha,i}^\tau$  defined by  $\Delta L_{\alpha,i}^\tau = L_\alpha([t_{i-1}, t_i]) \sim S_\alpha(\tau^{1/\alpha}, \beta, \mu)$  with  $\tau = t_i - t_{i-1}$  have been generated by the method given in (Janicki and Weron, 1993).

### 4.3. The Effect of Wiener and $\alpha$ -stable Lévy Power Fluctuations on the Rotor Angle Stability

Consider the SSMIB system given in (4.5). In the sequel, the numerical solutions of the phase portraits of generator angle and speed responses have been obtained for 1000 realizations for  $T = 200$  seconds with the step size  $\tau = 0.01$  and the noise intensity  $\epsilon = 0.01$ . The variation of the basin of attraction of the SEP and the limit cycle under the stochastic load fluctuations have been observed based on a single initial condition.

#### 4.3.1. Variation of Basin of Attraction of SEP by Increasing Impulsiveness and/or Skewness

Firstly, an initial condition has been chosen whose trajectory converges to the SEP for the deterministic SMIB and then for this initial condition 1000 trajectories which correspond to the realizations of stochastic SMIB have been obtained. Under the Wiener type fluctuations in the load ( $\alpha = 2, \beta = 0$ ) all realizations of the responses of rotor angle and rotating speed have converged to the SEP as shown in Figure 4.6 and the SEP has been observed to be stable in the mean square sense.

Thereafter by increasing the impulsiveness and/or skewness the variation of the basin of attraction of SEP has been analyzed. The impulsiveness at the load fluctuations has been chosen as  $\alpha = 1.95$  with  $\beta = 0$  the rotor angle responses have converged to the SEP as shown in Figure 4.7.

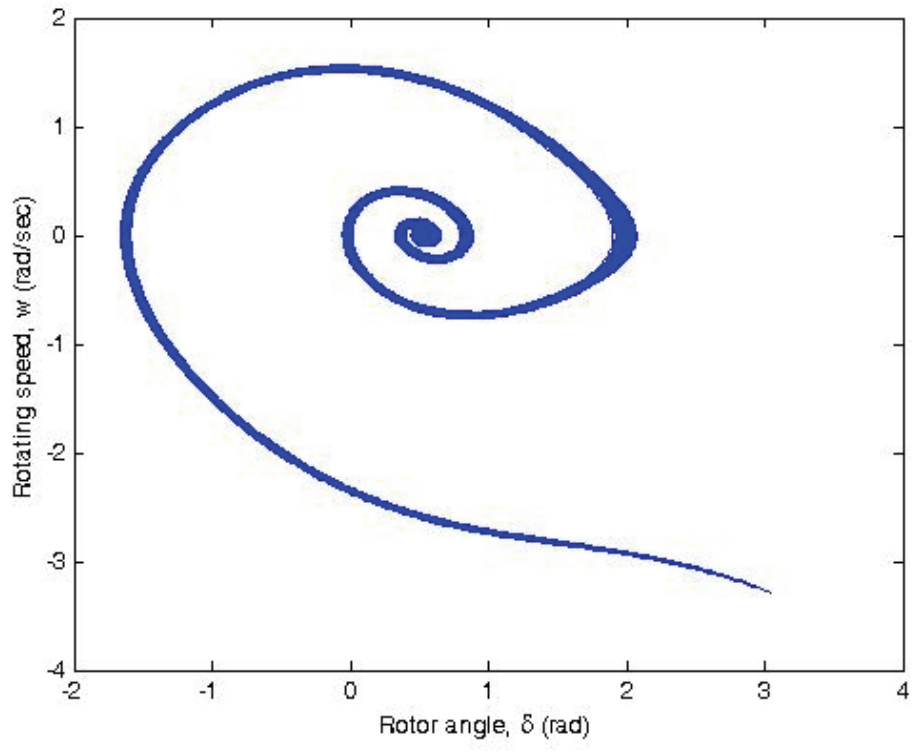


Figure 4.6. Wiener type fluctuations in the load  $\alpha = 2.0$  and  $\beta = 0$ .

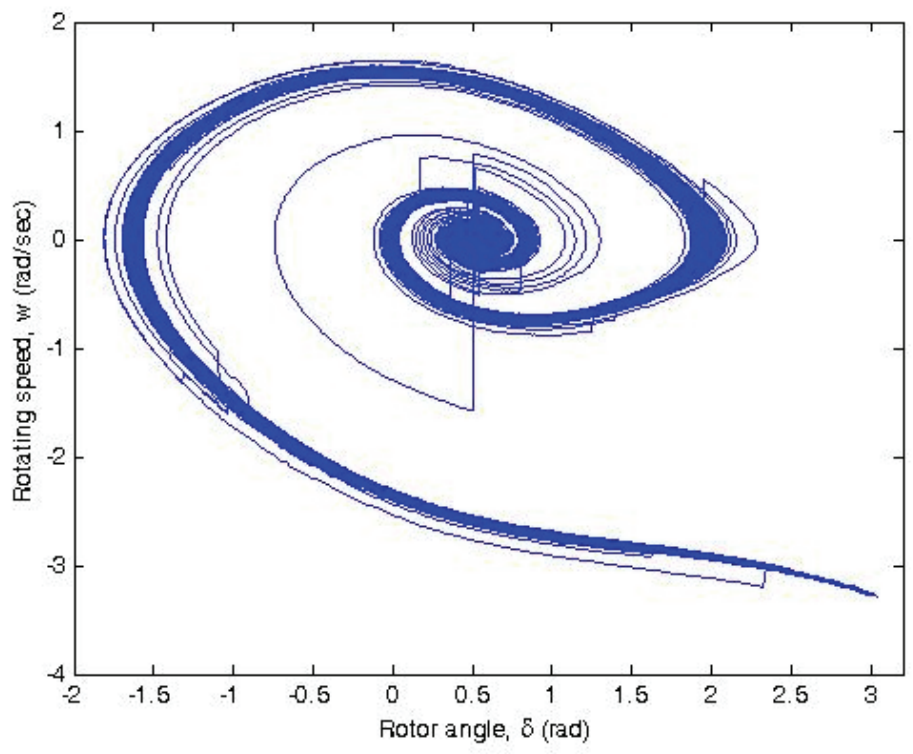


Figure 4.7. Lévy type fluctuations in the load with  $\alpha = 1.95$  and  $\beta = 0$ .



When the impulsiveness at the load fluctuations has been increased by choosing the characteristic exponent  $\alpha = 1.8$  while preserving the symmetry (i.e.,  $\beta = 0$ ) and hence the load fluctuations have become non-Gaussian. The majority of 1000 realizations has converged to the SEP but sudden jumps have occurred in the few of realizations of the rotor speed as shown in Figure 4.8. These trajectories have converged to the rotating orbit (limit cycle) which previously stated as undesired for the rotor angle stability. The SEP has been observed to be unstable in the mean square sense and stable in the sense of probability.

The deviation from the symmetry at the load fluctuations has been provided by increasing the skewness. Although the rotor angle responses have converged to the SEP for  $\alpha = 1.95$ ,  $\beta = 0$  as shown in Figure 4.7 by increasing the skewness  $\beta = 1$  few of realizations has converged to the rotating orbit as shown in Figure 4.9.

With these obtained results it has been observed that the increase of impulsiveness and/or the distortion of the symmetry at the load fluctuations lead to the change in the basin of attraction of the SEP. Some of the trajectories have converged to the limit cycle and the SEP have been observed to become unstable in the mean square sense.

This important observation is distinct from the observation in (Lu et al., 2015) which states that under the Wiener type fluctuations at the load the SEP is stable in the mean square sense.

### **4.3.2. Variation of Basin of Attraction of Limit Cycle by Increasing Impulsiveness and/or Skewness**

In the sequel, the variation of basin of attraction of limit cycle has been analyzed based on a single initial condition by increasing impulsiveness and/or skewness. An initial condition has been chosen such that the trajectory converges to the limit cycle for the deterministic SMIB and then for this initial condition 1000 trajectories have obtained which correspond to the realizations of stochastic SMIB.

The fluctuations at the load have been modeled as Wiener process ( $\alpha = 2.0$  and  $\beta = 0$ ). All of 1000 realizations have converged to the rotating orbit as shown in Figure 4.10. This situation have caused to be the rotor angle of the system unstable both in the mean square sense and in the sense of probability.

The random fluctuations in the load have been modeled as symmetric Lévy process with  $\alpha = 1.8$ ,  $\beta = 0$ . A few of the 1000 trajectories have converged to the SEP as shown in Figure 4.11 (i.e. zoomed version of red area), the majority of trajectories have converged to the rotating orbit (limit cycle) and hence the rotor angle is still unstable both in the sense of probability and in the mean square sense.



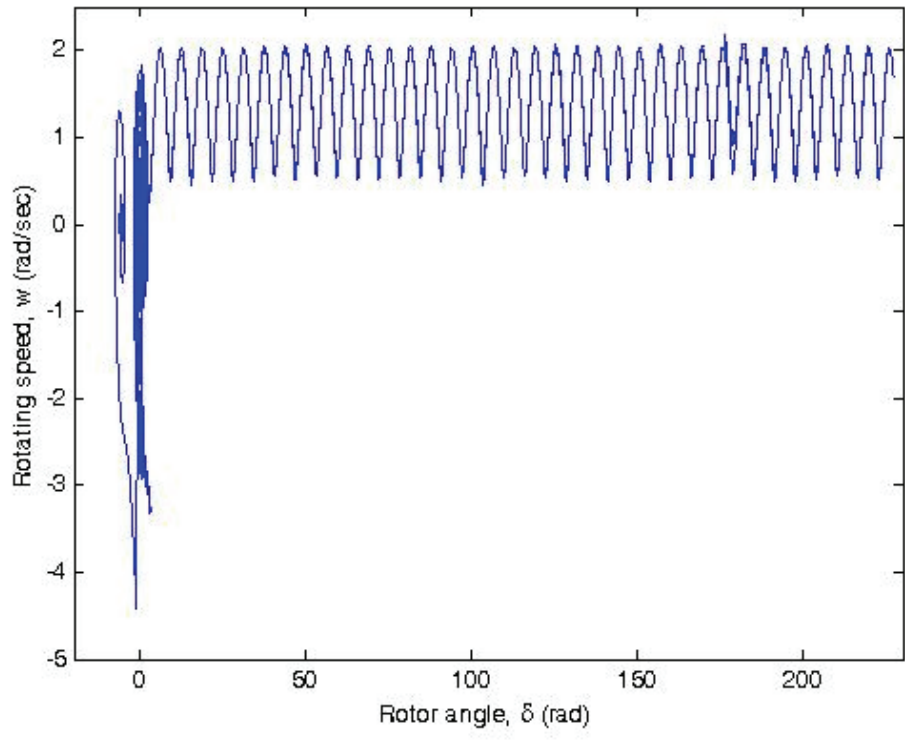


Figure 4.8. Lévy type fluctuations in the load with  $\alpha = 1.8$  and  $\beta = 0$ .

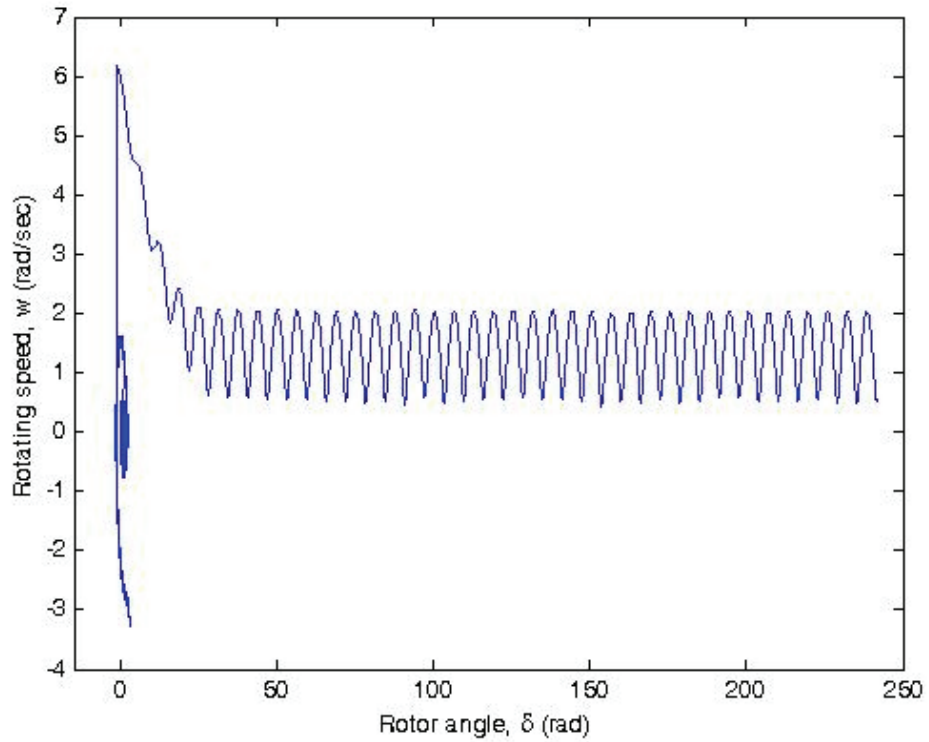


Figure 4.9. Lévy type fluctuations in the load with  $\alpha = 1.95$  and  $\beta = 1$ .

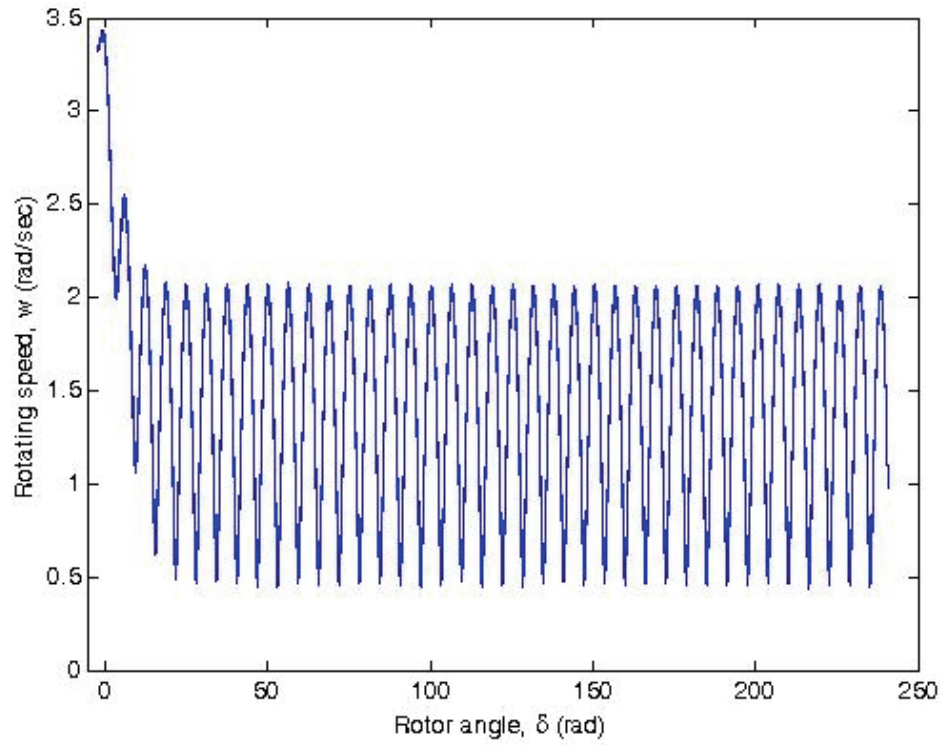


Figure 4.10. Wiener type fluctuations in the load with  $\alpha = 2.0$  and  $\beta = 0$ .

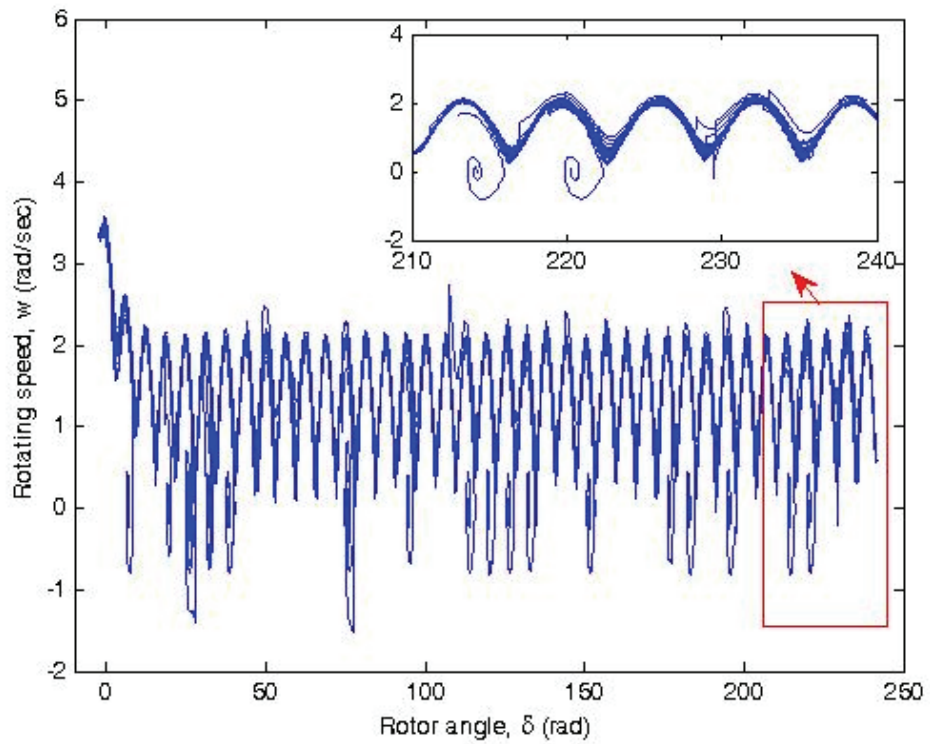


Figure 4.11. Lévy type fluctuations in the load with  $\alpha = 1.8$  and  $\beta = 0$ .

However, with the increase of impulsiveness, the percentage of trajectories which converge to the SEP for 1000 realizations has increased as shown in Table 4.1 and hence the stability of the rotor angle improves in the sense of probability. This important observation is distinct from the response of Wiener type fluctuations where the rotor angle is unstable in the sense of probability which has been observed as shown in Figure 4.10.

Table 4.1. Percentage of Stochastic Trajectories Converging to the SEP.

| $\beta \setminus \alpha$ | 1.9  | 1.8  | 1.6   | 1.5   | 1.4   | 1.2   |
|--------------------------|------|------|-------|-------|-------|-------|
| 0                        | 1.2% | 3.3% | 10.8% | 12.7% | 24.5% | 43.7% |
| -1                       | 1.7% | 4.8% | 19.3% | 26.4% | 38.1% | 61.0% |

With the asymmetric load fluctuations where  $\beta = -1$ , the percentage of trajectories which converge to the SEP have increased with the increase of impulsiveness as shown in Table 4.1. Therefore it has been observed that the stability of the rotor angle improves in the sense of probability.

However, for  $\beta = 1$  the trajectories have not converged to the SEP as shown in Figure 4.12, all trajectories have converged to the limit cycle. This observation has revealed that the tendency of the distribution at the load fluctuations is important for the rotor angle stability in the sense of probability.

For given initial condition, the trajectories converge to the limit cycle in the deterministic SMIB whereas in the stochastic SMIB some of these realizations have been observed which not converge to the limit cycle but converge to the SEP for  $\alpha$ -stable Lévy type load fluctuations. It has been concluded that the Lévy type fluctuations in the load have provided to change in the basin of attraction of the limit cycle. Therefore the stability of the rotor angle in the sense of probability has been improved. This important observation is distinct from the response of Wiener type fluctuations where the rotor angle is unstable in the sense of probability as shown in Figure 4.10.

Since the variation of basin of attraction of SEP and limit cycle have been observed based on a single initial condition then beyond these observations obtained from a single initial condition, in the following subsection, a largely set of initial conditions have been considered and hence the rotor stability have been extended in terms of basin stability.

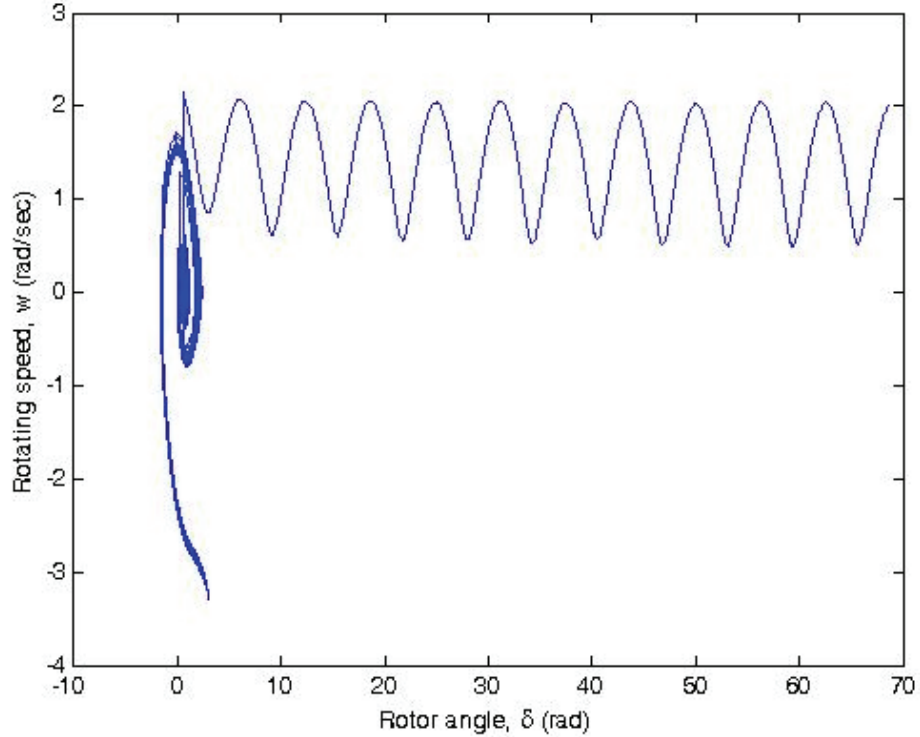


Figure 4.12. Lévy type fluctuations in the load with  $\alpha = 1.9$  and  $\beta = 1$ .

#### 4.4. Basin Stability of Stochastic Single Machine Infinite Bus Power System

The basin stability is a measure of the volume of the basin of attraction and it allows to quantify the probability to converge to the equilibrium point after being subjected to perturbations. The basin stability in deterministic SMIB systems has been presented in (Menck et al., 2013, 2014) and then the Northern European power grid has been considered as a case study. In (Ji and Kurths, 2014) the basin stability for deterministic SMIB system and four-node network have been investigated. By introducing the notion of stochastic basin of attraction, the basin stability has been generalized in (Serdukova et al., 2016) and applied to the three-well potential perturbed by two types of noises, Brownian motion and  $\alpha$ -stable Lévy motion.

The basin stability is a powerful method which can be applied to the many fields of science (Leng et al., 2016). For the practical purposes, the numerical computation of the basin stability is as follows:

- (i)  $K$  points have drawn uniformly at random from  $[-\pi, \pi] \times [-10, 10]$  which correspond to the  $K$  initial conditions of  $(\delta, \omega)$ .

- (ii) The system has been integrated long enough for these  $K$  points and 1000 random realizations have been carried out for each initial condition.
- (iii) The number  $M$  of the initial conditions which finally reach a SEP in the presence of disturbance has been counted.
- (iv) The criteria for the basin stability has been quantified by the percentage  $M/K$ .
- (v) The probability of the system returning to a SEP has been defined as the return probability.

In this part, to observe the possibility of the power system to reach the synchronous state in the presence of disturbances which occur due to such as short circuits, load fluctuations or renewable generations, these power fluctuations have been modeled as Wiener and  $\alpha$ -stable Lévy type, respectively and 400 initial conditions of  $(\delta, \omega)$  have been taken from  $[-\pi, \pi] \times [-10, 10]$  and 1000 random realizations have been carried out for each initial condition as given in our work (Yılmaz and Savacı, 2017b). Then the system has been integrated long enough and the percentage of the initial values converging to the SEP has been calculated.

In the case of deterministic SMIB system for different values of the mechanical power  $P_m$  and damping  $D$  parameters the basin stability diagram have been obtained as shown in Figure 4.13.

The colored circles represent the return probabilities which correspond to the related mechanical power and damping parameters. It can be expressed such that for the pair of parameters corresponding to the red circles, all trajectories converge to the SEP with the return probability one whereas for the pair of the parameters corresponding to the blue circles, the trajectories converge to the stable limit cycle (rotating orbit) with the return probability zero.

For the pair of mechanical and damping parameters corresponding to the yellow circles, it has been calculated that 600 of the 1000 realizations converge to the SEP. The rest of the colored circles have also been marked with the same approach.

The pair of mechanical power and damping parameters have been chosen as  $P_m = 0.5$  and  $D = 0.8$ . In the deterministic case all trajectories have converged to the SEP as observed in Figure 4.13.

When the power imbalance between the mechanical and electrical power has been modeled by Brownian motion ( $\alpha = 2, \beta = 0$ ) the return probability have been evaluated as 0.9965.

However, for various values of the characteristic exponent  $\alpha$  and for either symmetric or asymmetric  $\alpha$ -stable Lévy type power fluctuations the return probabilities have been evaluated and it has been observed that the return probabilities decrease with the decrease

of characteristic exponent  $\alpha$  (increase of impulsiveness) for either symmetric or asymmetric  $\alpha$ -stable Lévy motion as shown in Figure 4.14.

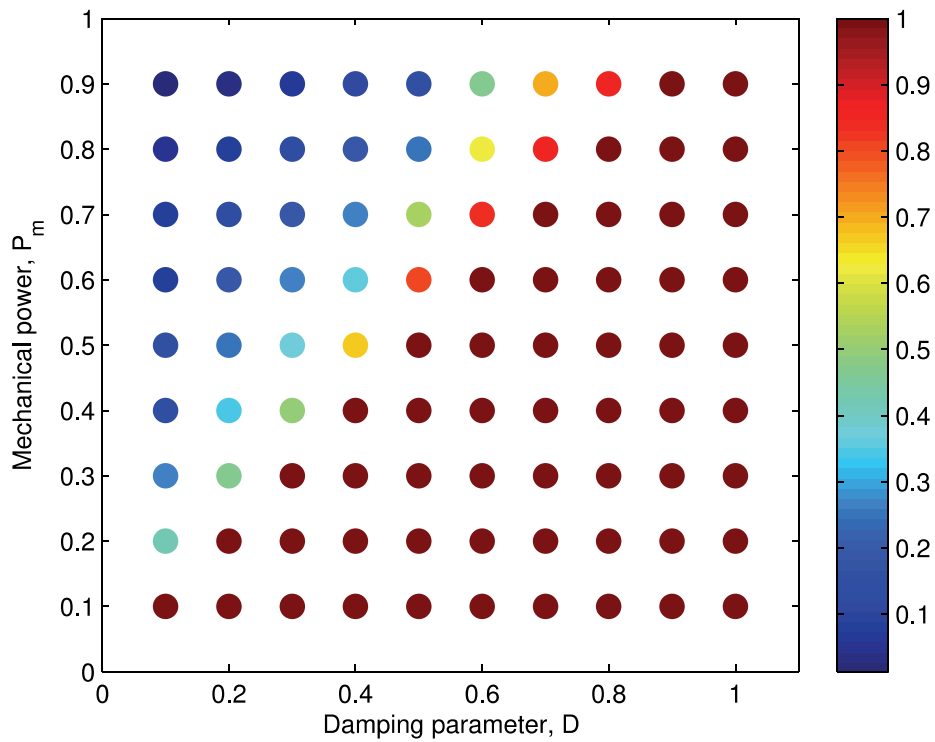


Figure 4.13. Basin stability diagram for deterministic case.

For positive-skewed  $\alpha$ -stable Lévy motion the return probability decreases with the decrease of characteristic exponent  $\alpha$  and then for  $\alpha = 1.2$  the return probability increases.

When the mechanical power  $P = 0.5$  and damping  $D = 0.2$  have been selected the return probabilities have been obtained as shown in Figure 4.15. For negative-skewed  $\alpha$ -stable Lévy type power fluctuations, it has been observed that the return probability increases with the decrease of characteristic exponent  $\alpha$  (increase of impulsiveness) and then for  $\alpha = 1.2$  return probability decreases.

The basin stability diagram over the parameter space  $P_m - D$  with the changes of values of characteristic exponent  $\alpha$  and skewness  $\beta$  parameters has been obtained as presented in Figures 4.16- 4.18. It can be seen from Figures 4.16- 4.17 that asymmetric  $\alpha$ -stable Lévy type power fluctuations with  $\alpha = 1.7$  provides a change in the basin stability diagram compared to the deterministic basin stability diagram. The return probability increases for some specific parameter pair value of  $(P_m, D)$  and hence the stability of the rotor angle is improved.

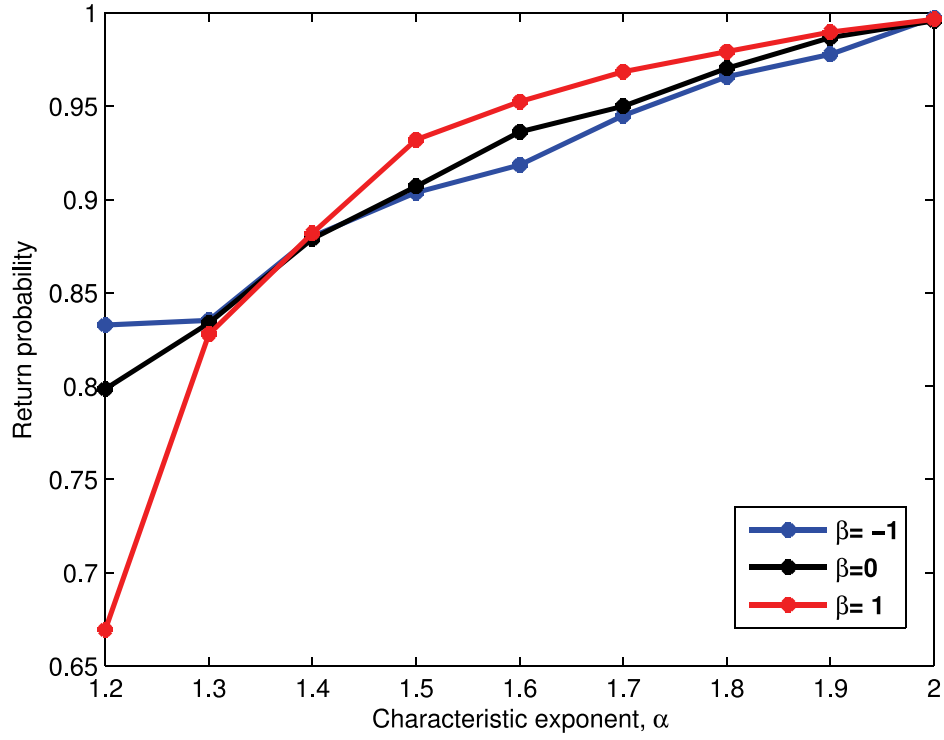


Figure 4.14. Return probability for  $P_m = 0.5$  and  $D = 0.8$ .

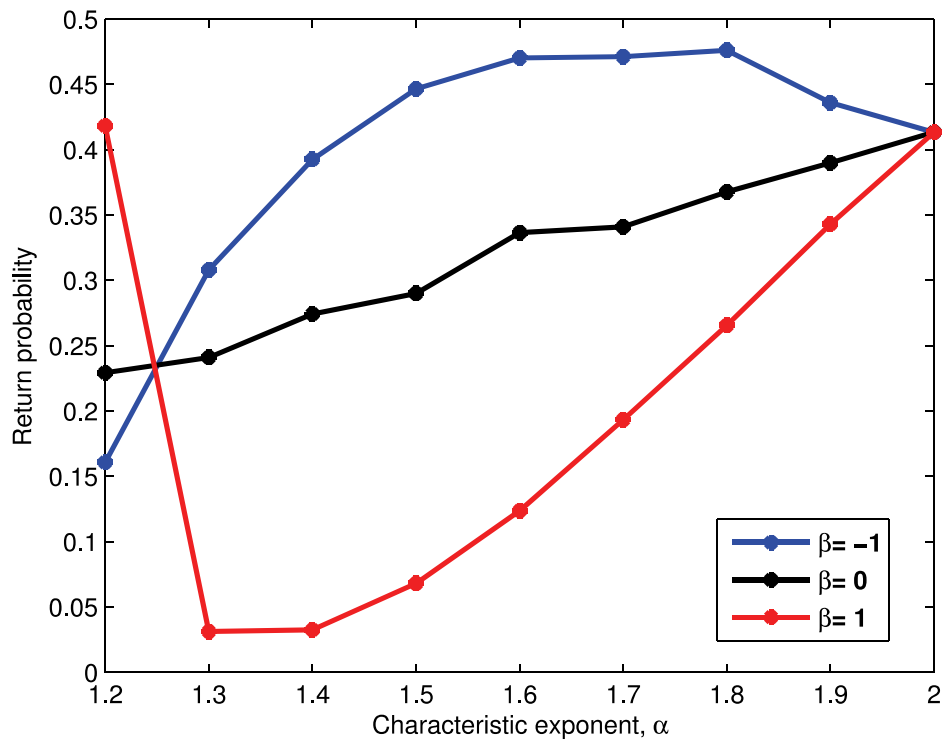


Figure 4.15. Return probability for  $P_m = 0.5$  and  $D = 0.2$ .

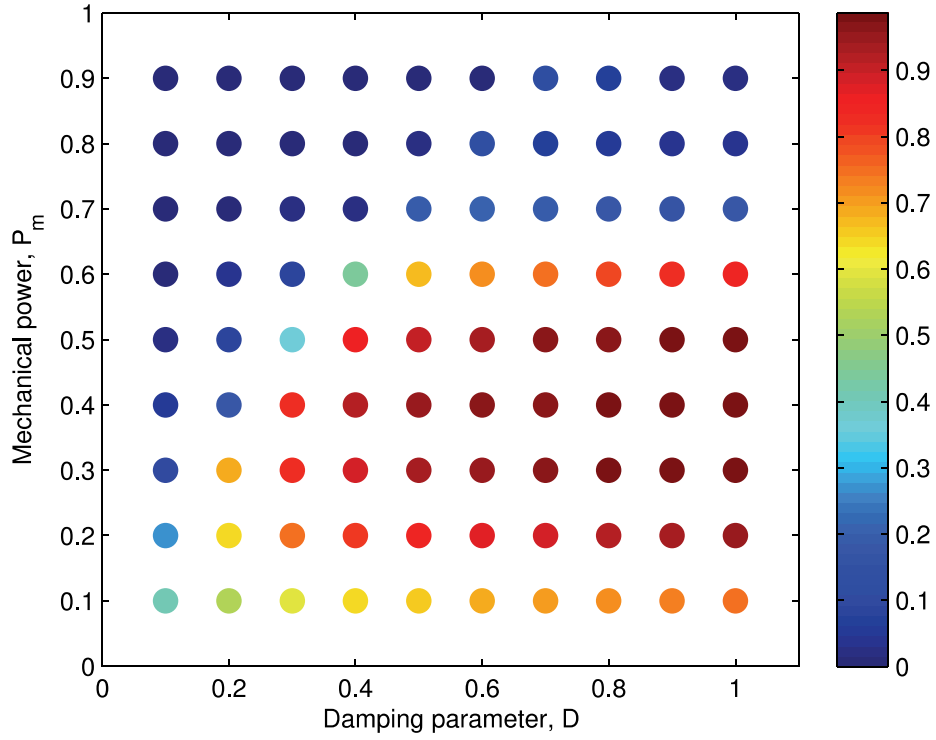


Figure 4.16. Basin stability diagram in the case of  $\alpha$ -stable Lévy type power fluctuations with  $\alpha = 1.7$ ,  $\beta = 1$ .

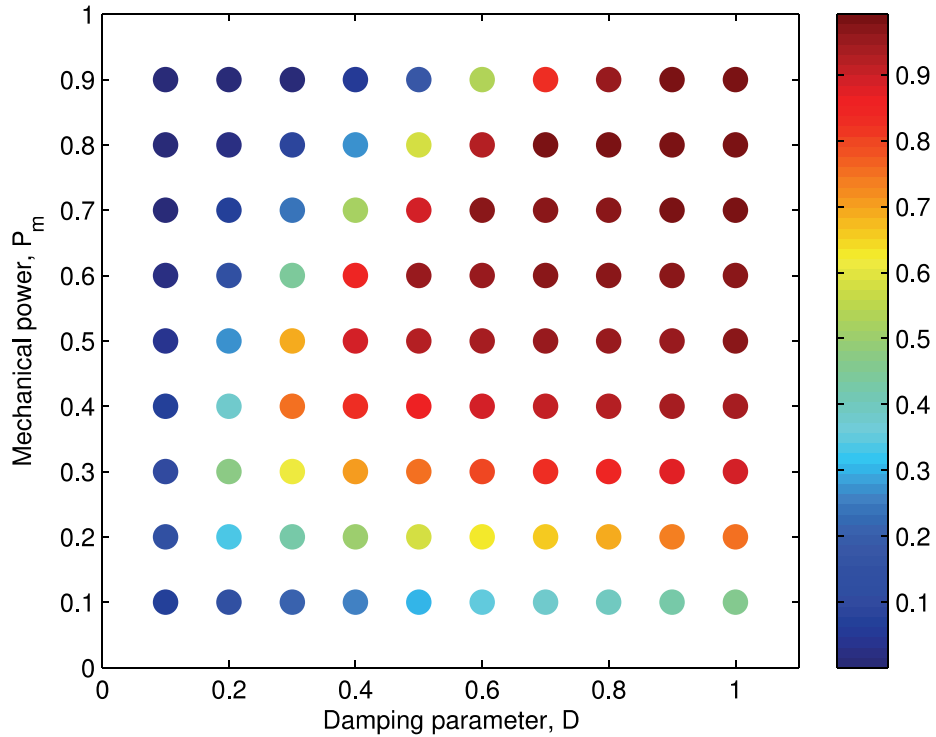


Figure 4.17. Basin stability diagram in the case of  $\alpha$ -stable Lévy type power fluctuations with  $\alpha = 1.7$ ,  $\beta = -1$ .



Furthermore how the basin stability over parameter space changes according to the skewness parameter  $\beta = 1$  and  $\beta = -1$  can be clearly seen from Figures 4.16- 4.17. For  $\alpha = 1.2$  and  $\beta = 1$  the region of basin stability for SEP becomes smaller as shown in Figure 4.18. Therefore it has been concluded that the system is not able to withstand to the perturbations.

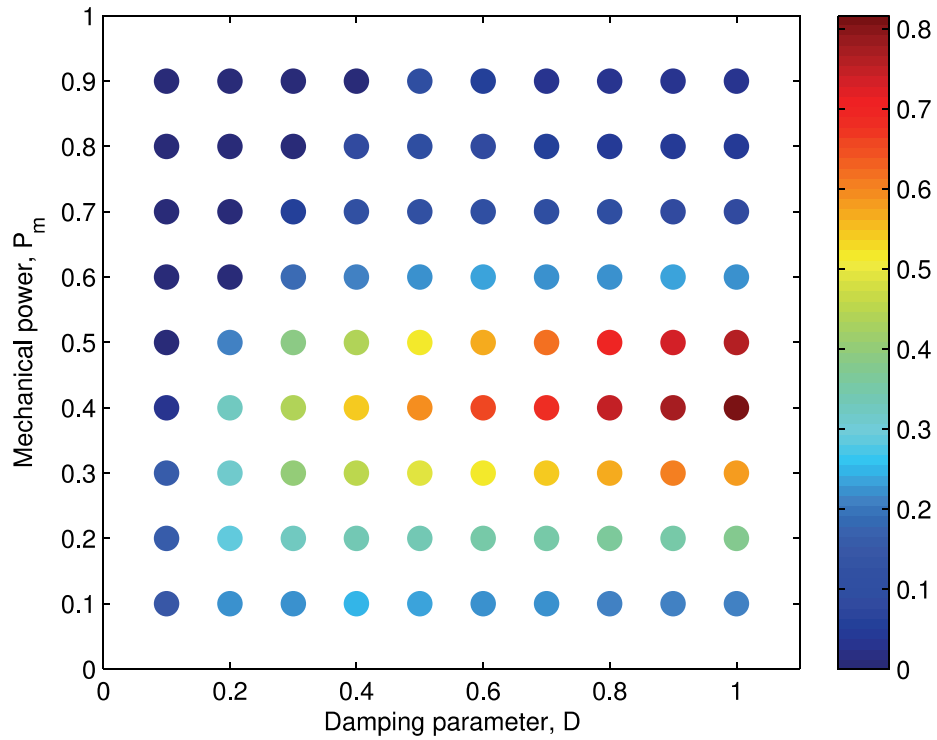


Figure 4.18. Basin stability diagram in the case of  $\alpha$ -stable Lévy type power fluctuations with  $\alpha = 1.2$ ,  $\beta = 1$ .

## CHAPTER 5

# CONTROL OF STOCHASTIC SINGLE MACHINE INFINITE BUS POWER SYSTEMS

In (Yang, 1997) H-infinity control method have been applied to find the optimal power system stabilizer for single machine infinite bus systems in the presence of disturbance. In (Rigatos et al., 2017) with the appropriately chosen Lyapunov function, nonlinear H-infinity control method have been applied to the linearized model of the distributed synchronous generators subject to the variations in the mechanical torque and measurement noises. In (Mahmud et al., 2017) by considering the effects of measurement noises which have been modeled as white Gaussian noises, a partial feedback linearization technique have been designed in which the feedback linearizing control law has been proposed to decouple the noises from the system. These noises have been incorporated during the simulation in (Mahmud et al., 2017).

In the first part of this chapter, the control of the rotor angle stability of SMIB power systems with Wiener type stochastic fluctuations has been achieved by minimizing the stochastic sensitivity function. In the second part of this chapter, an analytical expression for the rotor angle dispersion of SMIB in the presence of impulsive and asymmetric fluctuations have been derived. Those fluctuations have modeled by  $\alpha$ -stable Lévy processes and the minimization of the rotor angle dispersion has been achieved.

### 5.1. Controlling the Rotor Angle Stability in SMIB Power Systems by Minimizing Stochastic Sensitivity Function

In this section, the stochastic sensitivity analysis (SSA) introduced in (Ryashko and Bashkirtseva, 2008; Bashkirtseva et al., 2017) has been used for controlling the rotor angle stability of SMIB power system in the presence of Wiener type power fluctuations. Depending on the values of the ratio  $P_m/P_{max}$ , the damping parameter  $D$ , the initial conditions and the noise intensity of the stochastic fluctuations, the trajectories converge either to the SEP or to the stable limit cycle (unique rotating orbit) as stated previously. Since the rotating orbit is an undesired case in power systems this situation can be overcome by the control input which is synthesized by the feedback regulator. The control rule to stabilize the stochastic SMIB system have been derived through the stochastic sensitivity measure given in Chapter 3.

Consider the SSMIB system given in (4.5) in which the imbalance between the mechanical power and the electrical power has been modeled as Wiener process  $P_L = \epsilon B(t)$ . It has been assumed that the state variables  $\delta$  and  $\omega$  are available for measurements and a feedback  $u = k_1(y_1 - \bar{\delta}) + k_2(y_2 - \bar{\omega})$  with noisy measurements  $y_1$  and  $y_2$  :

$$\begin{aligned} y_1(t) &= \delta + \epsilon c_1 \eta_1(t) \\ y_2(t) &= \omega + \epsilon c_2 \eta_2(t) \end{aligned} \quad (5.1)$$

where  $k_1, k_2 \in R$  are the feedback coefficients,  $c_1, c_2 \in R$  are the intensity of noisy measurements and  $\eta_1, \eta_2$  are uncorrelated white Gaussian noises.

Using the feedback regulator given in (5.1), the matrices defined in (3.40) have been obtained as:

$$\begin{aligned} F &= \begin{bmatrix} 0 & 1 \\ -P_{max} \cos(\bar{\delta}) & -D \end{bmatrix}, \quad B = \begin{bmatrix} 0 \\ 1 \end{bmatrix}, \quad S = \begin{bmatrix} 0 & 0 \\ 0 & 1 \end{bmatrix}, \\ R &= \begin{bmatrix} c_1^2 & 0 \\ 0 & c_2^2 \end{bmatrix}, \quad K = [k_1 \quad k_2]. \end{aligned} \quad (5.2)$$

For the uncontrolled SMIB system (4.5) with Wiener type load fluctuations  $P_L = \epsilon B(t)$  the solution of matrix equation

$$FW + WF^T + S = 0 \quad (5.3)$$

gives the stochastic sensitivity matrix  $W$  as follows:

$$W = \begin{bmatrix} \frac{1}{2P_{max}D \cos(\bar{\delta})} & 0 \\ 0 & \frac{1}{2D} \end{bmatrix}. \quad (5.4)$$

In the presence of control input by using the conditions given in (3.44)-(3.45) a parametric description of the set of pairs  $(w_{11}, w_{22})$  for which the stochastic sensitivity matrix  $W$  is attainable has been obtained through the following inequality:

$$w_{11}^2 w_{22}^2 + 2D w_{11}^2 w_{22} c_2^2 - w_{11}^2 c_2^2 - P_{max}^2 w_{11}^2 c_1^2 c_2^2 - 2P_{max} \cos(\bar{\delta}) w_{11} w_{22} c_1^2 c_2^2 - w_{22}^2 c_1^2 c_2^2 \geq 0 \quad (5.5)$$

where  $w_{11}$  and  $w_{22}$  are the diagonal elements of the stochastic sensitivity matrix  $W$ .

The aim is to design a feedback regulator which minimizes the value of stochastic sensitivity and hence to stabilize the equilibrium  $(\bar{\delta}, 0)$ .

To construct a feedback regulator which minimizes the stochastic sensitivity function, the cost function  $J(W) = tr(W) = w_{11} + w_{22}$  has been considered.

The minimum of the cost function  $J_0 = \min J(W)$  geometrically corresponds to the tangent line to the border of the attainability region and the corresponding pair  $(w_{11}, w_{22})$  of the attainable set provides the minimization of stochastic sensitivity function.

For this minimal attainable value of the pair  $(w_{11}, w_{22})$ , the optimization problem can be directly solved without using the Lagrange function given in (3.49) for lower order dimensions and the coefficients of the optimal regulator coefficients have been found such that

$$k_1 = -\frac{w_{22}}{w_{11}} + P_{max} \cos(\bar{\delta}) \quad (5.6)$$

and the coefficient  $k_2$  satisfies the following equation:

$$k_2^2 c_2^2 + 2w_{22}(k_2 - D) + c_1^2 \left( \frac{-w_{22}}{w_{11}} + P_{max} \cos(\bar{\delta}) \right)^2 + 1 = 0 \quad (5.7)$$

which indeed implies that  $k_2$  should be as  $k_2 < D$ .

The designed feedback regulator given by (5.6)-(5.7) for controlling nonlinear stochastic SMIB power system has been based on the linearization of nonlinear stochastic system around its equilibrium point. These designed coefficients  $k_1$  and  $k_2$  have been verified through the simulations of the nonlinear stochastic SMIB system written in the Itô form:

$$d\mathbf{X}(t) = \mathbf{F}(t, \mathbf{X}(t))dt + \mathbf{G} d\mathbf{B}(t) \quad (5.8)$$

where the state variable  $\mathbf{X} = [\delta \ \omega]^T$ , the uncorrelated incremental Wiener process  $d\mathbf{B} = [dB^{(1)} \ dBB^{(2)} \ dB^{(3)}]^T$  and

$$\mathbf{F}(t, \mathbf{X}(t)) = \begin{bmatrix} \omega \\ -D\omega + P_m - \sin(\delta) + k_1(\delta - \bar{\delta}) + k_2\omega \end{bmatrix}$$

$$\mathbf{G} = \begin{bmatrix} 0 & 0 & 0 \\ \epsilon & \epsilon k_1 c_1 & \epsilon k_2 c_2 \end{bmatrix}. \quad (5.9)$$

The numerical solution of (5.8) can be approximated by using the Euler-Maruyama method (Kloeden and Platen, 1999) as

$$\mathbf{X}_{t_i} = \mathbf{X}_{t_{i-1}} + \mathbf{F}(t_{i-1}, \mathbf{X}(t_{i-1}))\tau + \mathbf{G}\Delta\mathbf{B}^T \quad (5.10)$$

where the increment of the Wiener process defined by  $\Delta B_\tau^{(l)} = B(t_i) - B(t_{i-1})$  with  $l = 1, 2, 3$  is Gaussian random variable  $N(0, \tau)$  and  $t_i = i\tau$  for  $i = 0, 1, \dots, n$ .

In the sequel, the parameters  $E = 1.0$  p.u,  $V = 1.0$  p.u and  $X_T = 1.0$  p.u have been chosen and the stochastic sensitivity analysis have been carried out for different parameters of the mechanical power  $P_m$  and damping coefficient  $D$ . The initial conditions of  $\delta(0)$  and  $\omega(0)$  have been selected as 100 evenly spaced points in the interval of  $[-\pi, \pi]$  and  $[-10, 10]$ , respectively.

Consider the values of mechanical power  $P_m = 1$  p.u and the damping coefficient  $D = 0.2$  p.u and  $c_1 = c_2 = c$ . In this case the SEP and the saddle point coalesce in a saddle-node bifurcation of fixed point  $\bar{\delta} = 1.5708$ ,  $\bar{\omega} = 0$ .

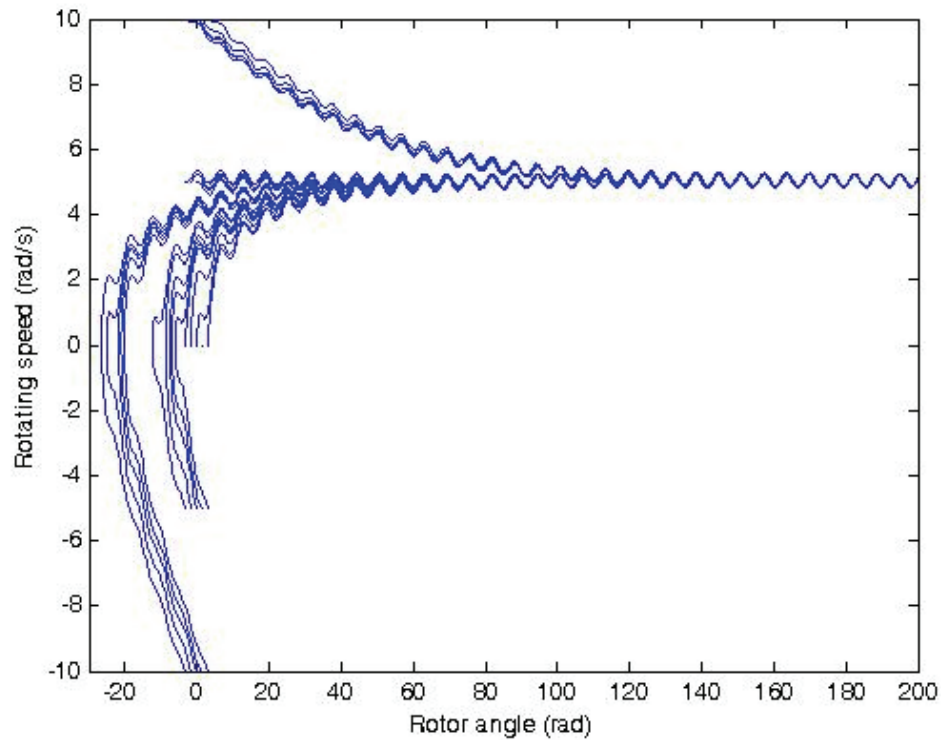


Figure 5.1. Phase portrait of rotor angle  $\delta$  vs. rotating speed  $w$  of deterministic ( $\epsilon = 0$ ) for the initial conditions  $\delta(0), \omega(0)$  in the interval of  $[-\pi, \pi]$  and  $[-10, 10]$ .

For the uncontrolled deterministic system (4.5) (i.e.,  $u = 0, \epsilon = 0$ ) it has been observed that all trajectories converge to a stable limit cycle (unique rotating orbit) as shown in Figure 5.1. Since for any initial condition the trajectories converge to the unique rotating orbit, the initial point has been kept to be as  $\delta(0) = 1, \omega(0) = 1$  to give a clear visualization of the response in the presence of power fluctuations.

The phase portraits of the stochastic responses over 1000 realizations have been shown in Figure 5.2 where the noise intensity  $\epsilon = 0.001$ . It has been seen from Figure 5.2 that the system has large-amplitude oscillations and it has been calculated that the uncontrolled stochastic SMIB power system (4.5) has  $w_{11} = 2.5$  and  $w_{22} = 2.5$  by using (5.4).

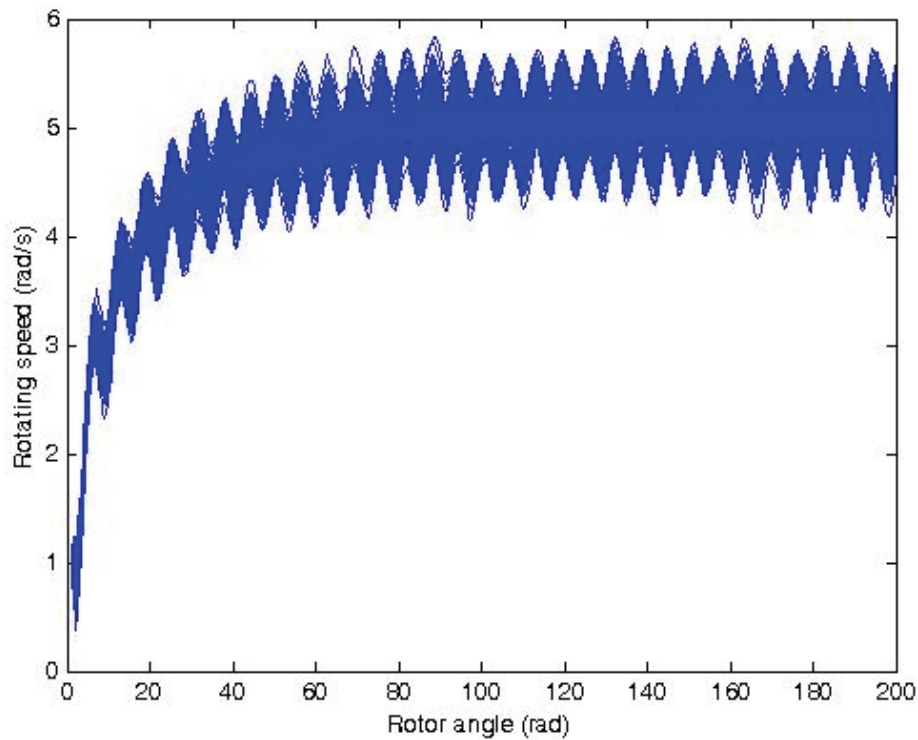


Figure 5.2. Phase portrait of rotor angle  $\delta$  vs. rotating speed  $w$  of stochastic uncontrolled SMIB power system ( $\epsilon = 0.001$ ) for  $\delta(0) = 1, \omega(0) = 1$ .

The attainability domains for the pairs  $(w_{11}, w_{22})$  of the stochastic sensitivity matrix  $W$  for the different intensity values of the noisy measurement “ $c$ ” have been obtained as shown in Figures 5.3-5.6. The blue region corresponds to the values of  $(w_{11}, w_{22})$  for which the stochastic sensitivity matrix  $W$  is attainable.

As it is seen from Figures 5.3-5.6 that the increase of  $c$  results in the contraction of the attainability region.

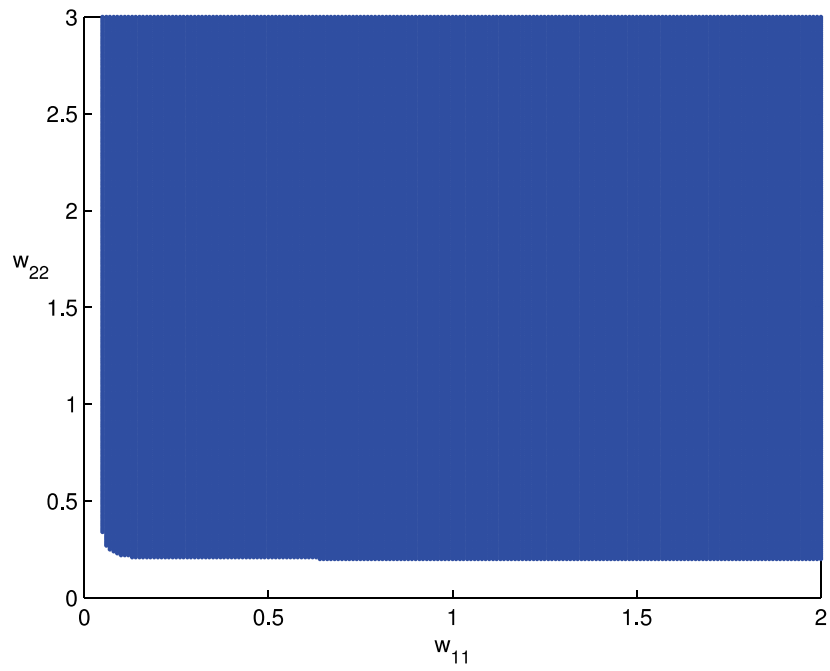


Figure 5.3. Attainability region of the stochastic sensitivity matrix  $W$  for  $P_m = 1$ ,  $D = 0.2$  and the intensity of noisy measurement  $c = 0.2$ .

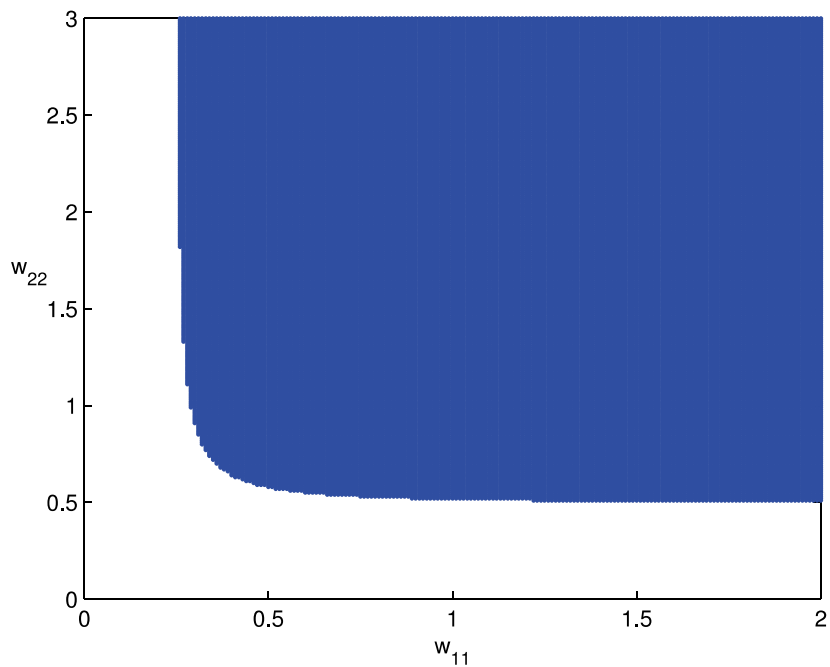


Figure 5.4. Attainability region of the stochastic sensitivity matrix  $W$  for  $P_m = 1$ ,  $D = 0.2$  and the intensity of noisy measurement  $c = 0.5$ .

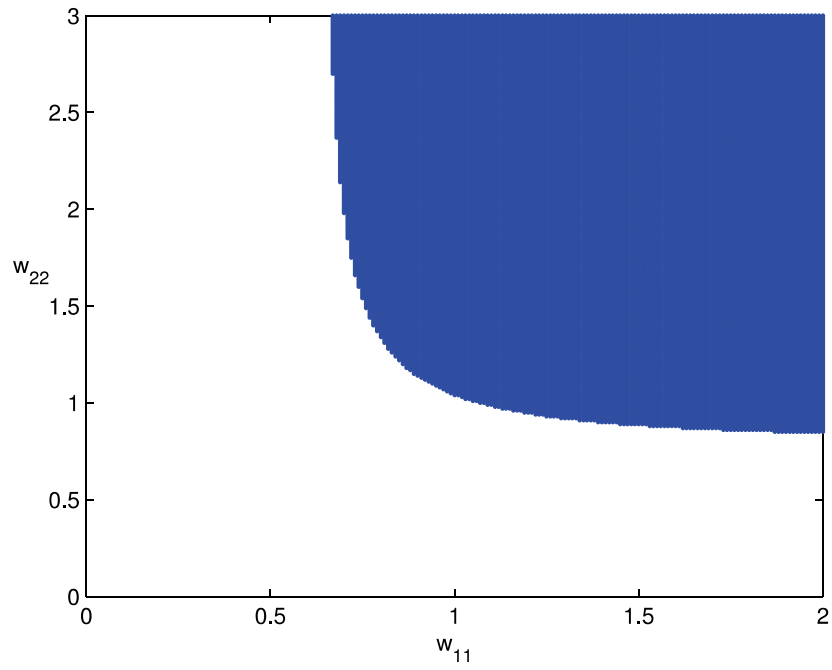


Figure 5.5. Attainability region of the stochastic sensitivity matrix  $W$  for  $P_m = 1$ ,  $D = 0.2$  and the intensity of noisy measurement  $c = 0.8$ .

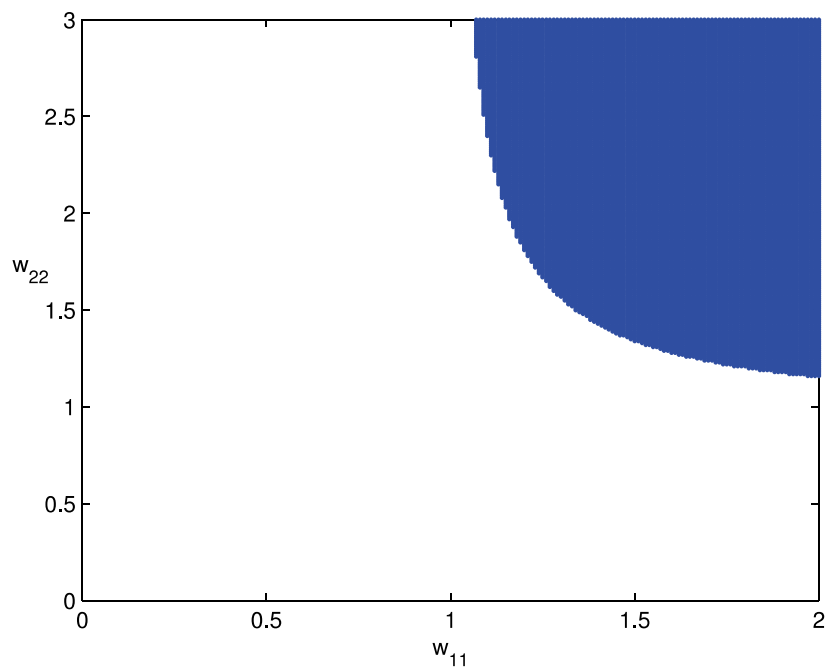


Figure 5.6. Attainability region of the stochastic sensitivity matrix  $W$  for  $P_m = 1$ ,  $D = 0.2$  and the intensity of noisy measurement  $c = 1.0$ .



Having obtained the attainability region for the pairs of  $(w_{11}, w_{22})$  of the stochastic sensitivity matrix  $W$ , the optimal regulator coefficients which minimize the cost function  $J(W) = w_{11} + w_{22}$  has been calculated as given in Table 5.1.

It has been seen that even if the feedback contains high noisy measurements (i.e. for high  $c$  values) the optimal regulator coefficients  $k_1$  and  $k_2$  can be obtained and the increase of the intensity of noisy measurements causes the optimal regulator coefficients  $k_1$  and  $k_2$  to become larger.

Table 5.1. Optimal parameters of stochastic sensitivity matrix and the optimal regulator coefficients.

| $c$ | $w_{11}$ | $w_{22}$ | $k_1$   | $k_2$    |
|-----|----------|----------|---------|----------|
| 0.2 | 0.07     | 0.25     | -3.5714 | -14.8708 |
| 0.5 | 0.4      | 0.64     | -1.60   | -6.037   |
| 0.8 | 0.89     | 1.15     | -1.2921 | -4.1931  |
| 1.0 | 1.38     | 1.45     | -1.0507 | -3.3543  |

Using these optimal regulator coefficients obtained as in Table 5.1 the dynamical behavior of the nonlinear system (5.8) have been numerically analyzed over 1000 realizations with the initial condition  $\delta(0) = 1$  and  $\omega(0) = 1$ .

The sample mean and 95% confidence interval for the mean have been computed over 1000 realizations. The 95% confidence intervals have been determined by the 2.5% and 97.5% percentiles of the simulated trajectories which correspond to the lower and upper bounds of the confidence interval, respectively.

The time series of the rotor angle  $\delta$  with the variations of  $c$  have been shown in Figures 5.7-5.10 in which the results have showed that the rotating orbit behavior disappears and the trajectories converge to the SEP even if the feedback contains high noisy observations. It has been also observed that the increase in noisy measurements in feedback regulator have resulted in the increase of the width of confidence intervals.

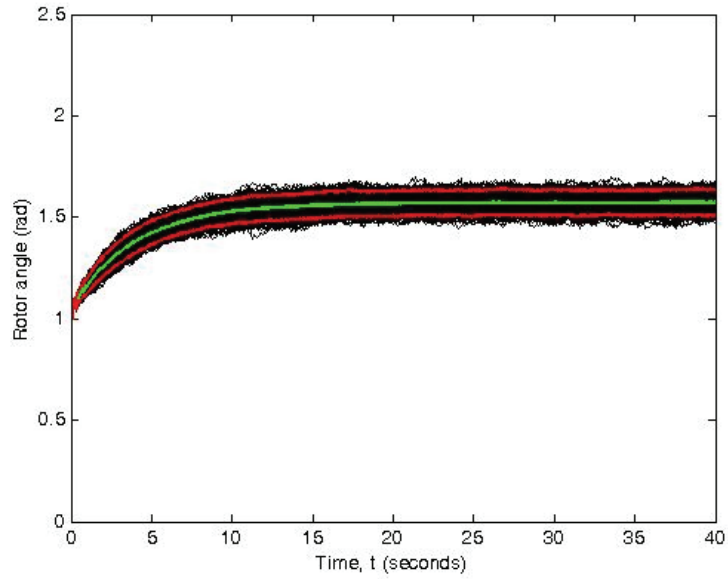


Figure 5.7. The stochastic rotor angle responses over 1000 trajectories (black) with optimal regulators, 95% confidence interval (red), empirical mean (green) for noise intensity with  $c = 0.2$ .

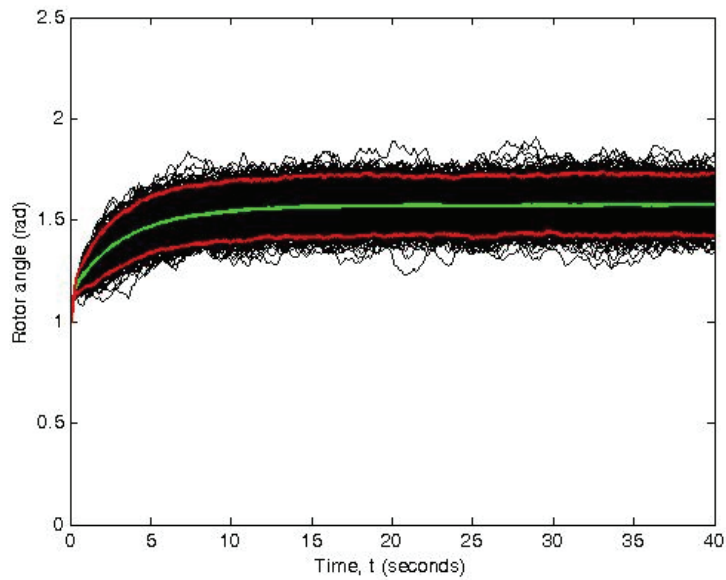


Figure 5.8. The stochastic rotor angle responses over 1000 trajectories (black) with optimal regulators, 95% confidence interval (red), empirical mean (green) for noise intensity with  $c = 0.5$ .

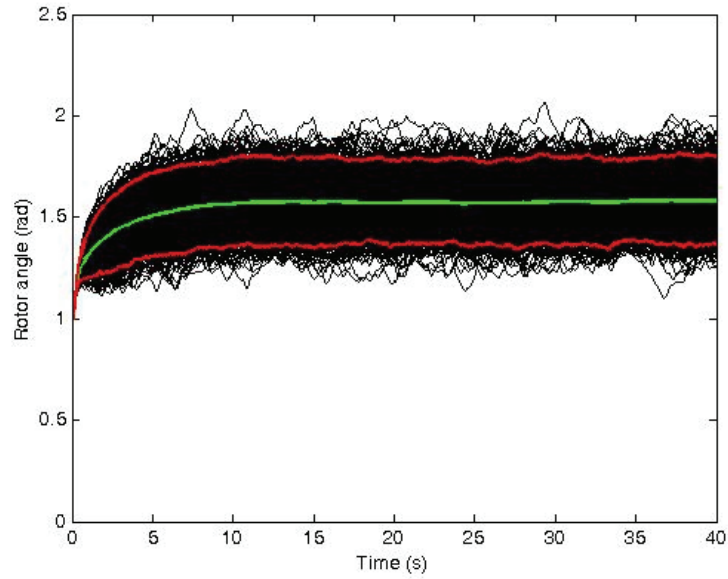


Figure 5.9. The stochastic rotor angle responses over 1000 trajectories (black) with optimal regulators, 95% confidence interval (red), empirical mean (green) for noise intensity with  $c = 0.8$ .

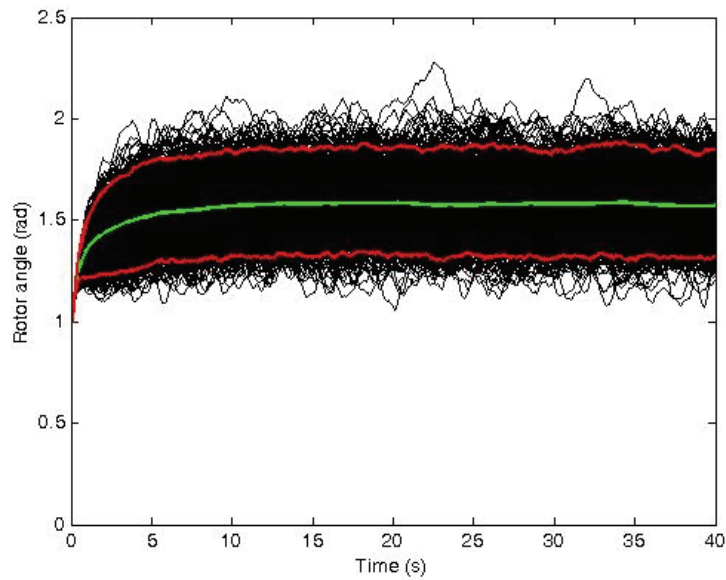


Figure 5.10. The stochastic rotor angle responses over 1000 trajectories (black) with optimal regulators, 95% confidence interval (red), empirical mean (green) for noise intensity with  $c = 1.0$ .

Consider the values of  $P_m = 0.5$  p.u and  $D = 0.2$  p.u in which the SEP is located at  $\bar{\delta} = 0.5236$ ,  $\bar{\omega} = 0$  with  $2\pi$  periodicity. The basin of attraction of deterministic and uncontrolled system of (5.8) has been shown in Figure 5.11. In this case the trajectories converge either to the stable equilibrium point with  $2\pi$  periodicity or a stable limit cycle (rotating orbit) depending on the initial conditions as stated previously.

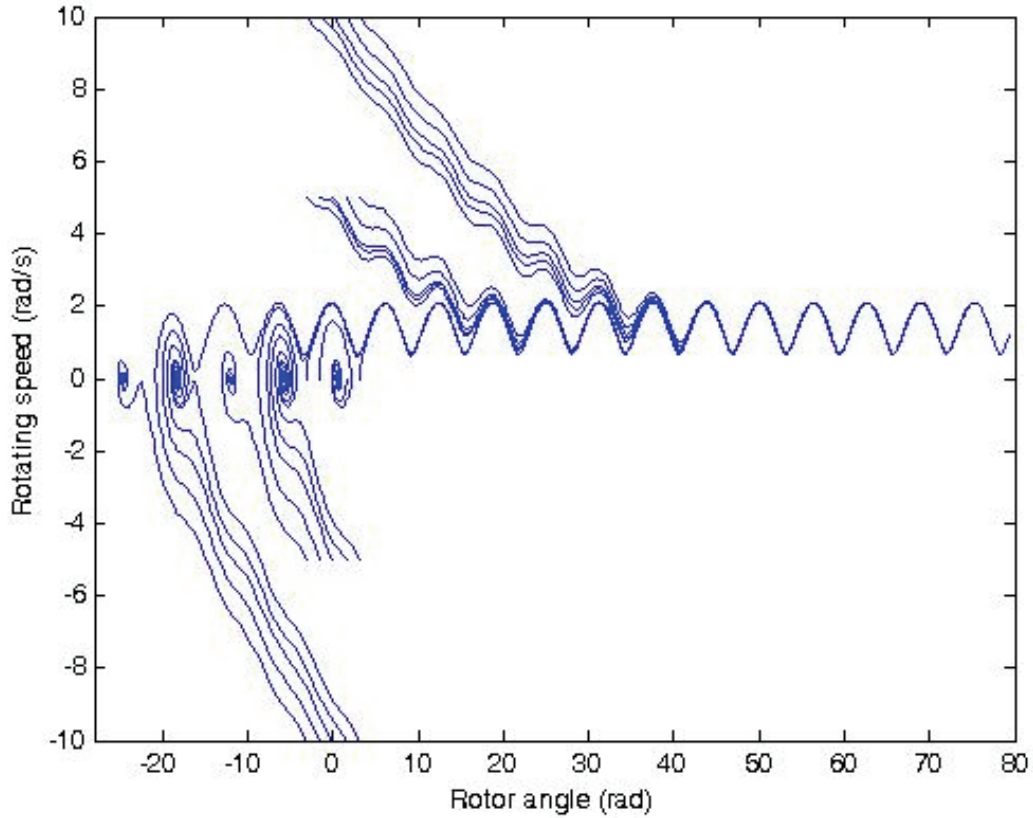


Figure 5.11. Phase portrait of rotor angle  $\delta$  vs. rotating speed  $\omega$  of the deterministic and uncontrolled system for  $P_m = 0.5$ .

The initial conditions have been chosen such that the trajectories converge to the limit cycle which is undesired for rotor angle stability. The stochastic sensitivity for the uncontrolled system of (5.8) has been calculated as  $w_{11} = 2.8868$  and  $w_{22} = 2.5$ . The designed feedback regulator which minimizes the value of the stochastic sensitivity stabilizes the equilibrium  $(\bar{\delta}, 0)$ .

With the feedback regulator which includes noisy observations, the attainability domains for the pair  $(w_{11}, w_{22})$  have been obtained as shown in Figures 5.12-5.15.

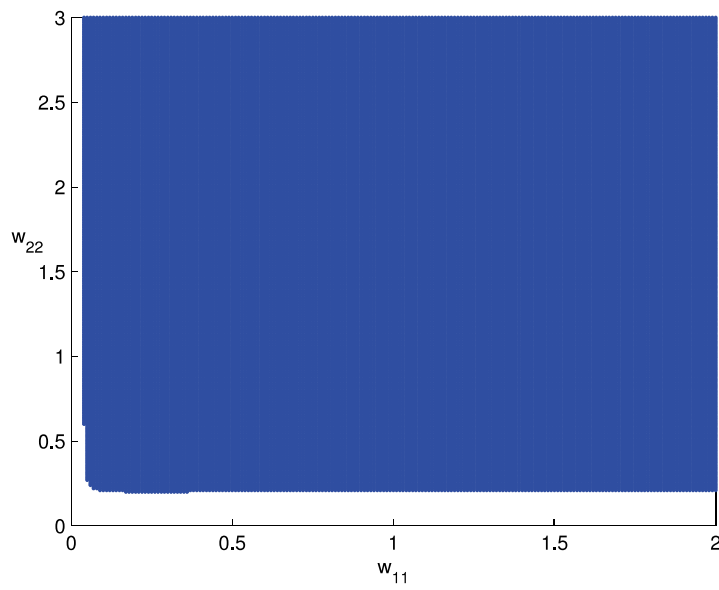


Figure 5.12. Attainability region of the stochastic sensitivity matrix  $W$  for  $P_m = 0.5$ ,  $D = 0.2$  and the intensity of noisy measurement  $c = 0.2$ .

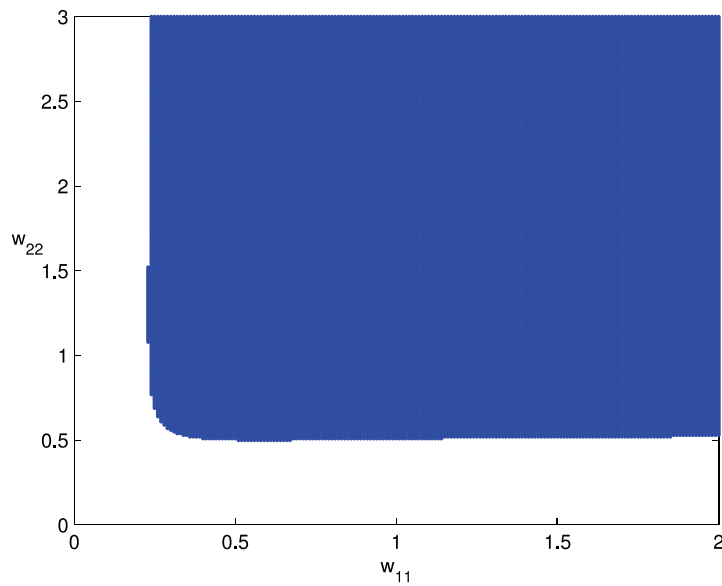


Figure 5.13. Attainability region of the stochastic sensitivity matrix  $W$  for  $P_m = 0.5$ ,  $D = 0.2$  and the intensity of noisy measurement  $c = 0.5$ .

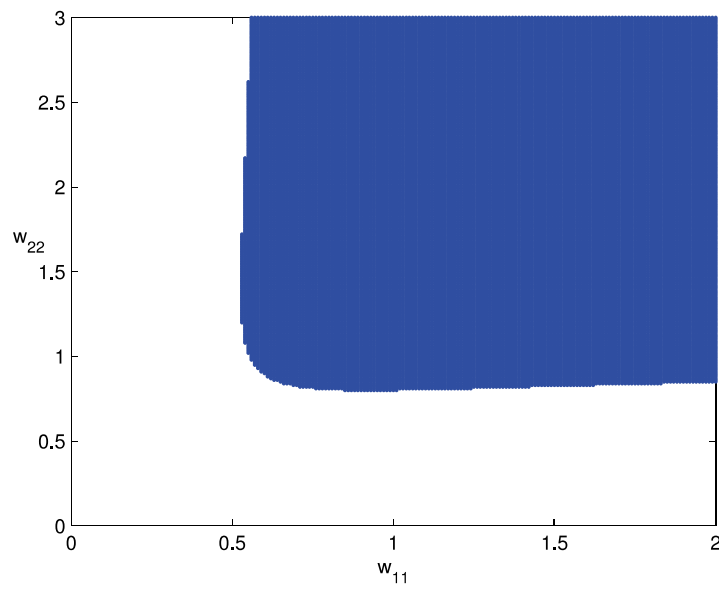


Figure 5.14. Attainability region of the stochastic sensitivity matrix  $W$  for  $P_m = 0.5$ ,  $D = 0.2$  and the intensity of noisy measurement  $c = 0.8$ .

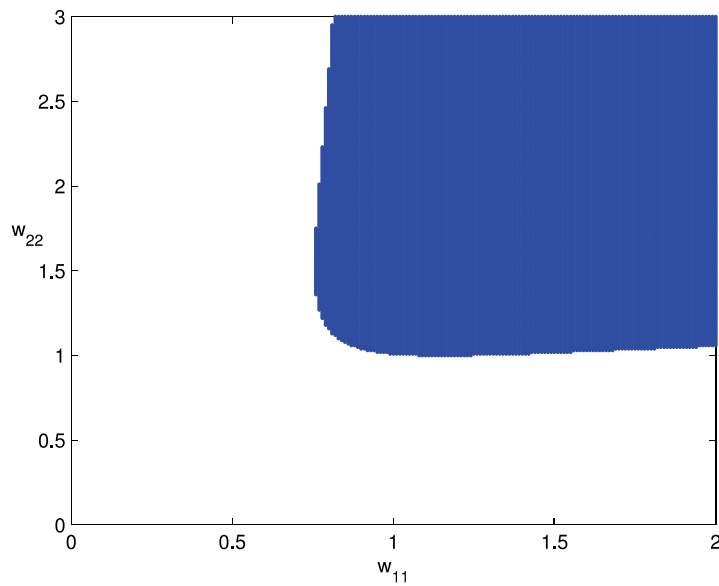


Figure 5.15. Attainability region of the stochastic sensitivity matrix  $W$  for  $P_m = 0.5$ ,  $D = 0.2$  and the intensity of noisy measurement  $c = 1.0$ .

The optimal regulator coefficients have been obtained by minimizing the cost function which implies the minimization of the dispersion of the states from the equilibria as shown in Table 5.2.

As it is seen from Table 5.2 that the stochastic sensitivity of equilibria  $(\bar{\delta}, \bar{\omega})$  has been minimized by the optimal regulators even if high noisy observations are present (i.e.,  $c = 1.0$ ).

Table 5.2. Optimal parameters of stochastic sensitivity matrix and the optimal regulator coefficients.

| $c$ | $w_{11}$ | $w_{22}$ | $k_1$   | $k_2$    |
|-----|----------|----------|---------|----------|
| 0.2 | 0.07     | 0.22     | -2.2768 | -13.1311 |
| 0.5 | 0.29     | 0.57     | -1.0995 | -5.3614  |
| 0.8 | 0.61     | 0.88     | -0.5766 | -3.1378  |
| 1.0 | 0.83     | 1.1      | -0.4593 | -2.5075  |

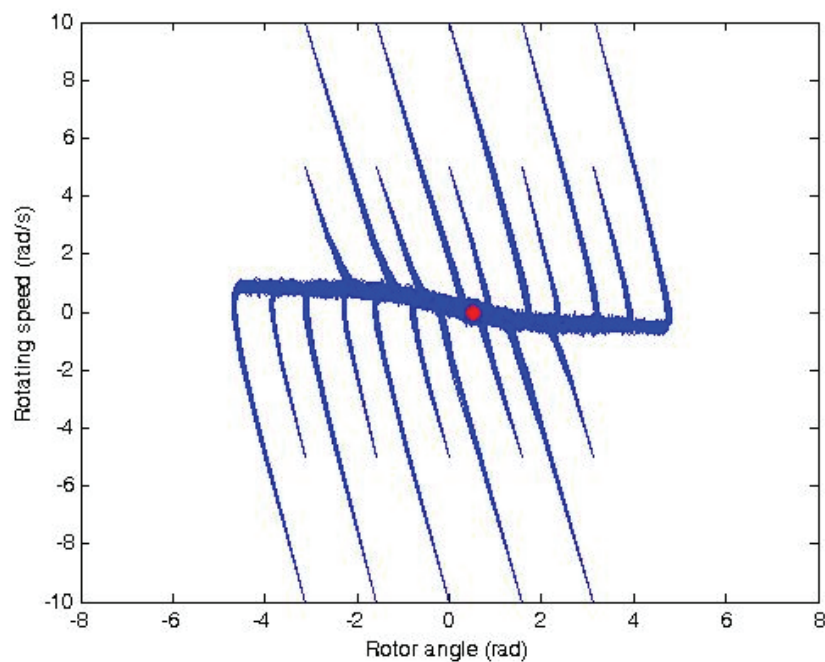


Figure 5.16. The stochastic rotor angle responses over 1000 trajectories with optimal regulators for  $P_m = 0.5$ ,  $D = 0.2$  and the intensity of noise measurements  $c = 0.5$ .

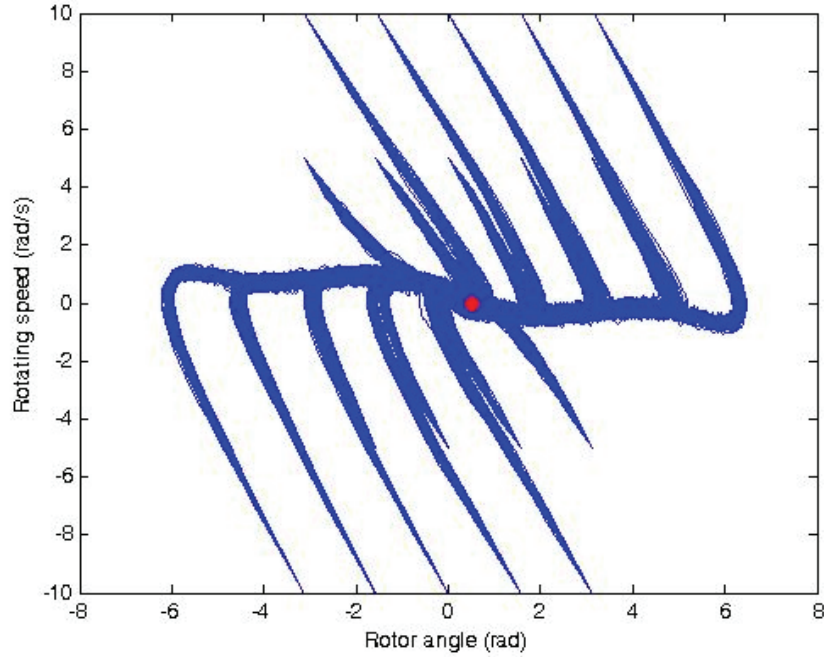


Figure 5.17. The stochastic rotor angle responses over 1000 trajectories with optimal regulators for noise intensity  $c = 1.0$ .

By using the optimal regulator parameters given in Table 5.2, the system (5.8) has been numerically analyzed over 1000 trajectories and the basin of attraction of the rotor angle  $\delta$  and rotating speed  $\omega$  with the variations of the intensity of noisy measurements  $c$  have been shown in Figures 5.16 and 5.17, respectively in which the SEP is indicated by red point.

As it can be seen from Figure 5.17, by the optimal regulators the responses of SMIB power systems can be stabilized even in the presence of high noisy observations in feedback regulator.

It has been also verified that using the optimal regulator parameters calculated theoretically, the control of the stochastic nonlinear SMIB power system has been numerically achieved for different values of mechanical power and damping parameters.

## 5.2. Controlling the Rotor Angle Stability in SMIB Power Systems with $\alpha$ -stable Lévy type power fluctuations

In this section, stochastic power fluctuations in SMIB systems have been modeled as  $\alpha$ -stable Lévy process to characterize the impulsive and asymmetric fluctuations proposed as in (Yılmaz and Savacı, 2017a,b). Then the expression of the rotor angle dispersion of SMIB



with Lévy type fluctuations analytically has been derived based on the study presented in (Grigoriu, 1995b) which uses the integral representations of alpha-stable processes (Samorodnitsky and Taqqu, 1994) and the control of the rotor angle stability has been also developed for the first time in the literature by minimizing the dispersion of this deviation (Savaci and Yilmaz, 2019).

As it was studied in (Yilmaz and Savaci, 2017a,b; Savaci and Yilmaz, 2019) the imbalance between the mechanical power input and the electrical power output in the SMIB power system given in (4.5) has been modeled by  $P_L(t) = \epsilon L_\alpha(t)$  where  $\epsilon$  is the noise intensity and  $L_\alpha(t)$  is the alpha-stable Lévy process and the increments of the Lévy process  $dL_\alpha(t)$  is  $\alpha$ -stable random variable (Samorodnitsky and Taqqu, 1994).

An  $\alpha$ -stable process with the integral representation (Samorodnitsky and Taqqu, 1994):

$$\{Y(t), t \in T\} \stackrel{d}{=} \left\{ \int_S f(t, y) M(dy), t \in T \right\} \quad (5.11)$$

can be interpreted as a linear combination of independent  $\alpha$ -stable variables  $M(dy)$  with coefficients  $f(t, y)$  satisfying some mild conditions (Grigoriu, 1995b).

The random measure in (5.11) have the Lebesgue control measure  $m(dy) = dy$  then the integral representation of  $\{L_\alpha(t), t \geq 0\}$  is as:

$$L_\alpha(t) = \int_0^t M(dy) = \int_0^\infty 1_{(0,t)} M(dy) \quad (5.12)$$

where  $1_{(0,t)}$  is the indicator function of set  $(0, t)$ .

The response  $X(t)$  of a linear system to an  $\alpha$ -stable input  $Y(t)$  is written in (Grigoriu, 1995b,a) as:

$$X(t) = \int_S g(t, s) dL_\alpha(s) \quad (5.13)$$

in which

$$g(t, s) = \int_0^t h(t, y) f(y, s) ds, \quad t \geq 0, \quad (5.14)$$

and  $h(t)$  is the unit impulse response function of the linear system.

Then the response  $X(t)$  is an  $\alpha$ -stable process with the scale in (Grigoriu, 1995b) is as follows:

$$\sigma(t) = \left[ \int_S |g(t, s)|^\alpha m(ds) \right]^{1/\alpha}. \quad (5.15)$$

Consider the following linearized stochastic SMIB system with the feedback regulator  $u = k_1(\delta - \bar{\delta}) + k_2(\omega - \bar{\omega})$  :

$$\begin{bmatrix} \dot{\delta} \\ \dot{\omega} \end{bmatrix} = \begin{bmatrix} 0 & 1 \\ k_1 - \cos\bar{\delta} & k_2 - D \end{bmatrix} \begin{bmatrix} \delta \\ \omega \end{bmatrix} + \begin{bmatrix} 0 \\ 1 \end{bmatrix} P_L \quad (5.16)$$

where  $P_L = \epsilon L_\alpha(t)$  represents  $\alpha$ -stable Lévy type power fluctuations.

The deviation of the rotor angle of the system (5.16) from the SEP  $(\bar{\delta}, \bar{\omega})$  has been given as:

$$X(t) = \delta(t) - \bar{\delta} \quad (5.17)$$

The control objective is to design a state feedback by minimizing the deviation of the response  $(\delta, \omega)$  from the SEP  $(\bar{\delta}, \bar{\omega})$  which implies the minimization of the dispersion parameter of the response  $X(t)$  within the minimum time settling down to the SEP  $(\bar{\delta}, \bar{\omega})$ .

In the sequel, the dispersion of SMIB with  $\alpha$ -stable Lévy power fluctuations have been obtained based on the approach in (Grigoriu, 1995b) where the response of the linear system subject to the alpha-stable input has been obtained.

The dispersion parameter of the response  $X(t)$  which corresponds to the scale parameter at power  $\alpha$  have been obtained using (5.14) in which the unit impulse response of a linearized SMIB system (5.16) is as follows:

$$h(t, y) = \frac{1}{\lambda} e^{0.5(k_2 - D)(t-y)} \sin(\lambda(t-y)) \quad (5.18)$$

with

$$\lambda = \sqrt{\cos\bar{\delta} - k_1 - \frac{(k_2 - D)^2}{4}} \quad (5.19)$$

and

$$f(y, s) = \epsilon 1_{(0,y)}(s). \quad (5.20)$$

then from (5.15) the scale parameter at  $\alpha$  has been derived as:

$$\sigma(t)^\alpha = \frac{\epsilon^\alpha}{\lambda^\alpha} \int_0^t |e^{0.5(k_2-D)z} \sin(\lambda z)|^\alpha dz. \quad (5.21)$$

The mechanical power  $P_m = 1.0$  p.u and the damping parameter  $D = 0.2$  p.u have been kept as fixed and the stochastic power fluctuations have been modeled as symmetric  $\alpha$ -stable Lévy process.

By using (5.21) the dispersion  $\sigma(t)^\alpha$  has been calculated for the range of  $k_1, k_2 \in [-10 - 1]$  with the noise intensity  $\epsilon = 0.001$ .

Considering the criteria of the minimum of  $\sigma^\alpha(t)$  and shorter settling time, the coefficients of feedback regulators have been evaluated as in Table. 5.3.

Table 5.3. The optimal regulator coefficients for  $P_m = 1.0$  p.u.

| $\alpha$ | $t_{min}(s)$ | $k_1$ | $k_2$ |
|----------|--------------|-------|-------|
| 2.0      | 1.096        | -8    | -3    |
| 1.9      | 1.6261       | -4    | -3    |
| 1.8      | 1.8284       | -3    | -2    |
| 1.7      | 2.3677       | -2    | -2    |
| 1.6      | 4.0264       | -2    | -1    |
| 1.5      | 4.1763       | -2    | -1    |
| 1.4      | 4.3901       | -2    | -1    |

As it has been seen from Table. 5.3 the time required to settle down to the equilibria increases with the decrease of characteristic exponent (i.e., the increase of impulsiveness). However, the control of the stabilization has been achieved by smaller amplitude of feedback regulator coefficients with the increase of impulsiveness.

The values of  $\sigma^\alpha(t_{min})$  obtained as the value of  $\sigma^\alpha(t)$  corresponding to the minimum settling time  $t_{min}$  have been presented in Figure 5.18 with the variation of the characteristic exponent  $\alpha$ . It has been observed that the time required to settle down to the equilibria increases with the decrease of characteristic exponent.

By using the optimal regulator coefficients obtained in Table. 5.3 the numerical solutions have been approximated by the Euler-Maruyama method (4.8) given in (Kloeden and Platen, 1999; Janicki and Weron, 1993).

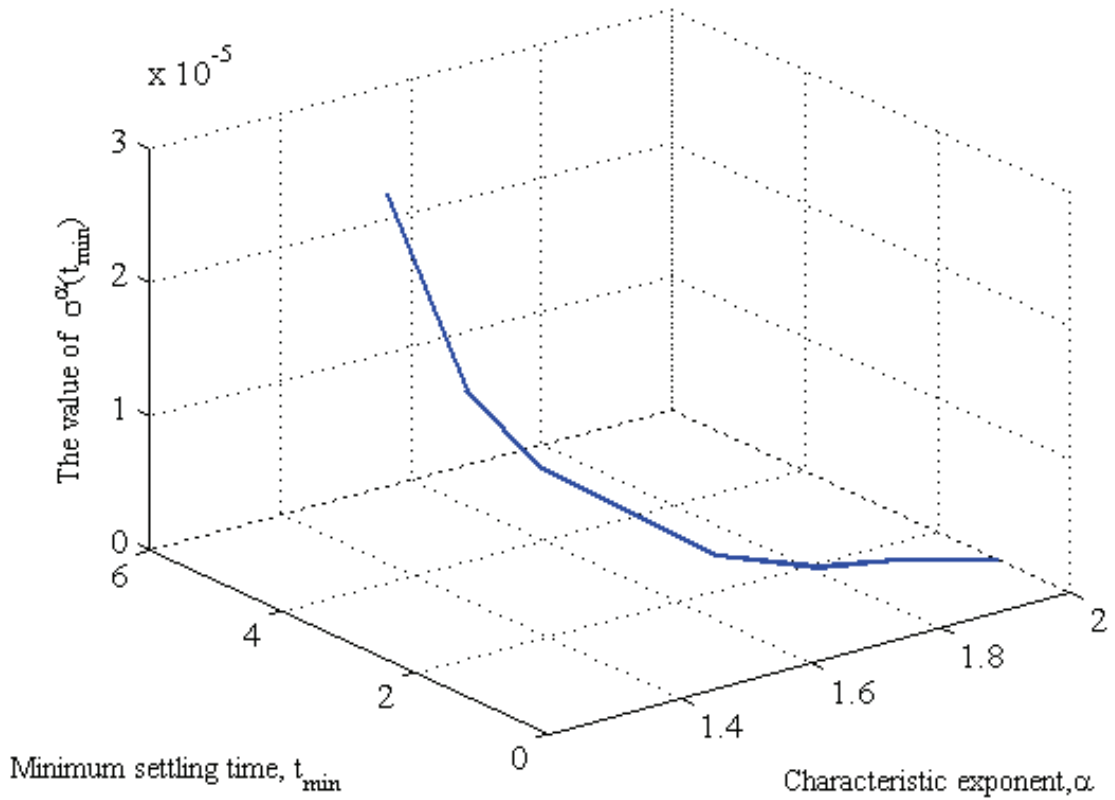


Figure 5.18. The values of the dispersion  $\sigma^\alpha$  versus to the minimum settling time with the variation of the characteristic exponent  $\alpha$ .

The numerical responses of rotor angle and rotating speed of nonlinear stochastic SMIB power system realizations have been obtained over 1000 as shown in Figures 5.19-5.20 in the presence of  $\alpha$ -stable Lévy type power fluctuations with  $\alpha = 1.5$ .

It has been observed from Figures 5.19-5.20 that the responses over 1000 realizations in the presence of  $\alpha$ -stable Lévy type power fluctuations have been stabilized and the trajectories of the rotor angle and the rotating speed have been converged to the SEP with much narrower confidence interval compared to the Wiener process.

When the mechanical power have been chosen as  $P_m = 0.5$  p.u and the damping parameter  $D = 0.2$  p.u by using (5.21) the coefficients of the feedback regulators have been found as  $k_1 = -2$  and  $k_2 = -2$  and the minimum settling time  $t_{min} = 1.8639$  seconds for the stochastic power fluctuations of  $\alpha$ -stable Lévy process type with  $\alpha = 1.8$  and  $\beta = 0$ .

The numerical responses of rotor angle and rotating speed of nonlinear SMIB system have been obtained over 1000 realizations for the 100 initial values of  $(\delta, \omega)$  from  $[-\pi, \pi] \times [-10, 10]$  as shown in Figure 5.21.

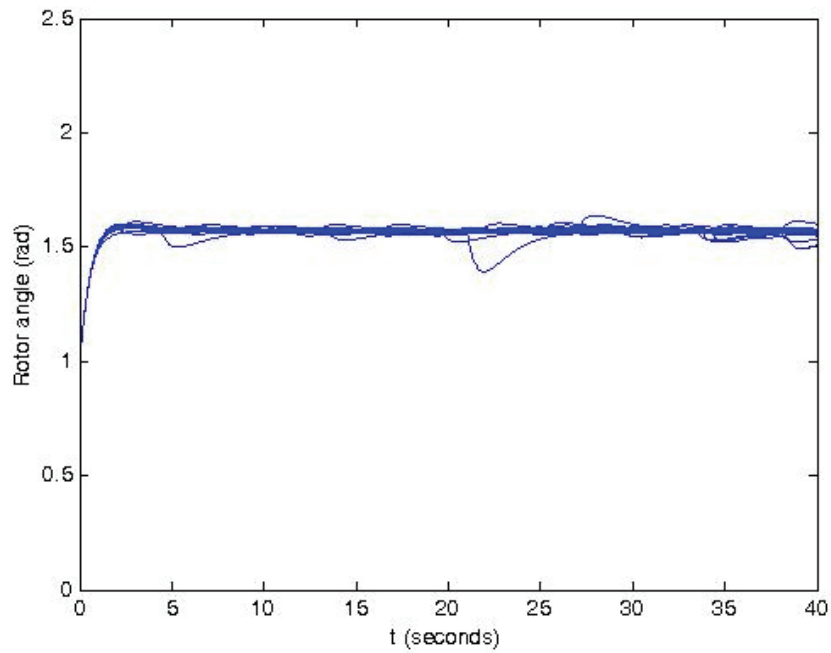


Figure 5.19. The stochastic responses of rotor angle of SMIB subject to  $\alpha$ -stable Lévy type power fluctuations with  $\alpha = 1.5$ ,  $\beta = 0$  over 1000 realizations in the presence of optimal regulator.

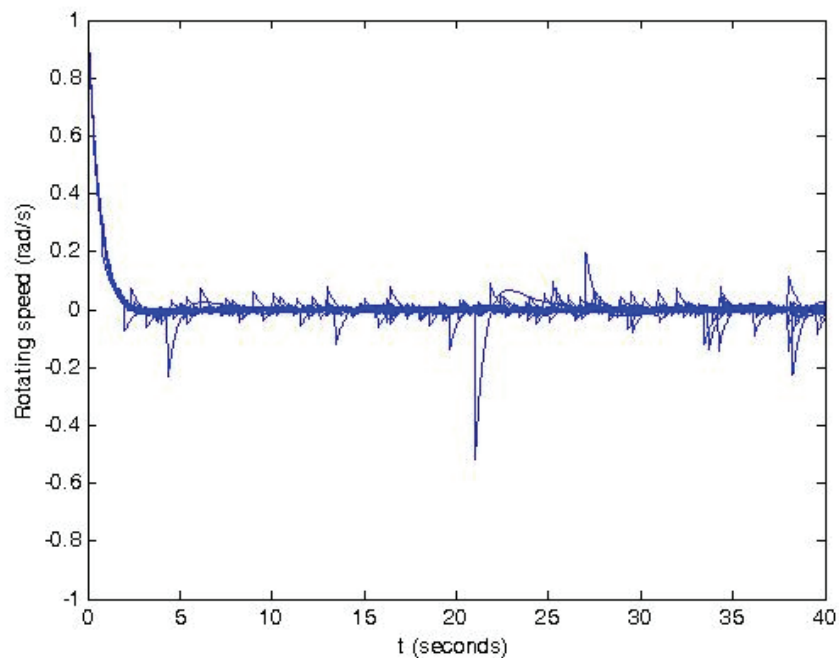


Figure 5.20. The stochastic responses of rotor speed of SMIB subject to  $\alpha$ -stable Lévy process with  $\alpha = 1.5$ ,  $\beta = 0$  over 1000 realizations in the presence of optimal regulator.

It is clearly seen that by the designed control rule the rotor angle  $\delta$  and the rotating speed  $\omega$  have been stabilized even in the presence of impulsive  $\alpha$ -stable Lévy type fluctuations and by such a feedback controller the basin of attraction have also been enlarged.

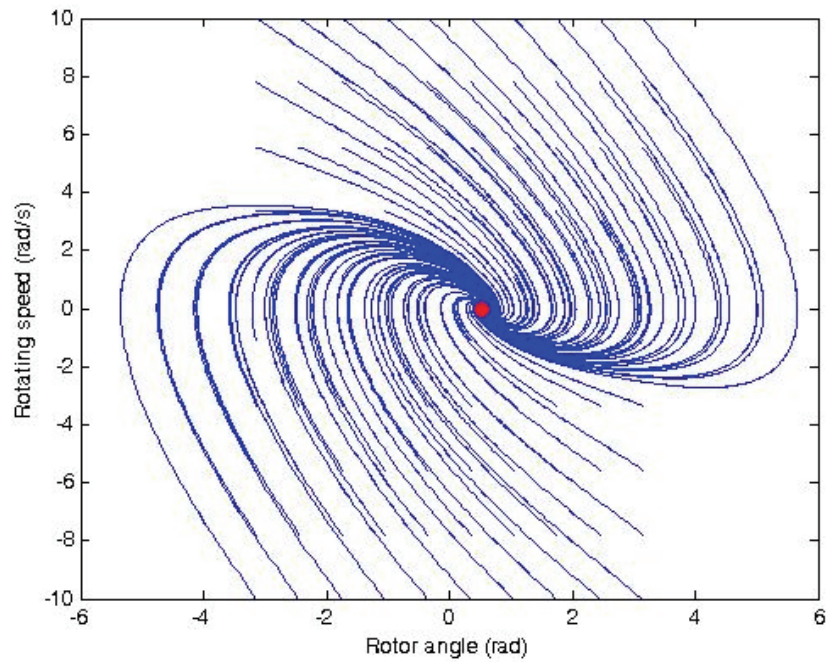


Figure 5.21. Phase portrait of the stochastic response of SMIB under  $\alpha$ -stable Lévy noise with  $\alpha = 1.8$ .

# CHAPTER 6

## CONCLUSIONS

In this dissertation, we have made progress on addressing the following questions: (1) What are effects of  $\alpha$ -stable Lévy fluctuations on the stability? 2) How should control rule be designed to achieve the synchronism in the presence of either Wiener or  $\alpha$ -stable Lévy type power fluctuations?

More specifically, we have investigated the effects of  $\alpha$ -stable Lévy type load fluctuations on the rotor angle stability in single machine infinite bus power system for different values of characteristic exponent and skewness parameters and derived the coefficients of the optimal feedback regulator to stabilize the single machine infinite bus power system in the presence of Wiener and  $\alpha$ -stable Lévy type fluctuations. It has been observed that the departing from the Gaussianity in distributions of load fluctuations either by increasing impulsiveness and/or distorting symmetry cause the instability of rotor angle in the mean square sense for the basin of attraction of synchronous state. However for the basin of attraction of limit cycle, the results show that Lévy type fluctuations improve the stability of rotor angle in the sense of probability. For some parameter pair of mechanical power and damping, the return probability decreases with the decrease of characteristic exponent (increase of impulsiveness) hence it becomes more difficult to converge to the synchronous state. The synchronous state's stability deteriorates when characteristic exponent decreases. However for some specific parameter pair value of mechanical power and damping, the return probability can be improved by injecting the stochasticity into the loads.

The coefficients of the optimal feedback regulator to stabilize the system have been derived in the presence of stochastic fluctuations modeled by Wiener process and  $\alpha$ -stable Lévy process. The control of the stability of single machine infinite bus power system with Wiener type power fluctuations have been studied by minimizing the stochastic sensitivity function. An expression has been derived for the rotor angle dispersion of the linearized stochastic SMIB and by selecting feedback gains, this dispersion has been numerically minimized. The stabilization of the rotor angle and rotating speed for nonlinear stochastic SMIB have been verified by the designed optimal regulators.

In the presence of  $\alpha$ -stable Lévy type power fluctuations, the proposed control rule has provided the stabilization of the responses of rotor angle and the rotating speed with narrower confidence interval and smaller gain constants compared to the Wiener type power fluctuations.

## REFERENCES

- Abe, S., Y. Fukunaga, A. Isono, and B. Kondo (1982). Power system voltage stability. *IEEE Transactions on Power Apparatus and Systems* (10), 3830–3840.
- Applebaum, D. (2009). *Lévy processes and stochastic calculus*. Cambridge university press.
- Astrom, K. J. (1971). *Introduction to Stochastic Control Theory*, Volume 70. Elsevier.
- Bashkirtseva, I., L. Ryashko, and G. Chen (2017). Controlling the equilibria of nonlinear stochastic systems based on noisy data. *Journal of the Franklin Institute* 354(3), 1658–1672.
- Bertram, J. and P. Sarachik (1959). Stability of circuits with randomly time-varying parameters. *IRE Transactions on Circuit Theory* 6(5), 260–270.
- Canizares, C. A. (1995). On bifurcations, voltage collapse and load modeling. *IEEE transactions on power systems* 10(1), 512–522.
- Chung, H.-Y. and W.-J. Chang (1994). Extension of the covariance control principle to nonlinear stochastic systems. *IEE Proceedings-Control Theory and Applications* 141(2), 93–98.
- Corsi, S. and C. Sabelli (2004). General blackout in italy sunday september 28, 2003, h. 03: 28: 00. In *Power Engineering Society General Meeting, 2004. IEEE*, pp. 1691–1702. IEEE.
- De Marco, C. and A. Bergen (1987). A security measure for random load disturbances in nonlinear power system models. *IEEE Transactions on Circuits and Systems* 34(12), 1546–1557.
- Deng, H. and M. Krstic (1999). Output-feedback stochastic nonlinear stabilization. *IEEE Transactions on Automatic Control* 44(2), 328–333.
- Dobson, I. (2013). Complex networks: synchrony and your morning coffee. *Nature Physics* 9(3), 133.



- Dobson, I. and H.-D. Chiang (1989). Towards a theory of voltage collapse in electric power systems. *Systems & Control Letters* 13(3), 253–262.
- Fredlin, M. and A. Wentzell (1984). Random perturbations of dynamical systems springer. *New York*.
- Frendal, M. and I. Rychlick (1992). Rainfall analysis. *Markov method. Technical report, Department of Mathematical Statistics, University of Lund, Sweden*.
- Grigoriu, M. (1986). Structural response to uncertain seismic excitations. *Journal of Structural Engineering* 112(6), 1355–1365.
- Grigoriu, M. (1995a). Linear and nonlinear systems with non-gaussian white noise input. *Probabilistic engineering mechanics* 10(3), 171–179.
- Grigoriu, M. (1995b). Linear systems subject to non-gaussian  $\alpha$ -stable processes. *Probabilistic engineering mechanics* 10(1), 23–34.
- Guckenheimer, J. and P. J. Holmes (2013). *Nonlinear oscillations, dynamical systems, and bifurcations of vector fields*, Volume 42. Springer Science & Business Media.
- Hotz, A. and R. E. Skelton (1987). Covariance control theory. *International Journal of Control* 46(1), 13–32.
- Janicki, A. and A. Weron (1993). *Simulation and chaotic behavior of alpha-stable stochastic processes*, Volume 178. CRC Press.
- Ji, P. and J. Kurths (2014). Basin stability of the kuramoto-like model in small networks. *The European Physical Journal Special Topics* 223(12), 2483–2491.
- Kloeden, P. E. and E. Platen (1999). *Numerical solution of stochastic differential equations*. Applications of mathematics. Berlin, New York: Springer.
- Kruczek, P., A. Wyłomańska, M. Teuerle, and J. Gajda (2017). The modified yule-walker method for  $\alpha$ -stable time series models. *Physica A: Statistical Mechanics and its Applications* 469, 588–603.
- Kundur, P., N. J. Balu, and M. G. Lauby (1994). *Power system stability and control*,

Volume 7. McGraw-hill New York.

- Kundur, P., J. Paserba, V. Ajjarapu, G. Andersson, A. Bose, C. Canizares, N. Hatziargyriou, D. Hill, A. Stankovic, C. Taylor, et al. (2004). Definition and classification of power system stability ieeecigre joint task force on stability terms and definitions. *IEEE transactions on Power Systems* 19(3), 1387–1401.
- Kushner, H. J. (1965). On the stability of stochastic dynamical systems. *Proceedings of the National Academy of Sciences of the United States of America* 53(1), 8.
- Kushner, H. J. (1967). Stochastic stability and control. Technical report, Brown Univ Providence Ri.
- Leng, S., W. Lin, and J. Kurths (2016). Basin stability in delayed dynamics. *Scientific reports* 6, 21449.
- Liscouski, B. and W. Elliot (2004). Final report on the august 14, 2003 blackout in the united states and canada: Causes and recommendations. *A report to US Department of Energy* 40(4), 86.
- Lu, Z., W. Zhao, D. Xie, and G. Li (2015). P-moment stability of power system under small gauss type random excitation. *Chaos, Solitons & Fractals* 81, 30–37.
- Ma, J., Y. Sun, X. Yuan, J. Kurths, and M. Zhan (2016). Dynamics and collapse in a power system model with voltage variation: The damping effect. *PloS one* 11(11), e0165943.
- Maas, G., M. Bial, and J. Fijalkowski (2007). Final report-system disturbance on 4 november 2006. *Union for the Coordination of Transmission of Electricity in Europe, Tech. Rep.*
- Mahmud, M., M. Hossain, H. Pota, and A. M. Oo (2017). Robust partial feedback linearizing excitation controller design for multimachine power systems. *IEEE Transactions on Power Systems* 32(1), 3–16.
- Mandelbrot, B. (1960). The pareto-levy law and the distribution of income. *International Economic Review* 1(2), 79–106.
- Menck, P. J., J. Heitzig, J. Kurths, and H. J. Schellnhuber (2014). How dead ends

- undermine power grid stability. *Nature communications* 5, 3969.
- Menck, P. J., J. Heitzig, N. Marwan, and J. Kurths (2013). How basin stability complements the linear-stability paradigm. *Nature Physics* 9(2), 89.
- Mil'Shtein, G. and L. Ryashko (1995). A first approximation of the quasipotential in problems of the stability of systems with random non-degenerate perturbations. *Journal of Applied Mathematics and Mechanics* 59(1), 47–56.
- Nikias, C. L. and M. Shao (1995). *Signal processing with alpha-stable distributions and applications*. Wiley-Interscience.
- Nolan, J. P. (1997). Numerical calculation of stable densities and distribution functions. *Communications in statistics. Stochastic models* 13(4), 759–774.
- Rigatos, G., P. Siano, A. Melkikh, and N. Zervos (2017). A nonlinear h-infinity control approach to stabilization of distributed synchronous generators. *IEEE Systems Journal* 12(3), 2654–2663.
- Rogers, G. (2012). *Power system oscillations*. Springer Science & Business Media.
- Ryashko, L. B. and I. A. Bashkirtseva (2008). On control of stochastic sensitivity. *Automation and Remote Control* 69(7), 1171–1180.
- Samorodnitsky, G. and M. S. Taqqu (1994). *Stable non-Gaussian random processes: stochastic models with infinite variance*, Volume 1. CRC press.
- Savaci, F. A. and S. Yılmaz (2019). Controlling the stability of stochastic single machine infinite bus power systems with wiener and alpha-stable levy type power fluctuations. *Systems and Control Letters* (Decision in Process).
- Schäfer, B., C. Beck, K. Aihara, D. Witthaut, and M. Timme (2018). Non-gaussian power grid frequency fluctuations characterized by lévy-stable laws and superstatistics. *Nature Energy* 3(2), 119.
- Serdukova, L., Y. Zheng, J. Duan, and J. Kurths (2016). Stochastic basins of attraction for metastable states. *Chaos: An Interdisciplinary Journal of Nonlinear Science* 26(7), 073117.

- Shi, Q., Y. Xu, Y. Sun, W. Feng, F. Li, and K. Sun (2018). Analytical approach to estimating the probability of transient stability under stochastic disturbances. In *2018 IEEE Power & Energy Society General Meeting (PESGM)*, pp. 1–5. IEEE.
- Skelton, R. E., T. Iwasaki, and D. E. Grigoriadis (1997). *A unified algebraic approach to control design*. CRC Press.
- Soong, T. T. (1973). *Random differential equations in science and engineering*. Elsevier.
- Strogatz, S. H. (2018). *Nonlinear dynamics and chaos: with applications to physics, biology, chemistry, and engineering*. CRC Press.
- Sun, J.-Q. (2006). *Stochastic dynamics and control*, Volume 4. Elsevier.
- TEIAS and ENTSO-E (2015). *Report on Blackout in Turkey on 31st March 2015*.
- Wang, X., Y. Chen, G. Han, and C. Song (2015). Nonlinear dynamic analysis of a single-machine infinite-bus power system. *Applied Mathematical Modelling* 39(10), 2951–2961.
- Wei, D. and X. Luo (2009). Noise-induced chaos in single-machine infinite-bus power systems. *EPL (Europhysics Letters)* 86(5), 50008.
- Weiss, M., M. Elsner, F. Kartberg, and T. Nilsson (2004). Anomalous subdiffusion is a measure for cytoplasmic crowding in living cells. *Biophysical journal* 87(5), 3518–3524.
- Weron, R. (2007). *Modeling and forecasting electricity loads and prices: A statistical approach*, Volume 403. John Wiley & Sons.
- Wojtkiewicz, S. and L. Bergman (2001). A moment specification algorithm for control of nonlinear systems driven by gaussian white noise. *Nonlinear Dynamics* 24(1), 17–30.
- Yang, T. C. (1997). Applying h-infinity optimisation method to power system stabiliser design part 1: Single-machine infinite-bus systems. *International journal of electrical power & energy systems* 19(1), 29–35.
- Yilmaz, S. and F. A. Savacı (2017a). Effect of levy type load fluctuations on the stability

of single machine infinite bus power systems. *2017 European Conference on Circuit Theory and Design (ECCTD)*. IEEE, 1–4.

Yılmaz, S. and F. A. Savacı (2017b). Basin stability of single machine infinite bus power systems with levy type load fluctuations. *International Conference on Electrical and Electronics Engineering (ELECO)*. IEEE, 125–129.

# VITA

## EDUCATION

### **2012 - 2019 Doctor of Philosophy in Electronics and Communication Engineering**

İzmir Institute of Technology, Turkey

Dissertation Title: Stability Analysis and Control of Stochastic Power Systems

### **2010 - 2012 Master of Science in Electronics and Communication Engineering**

İzmir Institute of Technology, İzmir -Turkey

Thesis Title: Stochastic Resonance in Chua's Circuit driven by Alpha-Stable Levy Noise

### **2004 - 2009 Bachelor of Science in Electrical and Electronics Engineering**

Gaziantep University, Gaziantep - Turkey

## PROFESSIONAL EXPERIENCE

### **2011 - 2018 Research and Teaching Assistant**

Department of Electrical and Electronics Engineering,

İzmir Institute of Technology, İzmir -Turkey

## PUBLICATIONS

Savaci, F. A. & Yilmaz, S., 2019: "Controlling the Stability of Stochastic Single Machine Infinite Bus Power Systems with Wiener and Alpha-Stable Levy Type Power Fluctuations" Systems and Control Letters, (Decision in Process).

Yilmaz, S., Cek, M.E. & Savaci, F. A., 2018: "Stochastic Bifurcation in Generalized Chua's Circuit driven by Skew-Normal Distributed Noise." Fluctuation and Noise Letters Vol.17, No.4.

Savaci, F. A. & Yilmaz, S., 2017: "Stochastic Bifurcation in Generalized Chua's Circuit through alpha-stable Levy noise." IEEE International Conference on Electronics, Circuits and Systems (ICECS), Batumi, Georgia, Dec 05-08, 2017.

Yilmaz, S. & Savaci, F. A., 2017: "Basin stability of single machine infinite bus power systems with Levy type load fluctuations." IEEE International Conference on Electrical and Electronics Engineering (ELECO), Bursa, Turkey, Nov 30 - Dec 02, 2017.

Yilmaz, S. & Savaci, F. A., 2017: "Effect of Levy type load fluctuations on the stability of single machine infinite bus power systems.", IEEE International Conference on Circuit Theory and Design (ECCTD), Catania, Italy, Sep 04-06, 2017.

Yilmaz, S. & Savaci, F. A., 2015: "Stochastic Resonance in Chua's Circuit driven by Alpha-Stable Levy noise.", International Conference on Physics and Control, İstanbul, Turkey, Aug 19-22, 2015, pp

Savaci, F. A. & Yilmaz, S., 2015: "Bayesian Stable Mixture Model of State Densities of Generalized Chua's Circuit.", International Journal of Bifurcation and Chaos, Vol.25, No.3 (2015).